



Doctoral Thesis in Biotechnology

Multifunctional carbohydrate-based soft materials from cereal by-products

SECIL YILMAZ TURAN

Multifunctional carbohydrate-based soft materials from cereal by-products

SECIL YILMAZ TURAN

Academic Dissertation which, with due permission of the KTH Royal Institute of Technology, is submitted for public defence for the Degree of Doctor of Philosophy on F3, Lindstedtsvägen 26, Stockholm, Sweden, 2021-11-04, 10.00 am

Doctoral Thesis in Biotechnology
KTH Royal Institute of Technology
Stockholm, Sweden 2021

© Secil Yilmaz Turan

ISBN 978-91-8040-005-3
TRITA-CBH-FOU-2021:39

Printed by: Universitetservice US-AB, Sweden 2021

Abstract

Cereal production generates large quantities of by-products every year, which still remain underutilized. The hemicellulose fractions from cereal by-products are anticipated to play an important role in tomorrow's sustainable and bio-based circular economy. This thesis addresses the valorization of hemicelluloses from cereal bran into films and hydrogels, starting from their isolation and expanding to the evaluation of material properties and potential use in future applications.

Initial isolation of arabinoxylans (AX) from wheat bran was achieved by a lab-scale subcritical water extraction (SWE) maintaining their functional groups (i.e. ferulic acid) and the effect of prior protein isolation on AX extraction was studied. The protein isolation resulted in a looser structure of wheat bran, which increased the polysaccharide yields in subsequent SWE. The polymeric structure and ferulic acid groups were preserved to a large extent after both protein isolation and SWE. The extracted AX fractions had considerable antioxidant activity, rendering them potential sources for further material development.

Further isolation of larger quantities of wheat bran AX was achieved by pilot scale SWE and alkaline extraction, resulting in feruloylated and non-feruloylated AX fractions, respectively. The film formation and properties of these AXs were investigated in comparison with a wheat endosperm AX. The three AX were also chemically modified by acetylation and applied in films. Higher purity, molecular weight, and degree of substitution of the AX extracts led to better thermal and mechanical properties of their films. The thermal stability of the films was significantly improved after chemical acetylation however, the mechanical performance and permeability properties did not change. Bound ferulic acid in feruloylated AX films was found to have considerably higher antioxidant activity than external incorporation of free ferulic acid.

Hydrogels were produced by enzymatic crosslinking of feruloylated AX from both wheat and corn bran, which show distinct molecular structure and ferulic acid content. For wheat bran AX, hydrogels were obtained by laccase crosslinking and the following regeneration process, and their biochemical and biophysical properties were studied. The rheological properties of feruloylated AX were enhanced by enzymatic crosslinking and further improved by the regeneration, proving that their mechanical strength can be modulated by chemical and physical adjustments. For corn bran AX, crosslinking was applied by laccase and peroxidase to compare the properties of the resulting hydrogels. Laccase formed a more elastic hydrogel network whereas peroxidase crosslinking resulted in hydrogels with larger covalent polymer networks. As a result of these differences between the two enzymes, the hydrogel obtained by peroxidase crosslinking contained larger aggregates with higher clustering strength. The crosslinking was followed by a cell application of the AX hydrogels, where their protective effect against chemically induced oxidative stress was demonstrated. Both corn bran AX hydrogels provided adequate scavenging against reactive oxygen species produced by human colon cells. It was shown that the gelation of wheat bran AX is governed by physical interactions between the xylan backbones of adjacent chains and interactions between larger scale aggregates in addition to the covalent crosslinks. The gelation mechanism of highly substituted corn bran AX was instead hypothesized to proceed by interactions between side chains together covalent crosslinks. This thesis demonstrated that AX-based hydrogels could find potential use in food and biomedical applications. The outputs of this thesis will contribute to the bioeconomy and sustainable development by valorizing food side fractions into new high-value materials.

Keywords

Wheat bran, corn bran, hemicellulose, arabinoxylan, ferulic acid, subcritical water extraction, acetylation, films, hydrogels, crosslinking, regeneration, antioxidant activity

Sammanfattning

Spannmålsproduktion genererar varje år biprodukter i stora mängder som fortfarande är outnyttjade. Hemicelluloser från spannmålsbiprodukter förväntas spela en viktig roll i framtidens hållbara och biobaserade cirkulära ekonomi. Denna avhandling omfattar valorisering av hemicelluloser från spannmålskli till filmer och hydrogeler, vilken startar med isolering och utvidgas till utvärdering av materialegenskaper och eventuell användning vid vidare applikationer.

Arabinoxylaner (AX) extraherades initialt genom att använda en subkritisk vattenextraktion (SWE) i laboratorieskala under vilken de funktionella grupperna (ferulysyra) behölls intakta och effekten av tidigare proteinisolering i AX extraktion studerades. Proteinisoleringen resulterade i en lösare struktur hos vetekliet, vilket ökade utbytet av polysackarid i efterföljande SWE. Polymerstrukturen och ferulysyra grupperna bibehölls i stor utsträckning efter både proteinisolering och SWE. De extraherade AX fraktionerna uppvisade avsevärd antioxidantisk aktivitet, vilket gör dem till potentiella källor för ytterligare materialutveckling.

Ytterligare isolering av vetekli AX i större mängder uppnåddes genom pilotskala SWE och alkalisk extraktion, vilket resulterade i feruloylerade och icke-feruloylerade AX-fraktioner. Filmbildningen och egenskaperna hos dessa AX undersöktes och jämfördes med en veteendosperm AX. De tre AX modifierades också kemiskt genom acetylering och applicerades i filmer. Högre renhet, molekylvikt och substitutionsgrad hos AX extrakten ledde till bättre termiska och mekaniska egenskaper hos dessa filmer. Filmernas termiska stabilitet förbättrades avsevärt efter kemisk acetylering, men de mekaniska prestanda och permeabilitetsegenskaperna förändrades inte. Bunden ferulysyra i AX filmerna uppvisade betydligt högre antioxidantisk aktivitet än extern införlivning av fri ferulysyra.

Hydrogeler producerades genom enzymatisk tvärbinding av feruloylerad AX från både vete och majscli, som båda uppvisar distinkt molekylstruktur och ferulysyrhalt. Hydrogeler producerades från vetekli AX genom lackas tvärbinding och den följande regenereringsprocessen samt deras biokemiska och biofysikaliska egenskaper studerades. De reologiska egenskaperna hos feruloylerad AX förstärktes genom enzymatisk tvärbinding och förbättrades vidare genom regenereringen, vilket bevisar att deras mekaniska hållfasthet kan moduleras genom kemiska och fysiska justeringar. För majscli AX applicerades tvärbinding med lackas och peroxidase för att jämföra egenskaperna hos de resulterande hydrogelerna. Lackas bildade ett mer elastiskt hydrogel nätverk medan peroxidase tvärbinding resulterade i hydrogeler med större kovalenta polymernätverk. Som ett resultat av dessa skillnader mellan de två enzymerna uppvisade hydrogelerna från peroxidase tvärbinding större aggregat med högre klusterstyrka. Tvärbindingen följdes av en cellapplicering av AX hydrogelerna, där deras skyddande effekt mot kemiskt inducerad oxidativ stress påvisades. Båda majscli AX hydrogelerna uppvisade god avlägsningsförmåga gentemot reaktiva syreföreningar som produceras av humana kolonceller. Det visades att gelningen av vetekli AX styrs av fysikaliska interaktioner mellan xylan skelettet i angränsande AX kedjor och interaktioner mellan aggregat i större skala i tillägg till de kovalenta tvärbindingarna. Geleringsmekanismen för starkt substituerad majscli AX antogs istället gå vidare genom interaktioner mellan sidokedjor tillsammans kovalenta tvärbindingar. Denna avhandling visade att AX-baserade hydrogeler kan hitta potentiell användning inom livsmedel och biomedicinska tillämpningar. Resultatet av denna avhandling kommer att bidra till bioekonomi och hållbar utveckling genom att valorisera livsmedelsfraktioner till nya högvärdiga material.

Nyckelord

Vetekli, majscli, hemicellulosa, arabinoxylan, ferulysyra, subkritisk vattenextraktion, acetylering, filmer, hydrogeler, tvärbinding, regeneration, antioxidant aktivitet

Public defense of dissertation

This thesis will be defended on November 4th, 2021 at 10 a.m. in F3, Lindstedtsvägen 26, Stockholm, Sweden.

Respondent:

Secil Yilmaz Turan
Department of Chemistry
School of Engineering Sciences in Chemistry, Biotechnology and Health
KTH Royal Institute of Technology, Sweden

Faculty Opponent:

Professor Anna Ström
Chemistry and Chemical Engineering
Chalmers University of Technology, Sweden

Evaluation committee:

Professor Ulrica Edlund,
Department of Fibre and Polymer Technology
School of Engineering Sciences in Chemistry, Biotechnology and Health
KTH Royal Institute of Technology, Sweden

Professor Tommy Nylander
Department of Chemistry, Division of Physical Chemistry
Lund University, Sweden

Associate Professor Bjørge Westereng
Department of Chemistry, Biotechnology and Food Science
Norwegian University of Life Sciences, Norway

Chairperson:

Dr. Lauren Sara McKee
Department of Chemistry
School of Engineering Sciences in Chemistry, Biotechnology and Health
KTH Royal Institute of Technology, Sweden

Respondent's main supervisor:

Associate Professor Francisco Javier Vilaplana Domingo
Department of Chemistry
School of Engineering Sciences in Chemistry, Biotechnology and Health
KTH Royal Institute of Technology, Sweden

List of appended papers

This thesis is a summary of the following four papers. Full versions are appended at the end of this thesis.

Paper I

Cascade extraction of proteins and feruloylated arabinoxylans from wheat bran

Secil Yilmaz Turan, Amparo Jiménez-Quero, Rosana Moriana, Elisa Arte, Kati Katina, and Francisco Vilaplana, *Food Chemistry*, **2020**, 333, 127491

Paper II

Bio-based films from wheat bran feruloylated arabinoxylans: Effect of extraction technique, acetylation and feruloylation

Secil Yilmaz Turan, Amparo Jiménez-Quero, Carolin Menzel, Danila Morais de Carvalho, Mikael E. Lindström, Olena Sevastyanova, Rosana Moriana, and Francisco Vilaplana, *Carbohydrate Polymers*, **2020**, 250, 116916

Paper III

Revealing the mechanisms of hydrogel formation by laccase crosslinking and regeneration of feruloylated arabinoxylan from wheat bran

Secil Yilmaz Turan, Patricia Lopez-Sanchez, Amparo Jiménez-Quero, Tomás S. Plivelic, and Francisco Vilaplana, *Submitted*

Paper IV

Enzymatic production of hydrogels from corn bran feruloylated arabinoxylan with protective effects against reactive oxygen species

Secil Yilmaz Turan, Kun Jiang, Patricia Lopez-Sanchez, Amparo Jiménez-Quero, Thomas Crouzier, Tomás S. Plivelic, and Francisco Vilaplana, *Manuscript*

List of author's contributions to the appended papers

Paper I

First author. Planned and performed all experimental and characterization work, but not the SEC. Analyzed and summarized all results and wrote a large part of the manuscript.

Paper II

First author. Planned the experimental work, performed chemical acetylation, film preparation, characterization and analyzed the data. Prepared the manuscript.

Paper III

First author. Designed and performed most experiments except HPLC-ESI-MS and cryo-SEM. Analyzed all the data and prepared the manuscript.

Paper IV

First author. Planned most experiments, performed hydrogel preparation, most of the characterization work and prepared the major part of the manuscript.

Other publications not included in this thesis

Paper V

Regulation of colony morphology and biofilm formation in *Shewanella algae*

Alberto J. Martín-Rodríguez, Katia Villion, [Secil Yilmaz Turan](#), Francisco Vilaplana, Åsa Sjöling, and Ute Römling, *Microbial Biotechnology*, **2021**, 14(3), 1183-1200

Paper VI

Macroalgae suspensions prepared by physical treatments: Effect of polysaccharide composition and microstructure on the rheological properties

Loredana Malafrente, [Secil Yilmaz Turan](#), Annika Krona, Marta Martinez-Sanz, Francisco Vilaplana, and Patricia Lopez-Sanchez, *Food Hydrocolloids*, **2021**, 120, 106989

ABBREVIATIONS

4- <i>O</i> -MeGlcA	4- <i>O</i> -methyl glucuronic acid
Araf	Arabinofuranose
ASE	Accelerated Solvent Extractor
AX	Arabinoxylan
A/X	Arabinose to xylose ratio
Cryo-SEM	Cryogenic Scanning Electron Microscopy
DA	Degree of acetylation
di-FA	Ferulic acid dehydrodimer
DMSO	Dimethyl sulfoxide
DPPH	1,1-diphenyl-2-picrylhydrazyl
DS	Degree of substitution
DSC	Differential Scanning Calorimetry
DW	Dry weight
EC ₅₀	Half-maximal effective concentration
FA	Ferulic acid
F-AX	Feruloylated arabinoxylan
FE-SEM	Field Emission Scanning Electron Microscopy
FTIR	Fourier Transform Infrared Spectroscopy
Fuc	Fucose
G'	Storage modulus
G''	Loss modulus
GalA	Galacturonic acid
GAX	Glucuronoarabinoxylan
Glc	Glucose
GlcA	Glucuronic acid
H ₂ O ₂	Hydrogen peroxide
HPAEC-PAD	High-Performance Anion Exchange Chromatography with Pulsed Amperometric Detection
HPF	High pressure freezing
HPLC	High-Performance Liquid Chromatography

HPLC-ESI-MS	High-Performance Liquid Chromatography with Electrospray Ionization mass spectrometry
HRP	Horseradish peroxidase
L-Ara	L-arabinose
L-Gal	L-galactose
MALLS	Multi-Angle Laser Light Scattering
Man	Mannose
MLBG	Mixed linkage β -glucan
\bar{M}_n	Number average molecular weight
\bar{M}_w	Weight average molecular weight
Mw	Molecular weight
OP	Oxygen Permeability
OTR	Oxygen Transmission Rate
Rha	Rhamnose
R_h	Hydrodynamic radius
SAXS	Small Angle X-ray Scattering
SEC	Size Exclusion Chromatography
SWE	Subcritical Water Extraction
T_g	Glass transition temperature
TGA	Thermogravimetric Analysis
T_{onset}	Initial decomposition temperature
tri-FA	Ferulic acid dehydrotrimer
UV/Vis	Ultraviolet Visible Spectroscopy
V_{el}	Elution volume
WAXS	Wide Angle X-ray Scattering
WB	Wheat bran
WVP	Water Vapor Permeability
WVTR	Water Vapor Transmission Rate
X_c	Degree of crystallinity
Xylp	Xylopyranose

Table of Contents

1 PURPOSE OF THE STUDY	1
2 INTRODUCTION	2
2.1 CEREALS.....	2
2.2 CEREAL BRAN AND ITS COMPONENTS.....	2
2.2.1 Arabinoxylans.....	3
2.2.2 Mixed linkage β -glucan and cellulose	6
2.2.3 Proteins	6
2.2.4 Lignin and other components	7
2.2.5 Cell wall recalcitrance	7
2.3 EXTRACTION OF ARABINOXYLANS AND CHALLENGES	8
2.4 FUNCTIONALITY AND UTILIZATION OF ARABINOXYLANS	9
2.4.1 Modification tools of arabinoxylans	10
2.4.1.1 Esterification	10
2.4.1.2 Etherification and oxidation.....	11
2.4.1.3 Covalent cross-linking	11
2.4.2 Material applications of arabinoxylans.....	13
2.4.2.1 Films from arabinoxylans	13
2.4.2.2 Hydrogels from arabinoxylans	15
3 EXPERIMENTAL.....	18
3.1 MATERIALS AND CHEMICALS	18
3.2 ARABINOXYLAN EXTRACTION (Paper I, II, III, IV).....	18
3.3 ACETYLATION OF ARABINOXYLANS (Paper II).....	20
3.4 FILM FORMATION (Paper II).....	20
3.5 PREPARATION OF HYDROGELS (Paper III, IV).....	21
3.6 INSTRUMENTATION AND CHARACTERIZATION	22
4 RESULTS AND DISCUSSION.....	29
4.1 Sequential extraction of wheat bran proteins and arabinoxylans (Paper I)	29
4.1.1 Effect of extraction conditions on the yields and molecular characteristics of F-AX	30
4.2 Arabinoxylan films (Paper II)	33
4.2.1 Upscaled SWE and alkaline extraction of arabinoxylans	33
4.2.2 Acetylation as a tool to improve the material properties of AX films	34

4.2.3 Material properties and bioactivity of native and acetylated AX films	35
4.3 Arabinoxylan hydrogels (Paper III and IV).....	40
4.3.1 Properties of crosslinked AX from wheat bran	41
4.3.2 Comparison of laccase and peroxidase crosslinking of corn bran AX.....	48
4.3.3 Physicochemical properties and antioxidative potential of hydrogels from corn bran AX	50
4.3.4 Comparison of the gelation mechanisms of wheat bran and corn bran AX.....	56
5 CONCLUSIONS	59
6 UNITED NATIONS SUSTAINABLE DEVELOPMENT GOALS.....	61
7 FUTURE PERSPECTIVES.....	62
8 ACKNOWLEDGEMENTS	63
9 REFERENCES	64

1 PURPOSE OF THE STUDY

Our society is currently experiencing a transition to a bio-based economy that requires innovative and efficient use of bio-based resources to generate future's functional and sustainable materials. Cereal by-products accommodate hemicelluloses that have been widely recognized for their great potential for use in food and biomedical applications as polymeric matrices. Effective exploitation of cereal by-products is fundamental for the efficient implementation of their hemicelluloses in subsequent materials. The purpose of this study was therefore to design and develop a range of different polymeric materials while using efficient extraction strategies for the biomolecules from cereal by-products. The specific aims of this thesis were:

- Evaluating how the isolation of wheat bran proteins influenced the extraction of arabinoxylans in a cascade process.
- Developing free-standing films from wheat bran arabinoxylans and unveiling the relationship between the molecular properties of arabinoxylans and film properties.
- Assessing the potential of chemical acetylation to introduce internal plasticization, hydrophobicity, and thermal stability to arabinoxylan-based films.
- Enzymatically and physically tailoring arabinoxylans to develop hydrogels from wheat and corn bran with enhanced gel properties and elucidate their gelation mechanism.
- Investigating the impact of crosslinking by different enzymes on the characteristics of arabinoxylan-based hydrogels.
- Demonstrating the proof of concept for the biomedical application of arabinoxylan-based hydrogels.

2 INTRODUCTION

2.1 CEREALS

Agricultural crops are interesting and versatile in many aspects, not only providing food to humankind and animals but also representing valuable sources for industrial product making. Cereal grains are the main components of the human diet and animal feeding, which were the earliest plants that were cultivated by humankind in ancient times. Nowadays, the most grown cereals in the world are wheat, rye, oats, barley, corn, and rice.

Cereal production takes an important place in Sweden's agriculture, and cereal products represent one-third of the increase in the country's export (Jordbruksverket, 2009). In 2019, the total production of cereal grains in Sweden reached 6.0 M tons (FAOSTAT, 2019). The processing of grains to produce cereal products generates significant amounts of by-products such as bran, husk, and straw. The majority of these by-products find their main use in animal feeding as low-cost ingredients. Cereal by-products are, however, renewable resources composed of valuable components and hence, can be used as feedstocks for advanced chemical, nutritional and material applications.

2.2 CEREAL BRAN AND ITS COMPONENTS

Cereal grain is constituted by three main parts: endosperm, germ (embryo) and bran, which are separated during the milling process. The starchy endosperm is mainly used for flour production whereas the germ contains high levels of lipids and is used in animal feeding. Bran layers of cereal grains are separated as by-products during milling operations and represent a rich source of fiber polysaccharides, vitamins and minerals. The morphology and composition of cereal bran vary depending on the source, variety of the grain, cultivation conditions and harvest time. In this thesis, bran layers from wheat and corn kernels have been used.

The bran of wheat accounts for 14-16 % of the whole kernel and is composed of arabinoxylans (AX) (20-40 %), mixed linkage β -glucans (MLBG) (2.5 %), cellulose (9-11 %), protein (14-20 %), lignin (9 %), phenolic compounds (0.2-1.0 %), fat (3-4 %), vitamins and minerals (3-4 %), water and phytochemicals (flavonoids, alkylresorcinols) (Apprich et al., 2014; Marta S. Izydorczyk & Biliaderis, 1995; Rosa-Sibakov, Poutanen,

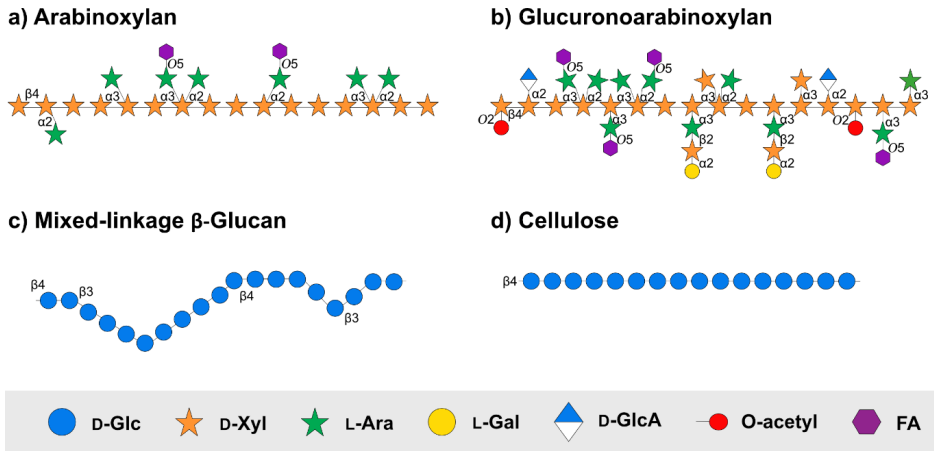
& Micard, 2015). Wheat bran is constituted by several different layers, namely the pericarp, testa, hyaline and aleurone (Hemery, Rouau, Lullien-Pellerin, Barron, & Abecassis, 2007). The inner and outer pericarp are rich in highly substituted AX, MLBG, cellulose, lignin and phenolic acids (Parker, Ng, & Waldron, 2005), the testa layer consists of lignin and the hyaline layer is rich in AX and phenolic compounds (Barron, Surget, & Rouau, 2007). The aleurone layer is made of less substituted AX, MLBG, phenolic compounds and proteins (Barron et al., 2007; Jerkovic et al., 2010; Rhodes & Stone, 2002).

The bran of corn accounts for 5 % of the kernel and contains AX (30-50 %), β -glucans (MLBG and cellulose) (15-20 %), protein (4-12 %), fat (2 %), lignin (0.7-2.6 %) and phenolic compounds (4 %) (Gáspár, Juhász, Szengyel, & Réczey, 2005; Gwirtz & Garcia-Casal, 2014; Huisman, Schols, & Voragen, 2000; D. J. Rose, Patterson, & Hamaker, 2010; L. Saulnier, Vigouroux, & Thibault, 1995).

2.2.1 Arabinoxylans

AX is found in the cell walls of cereal grains and other plants such as psyllium and bamboo (Cui, Wu, & Ding, 2013). In cereal grains, AX locates in the cell walls of the endosperm, the aleurone layer and mostly in the bran layers, where their abundance and structure show tissue-specific characteristics. The endosperm of wheat grain contains 2-4 % AX whereas the bran layers consist of 20-40 % AX (Barron et al., 2007). Among the different layers of wheat bran, the testa layer contains the highest AX content with 80-85 %. This is followed by the pericarp (50-75 %), aleurone (60-70 %) and hyaline (50-60 %) (Jerkovic et al., 2010; Parker et al., 2005). The total count of AX in corn bran is 30-50 % (Gáspár et al., 2005) however, the composition of individual corn bran layers has not been fully studied.

Structurally, AX is composed of a backbone of (1 \rightarrow 4) linked β -D-xylopyranosyl (Xylp) substituted by α -L-arabinofuranose (Araf) units at C(O)-2 and/or C(O)-3 positions. α -D-glucuronic acid (D-GlcA) or its 4-O-methyl derivative (4-O-MeGlcA) can be present at the C(O)-2 position of Xylp (Ebringerová, 2005; Huisman et al., 2000) (**Figure 1a**). AX of corn bran is substituted by D-GlcA or 4-O-MeGlcA to a higher extent, and therefore it can be named glucuroarabinoxylan (GAX). Corn bran AX has a highly complex structure, with oligomeric side chains composed of additional sugar units including xylose and galactose. The complexity of the corn bran AX is further increased by the ester-linked acetyl groups (**Figure 1b**).



e) Structure of cereal cell wall

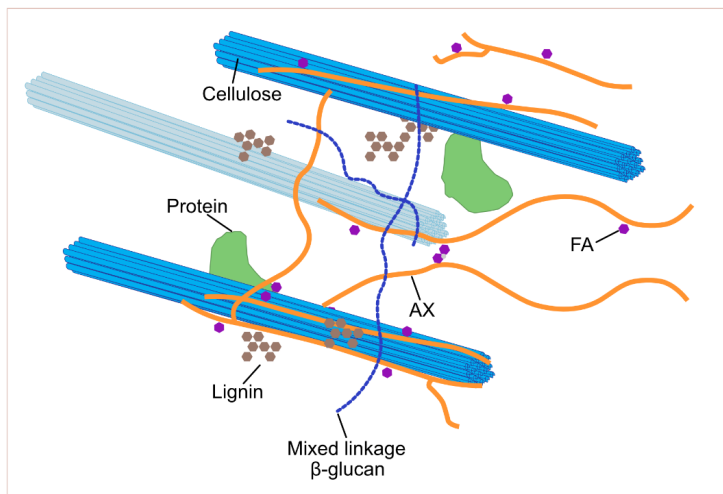


Figure 1. (a-d) Major polysaccharides of cereal bran, (e) Structural organization of cereal cell wall components.

The molecular weight (M_w) of AX varies depending on their plant origin as well as the extraction method. The M_w profiles of AX from cereal bran indicate very broad distributions that have been reported between 140 and 670 kDa (Aguedo, Fougnyes, Dermience, & Richel, 2014; Marta S. Izydorczyk & Biliaderis, 1995; Merali et al., 2015; Vinkx & Delcour, 1996; Y. Zhang et al., 2011). An important characteristic of AX in terms of its solubility and applications is the degree

of substitution (DS). DS of AX is usually expressed as A/X ratio inferring the proportion of Araf units to Xylp units, which varies between different plant tissues. In general, the A/X ratio of cereal grains increases from aleurone to the outer layers. The A/X ratio of AX from the wheat endosperm, aleurone and pericarp varies between 0.5-0.7, 0.3-0.4, and 0.8-1.1, respectively (Antoine et al., 2003; Gartaula, Dhital, Fleming, & Gidley, 2017; C. Maes & J. A. Delcour, 2002). Corn bran AX has relatively higher A/X compared to other cereal grains due to its highly substituted structure. Similar to wheat, AX from corn bran has more DS than that of the endosperm (Yadav, Johnston, Hotchkiss, & Hicks, 2007). Furthermore, the oligomeric side chains in corn bran AX increase its DS.

The most interesting feature of cereal AX is their phenolic acid substitutions, which are ester-linked to the arabinose moieties at the C(O)-5 position. The abundant phenolic compounds in cereal bran are ferulic acid (FA), sinapic acid and *para*-coumaric acid. FA is the most predominant phenolic acid in cereal grains, which can be found in monomeric, dimeric (dehydrodimers, di-FAs), or trimeric (dehydrotrimers, tri-FAs) forms. Wheat bran contains 0.2-1.7 % (of DW) phenolic acids, of which 90-95 % is FA (Rosa-Sibakov et al., 2015). The FA content of corn bran is notably higher than that of other cereal grains (3.3-4.0 % of DW) (Chateigner-Boutin et al., 2016; Schendel, Meyer, & Bunzel, 2015). The distribution of monomeric FA, di-FAs and tri-FAs in different bran layers may vary depending on the source. For example, monomeric FA in wheat bran is centered in the aleurone layer and the di-FAs are mostly localized in the outer pericarp (Barron et al., 2007; Parker et al., 2005).

FA is composed of a phenolic nucleus, on which methoxy and hydroxy substituents are present at positions 3 and 4, respectively (**Figure 2**). Its phenolic nucleus and unsaturated side chain allow it to easily form a resonance stabilized phenoxy radical by abstracting a hydrogen atom in the event of colliding with a reactive radical. This resonance stabilization of FA accounts for its antioxidant activity. Apart from its antioxidant activity, many studies have reported various therapeutic effects of FA such as anti-diabetic, anti-inflammatory and anti-aging actions (Srinivasan, Sudheer, & Menon, 2007).

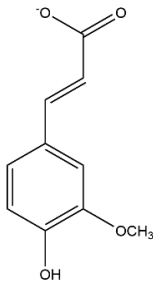


Figure 2. Chemical structure of ferulic acid.

2.2.2 Mixed linkage β -glucans and cellulose

MLBG is found in most cereal grains, foremost barley and oats are rich in MLBG. MLBG is concentrated in the endosperm and the aleurone layer of cereal grains (Fincher & Stone, 2004). Structurally, MLBG is made up of linear β -D-glucopyranosyl monomers linked by irregularly arranged (1 \rightarrow 3) and (1 \rightarrow 4) linkages (**Figure 1c**). MLBG has been shown to interact with AX strongly and spontaneously by hydrogen bonds, which occur between the unsubstituted regions of AX chains and β -(1 \rightarrow 4)-linked fragments of MLBG (M. S. Izydorczyk & MacGregor, 2000).

Cellulose is another component of the cereal cell wall, which may occur in a minor concentration in endosperm and aleurone but with a higher amount in the bran layers. Cellulose is a linear polysaccharide composed of (1 \rightarrow 4) linked β -D-glucopyranosyl (**Figure 1d**) that may reach 10 000-15 000 units. Cellulose exists in the form of microfibrils that are formed by parallel packing of the chains by hydrogen bonding, van der Waals forces and hydrophobic forces (Fincher & Stone, 2004). These microfibrils consist of both crystalline and amorphous regions. The association of cellulose microfibrils with AX and MLBG occurs through hydrogen bonding and non-specific surface interactions (Mikkelsen, Flanagan, Wilson, Bacic, & Gidley, 2015).

2.2.3 Proteins

Proteins constitute a considerable portion of the composition of cereal bran. The protein content of wheat bran and corn bran have been reported between 13.2-20.2 % (Apprich et al., 2014; Ruthes, Martínez-Abad, Tan, Bulone, & Vilaplana, 2017) and 4.8-12.0 % (D. J. Rose et al., 2010; Luc Saulnier, Marot, Chanliaud, & Thibault, 1995), respectively. Wheat bran proteins are prevalently localized in the aleurone layer and include structural, storage and defense-related proteins (Jerkovic et al., 2010), mostly albumins and globulins that consist of a greater amino

acid range compared to the endosperm proteins (Apprich et al., 2014; Rhodes & Stone, 2002). Corn bran proteins are richer in leucine amino acids as compared to the corn endosperm proteins (Kelzer et al., 2010). This substantiality of cereal bran proteins renders superior nutritional and functional properties and represent inexpensive and rich protein sources as potential ingredients of functional foods or special animal feed.

2.2.4 Lignin and other components

Lignin is an aromatic compound made up of several monolignols, mostly *p*-coumaryl alcohol, coniferyl alcohol and sinapyl alcohol. Lignin is one of the major components of woody plants contributing to the woody characteristics of the cell wall and may also be found in the outer pericarp layers of cereal tissues to a lesser extent (Antoine et al., 2003; Fincher & Stone, 2004). The lignin content of wheat bran and corn bran is 5.6-9.0 % (Rosa-Sibakov et al., 2015; Ruthes et al., 2017) and about 2.6 % (D. J. Rose et al., 2010), respectively.

Nutritionally, vitamins and minerals are also important components of the outer layers of cereal grains. Wheat bran contains almost all B-group vitamins (1.0-4.5 mg/100 g) and vitamin E (0.1-9.5 mg/100 g) (Onipe, Jideani, & Beswa, 2015). Wheat bran minerals include phosphorus, magnesium, zinc, iron manganese and copper (1.4-2.5 g/100 g), which may promote health benefits. However, most of these minerals are present as complexes with phytic acid, an anti-nutrient that is found with high amounts in wheat bran (3.1-5.8 % of DW). Therefore, the bioavailability of wheat bran minerals is considered to be low (Stevenson, Phillips, O'Sullivan, & Walton, 2012). Similarly, corn bran is rich in B-group vitamins (8.0 mg/100 g). The mineral content of corn bran is richer with calcium, iron, magnesium, phosphorus, potassium, sodium, zinc, copper, manganese and selenium (234.0 mg/100 g). The bioavailability of corn bran minerals is also higher as more than 80 % of phytic acid is concentrated in the germ of the corn grain (Zitterman, 2003).

2.2.5 Cell wall recalcitrance

The abovementioned components are placed in an entangled structure in the cell wall (**Figure 1e**) and associated with each other through intra- and intermolecular interactions. AX and MLBG interact with cellulose through extensive hydrogen bonding or non-specific surface interactions (Ebringerová & Heinze, 2000; Mikkelsen et al., 2015). Proteins not only covalently link to each other through tyrosine-tyrosine bridges (Rhodes & Stone, 2002) but also form covalent bridges between their tyrosine units and the phenolic acid substitutions of the AX

(Ebringerová, Hromádková, & Berth, 1994; Piber & Koehler, 2005). Furthermore, FA moieties dimerize and crosslink adjacent AX (Marta S. Izydorczyk & Biliaderis, 1995) and lignin (Kenji Iiyama, Lam, & Stone, 1990). Lignin plays an important role in the recalcitrance of the cereal cell wall as it is covalently linked to polysaccharides by ester and ether linkages. FA, both in monomeric and dimeric form, acts as a bridging unit between polysaccharides and lignin through ether linkages (Ebringerová & Heinze, 2000; K. Iiyama, Lam, & Stone, 1994). From a technological point of view, the localization of the cell wall components of cereals and interactions are of great importance as they affect the industrial processing of cereal grains and the isolation of individual components.

2.3 EXTRACTION OF ARABINOXYLANS AND CHALLENGES

To exploit the antioxidant and prebiotic properties of AXs and to use them as feedstock for nutritional and material applications, they have to be isolated from other cell wall components. However, the extraction of AX from cereal bran is challenging due to the supramolecular interactions in the cell wall and the highly cross-linked structure of the cell wall. The extraction of AX is restricted by the presence of covalent and non-covalent linkages between cell wall components, hence they cannot be extracted using water alone and requires more rigorous and usually multi-staged treatments. Extraction of AX from cereal by-products is typically achieved by acidic (Xu et al., 2006), neutral (C. Maes & J. Delcour, 2002) or alkaline (Doner, Chau, Fishman, & Hicks, 1998; Ragaee et al., 2008; Y. Zhang et al., 2011) solvents, mechanical-chemical techniques (i.e. ultrasound, microwave, extrusion) (Hollmann, Elbegzaya, Pawelzik, & Lindhauer, 2009; Devin J. Rose & Inglett, 2010; Zeitoun, Pontalier, Marechal, & Rigal, 2010), or enzyme-aided treatments (Figuerola-Espinoza, Poulsen, Borch Soe, Zargahi, & Rouau, 2004; Swennen, Courtin, Lindemans, & Delcour, 2006; Zhou et al., 2010).

Alkaline extraction is the most common technique used to extract AX with high efficiency from cereal biomass. Monovalent hydroxides such as sodium hydroxide (NaOH) (Thuvander, Arkell, & Jönsson, 2014) and divalent hydroxides such as calcium hydroxide (Ca(OH)₂) (Schooneveld-Bergmans, Hopman, Beldman, & Voragen, 1998) or barium hydroxide (Ba(OH)₂) (Nilsson, 1996) are usually employed for the alkaline extraction of AX. The hydroxyl ions of alkaline solvents break the hydrogen bonds and disrupt the ester linkages between cell wall components within the network. Alkaline conditions may cause the release of some other polysaccharides

and lignin, interfering with the AX extraction (Egues et al., 2014). Besides, the disruption of ester linkages between AX and phenolic acids results in the loss of valuable moieties such as FA.

The use of water for the extraction of AX has drawn interest as an abundant, inexpensive and environmentally friendly solvent. The properties of water need to be manipulated by means of high temperature and high pressure to make it capable of penetrating the recalcitrant structure of the cereal cell wall and extracting AX. Water in subcritical conditions is defined as liquid water that does not exceed the critical temperature (374 °C) and/or pressure (22.1 MPa) (Rabemanolontsoa & Saka, 2016) and represents an efficient means for the extraction of AX. In the subcritical state, the hydrolytic degradation capacity of water increases due to its ionic products and thus fractionation of the biomass can be achieved (Cocero et al., 2018). The most favorable feature of subcritical water extraction (SWE) is the preservation of phenolic substitutions of AX together with the polymeric structure (Rudjito, Ruthes, Jiménez-Quero, & Vilaplana, 2019; Ruthes et al., 2017).

2.4 FUNCTIONALITY AND UTILIZATION OF ARABINOXYLANS

AX, as an abundant constituent of cereal tissues, exerts many potential health benefits. Numerous studies have shown the antioxidant activity of cereal AX originating from their phenolic acid content (Adom & Liu, 2002; Fabiola E. Ayala-Soto, Serna-Saldívar, García-Lara, & Pérez-Carrillo, 2014; Hromadkova, Paulsen, Polovka, Kostalova, & Ebringerova, 2013; Verma, Hucl, & Chibbar, 2009). Under oxidative conditions, FA undergoes radical chain reaction and confer radical scavenging activity, hence provides an exceptional functionality to cereal AX. Feruloylated AX (F-AX), therefore, represents a valuable source for the development of multifunctional materials such as films or hydrogels.

Another potential application area of AX is its use in nutritional supplements. As a part of the dietary fiber content of cereals, AX also exerts potential beneficial effects on human health. The non-digestible AX oligosaccharides may alter the activity of the microbial flora in the gut by affecting their enzymatic activity and enhance the end products of the bacterial metabolism. The prebiotic effect of the xylooligosaccharides of cereal AX is well-accepted as many studies have shown their stimulating effect on the growth and/or activity of potentially health-promoting bacteria in the colon (Gong et al., 2019; Rogowski et al., 2015; D. J. Rose et al., 2010; Rumpagaporn et al., 2015).

2.4.1 Modification tools of arabinoxylans

The utilization of AX as ingredients or building blocks for novel products can be expanded by several modification strategies thanks to their chemical structure. The reactive hydroxyl groups of AX in each repeating unit make them suitable for chemical and enzymatic modification. Chemical modification has been studied to introduce new functional groups and new properties to cereal AX, such as altered solubility or thermoplasticity. Chemical or enzymatic covalent cross-linking is another modification approach to establish functional derivatives of AX and to broaden their application area.

2.4.1.1 Esterification

Among different chemical reactions, esterification has been the most common reaction applied for the modification of AX (e.g. acetate, propionate or laurate esters) (Buchanan et al., 2003; Stepan, Höije, Schols, de Waard, & Gatenholm, 2012). Esterification of acetyl groups (acetylation) is based on the replacement of the hydroxyl groups of AX by acetate groups (**Figure 3**), with the principal aim of increasing the degree of acetylation (DA) and hence, improving the hydrophobicity of AX. DA indicates the average number of substituted hydroxyl groups of AX and a fully acetylated AX has a DA of 2.0 as each unsubstituted xylose and arabinose contains two free hydroxyl groups. Generally, acetylation of xylans improves their thermal stability and solubility in organic solvents and the DA substantially determines the characteristics of the acetylated AX (Egues et al., 2014; Morais de Carvalho et al., 2019; Xueqin Zhang, Zhang, Liu, & Ren, 2016). Acetylation of AX can be carried out in different reaction media, such as N,N-dimethylformamide/lithium chloride (Fang, Sun, Fowler, Tomkinson, & Hill, 1999) or formamide/pyridine (Egues et al., 2014), but the main acetylating agent used remains acetic anhydride. Recently, dimethyl sulfoxide (DMSO) in combination with *N*-methylimidazole (NMI) as a catalyst has been explored as a potent reaction medium for the derivatization of xylan-type hemicelluloses under relatively mild conditions at room temperature (Xueqin Zhang et al., 2016).

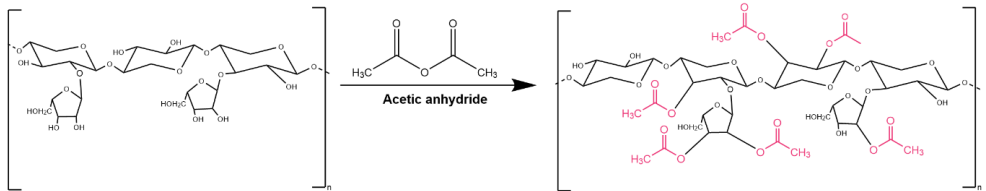


Figure 3. Acetylation reaction of AX with acetic anhydride and potential acetylated groups.

2.4.1.2 Etherification and oxidation

Etherification is another common modification strategy for AXs to improve their hydrophobicity and thermoplasticity by replacing the hydroxyl groups with alkoxy moieties. Among different etherification tools, AX have been etherified by methylation (Nylander, Svensson, Josefson, Larsson, & Westman, 2019), carboxymethylation (Velkova et al., 2015) and butyl glycidyl etherification (P. K. Deralia et al., 2021). Recently oxidation has been applied to modify AXs (Borjesson, Larsson, Westman, & Strom, 2018), which has been further combined with etherification (Borjesson, Westman, Larsson, & Strom, 2019; Parveen Kumar Deralia et al., 2021).

2.4.1.3 Covalent cross-linking

As another modification tool, covalent crosslinking of AX is accomplished using chemical agents or enzymes. The enzymatic crosslinking potential is a feature of cereal AX arising from the dimerization mechanism of FA under oxidative conditions. F-AX solutions are capable of forming hydrogels in a system containing a free radical-generating agent and an oxidative enzyme such as O_2 /laccase or hydrogen peroxide (H_2O_2)/peroxidase (Nino-Medina et al., 2010) (**Figure 4**). When oxidatively crosslinked, FA dimerizes into five main dimers, namely 5-5', 8-5', 8-O-4', 8-8' and 8-5' benzofuran di-FAs (Carvajal-Millan, Landillon, et al., 2005; Ng, Greenshields, & Waldron, 1997), which are also found in the cell wall (Buanafina, 2009) (**Figure 5**). Furthermore, some studies have identified the 4-O-8', 5-5'' trimer of FA in small amounts in crosslinked AX (Carvajal-Millan, Guigliarelli, Belle, Rouau, & Micard, 2005; Marquez-Escalante et al., 2018).

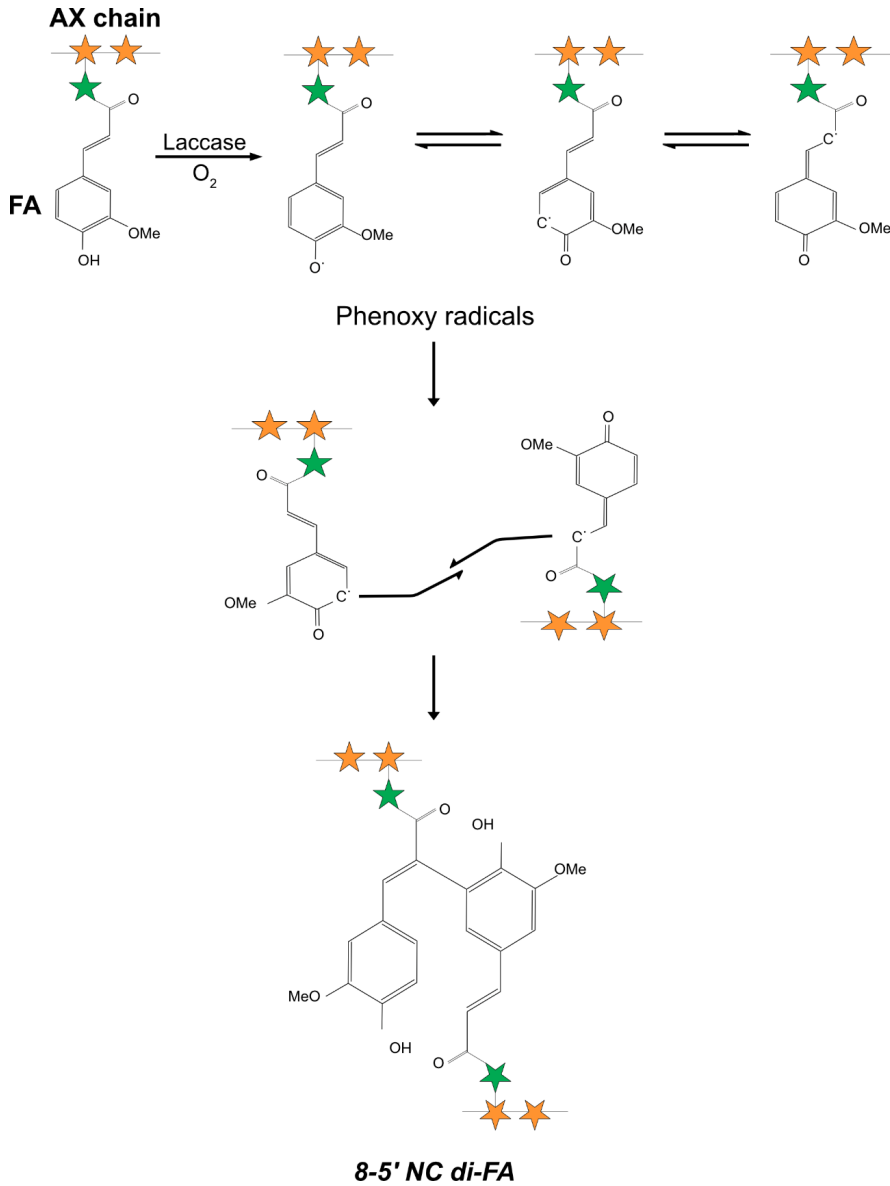


Figure 4. Covalent coupling of feruloylated arabinoxylan chains by O_2 /laccase or hydrogen peroxide (H_2O_2)/peroxidase.

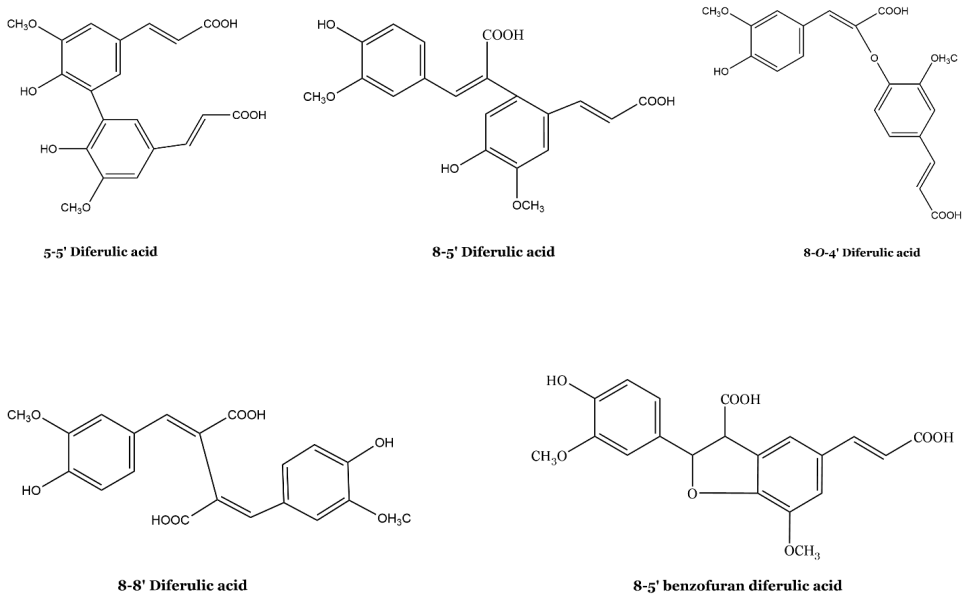


Figure 5. Dehydrodimers of ferulic acid.

2.4.2 Material applications of arabinoxylans

The abovementioned functional properties of AX, together with their polymeric structure and renewability, make them excellent resources for materials to replace fossil-based materials and contribute to a circular bio-based economy as the underutilized side streams of cereal processing are used. In this direction, film and gel preparations have been the most studied applications of AX, which targeted various uses in the food and biomedical fields. (Mendez-Encinas, Carvajal-Millan, Rascon-Chu, Astiazaran-Garcia, & Valencia-Rivera, 2018; Mikkonen & Tenkanen, 2012).

2.4.2.1 Films from arabinoxylans

The film-forming properties of AX are essentially determined by their molecular structure, which includes the A/X ratio, substitution pattern and molar mass. The A_{raf} substitution is the key factor that influences the solubility of AX in water, ultimately affecting the film properties. Many studies have shown that AX with a higher A/X ratio form more stable films in terms of mechanical and thermal properties (S. L. Heikkinen et al., 2013; Hoije, Sternemalm, Heikkinen,

Tenkanen, & Gatenholm, 2008; Sternemalm, Hoije, & Gatenholm, 2008). The lack of Araf substitutions promotes the unsubstituted Xylp units to interact with each other and hence, results in the formation of insoluble aggregates in an aqueous solution. These, in turn, may act as stress concentration points in AX films and lead to weak mechanical properties. On the other hand, a higher Araf substitution may bind more water that acts as a plasticizer in a film, yielding less brittle films but negatively affecting the water and oxygen barrier properties of the films. Film properties are also affected by the molar mass of AX, whereby higher molar masses have been correlated with good film properties (Susanna L. Heikkinen et al., 2014).

AX-based films are especially of interest due to their excellent oxygen barrier properties. The oxygen permeability (OP) values of AX films from different cereal sources have been reported between $0.2\text{-}0.9\text{ cm}^3\text{ }\mu\text{m m}^{-2}\text{ day}^{-1}\text{ kPa}^{-1}$ (Gröndahl & Gatenholm, 2007; Hoije et al., 2008; Mikkonen et al., 2009; Sárossy, Tenkanen, Pitkänen, Bjerre, & Plackett, 2013). These values are in the same range as the OP values of the synthetic polymer ethylene vinyl alcohol (EVOH) ($0.01\text{-}0.98\text{ cm}^3\text{ }\mu\text{m}^2\text{ day kPa}$) (McKeen, 2017), which is often used in packaging applications as a good oxygen barrier.

A challenge of AX, in terms of film applications, is the abundance of hydroxyl groups in their structure, which may cause moisture sensitivity. The moisture barrier properties of films are usually expressed in terms of water vapor permeability (WVP). The WVP of cereal AX films varies between $2.5\text{ and }21.0\text{ g mm m}^{-2}\text{ day}^{-1}\text{ kPa}^{-1}$ (Susanna L. Heikkinen et al., 2014; Sarossy et al., 2012; Sárossy et al., 2013; P. Zhang & Whistler, 2004), depending on the AX source and plasticization.

Mechanical properties of AX films are important as they indicate their integrity and durability over a time period and hence, their applicability in certain applications. Among many defined mechanical properties of polymeric materials, tensile properties, i.e. tensile strength, Young's modulus, elongation at yield and break, are the most commonly considered and measured. The tensile strength, elongation at break and Young's modulus values of films from cereal AX have been reported between $15\text{-}60\text{ MPa}$, $2\text{-}7\%$ and $550\text{-}2930\text{ MPa}$, respectively (Borjesson et al., 2019; Egues et al., 2014; Höije, Gröndahl, Tømmeraaas, & Gatenholm, 2005; Sárossy et al., 2013; Stevanic et al., 2011; Stoklosa, Latona, Bonnaillie, & Yadav, 2019). AX films have been recognized in many studies to show high brittleness due to their chain stiffness and low Mw, therefore plasticization has been a common tool to improve their mechanical performance.

Glycerol, sorbitol and propylene glycol have been used for the plasticization of the films of cereal AX (Anderson & Simsek, 2019; S. Heikkinen et al., 2016; Susanna L. Heikkinen et al., 2014; Mikkonen et al., 2009; P. Zhang & Whistler, 2004). Mikkonen et al. (2009) have reported that the mechanical properties of AX films change depending on the concentration of glycerol and sorbitol in film preparations. Accordingly, when glycerol was used at 10 % (w/w) the tensile strength and stiffness of AX films was higher than those plasticized with the same amount of sorbitol, whereas 40 % plasticized content resulted in opposite findings (Mikkonen et al., 2009). Plasticization has been reported to affect not only the mechanical and thermal properties but also the water vapor and gas permeability of AX films. Several studies have shown that sorbitol has a reducing effect on the WVP due to less plasticization compared to glycerol and propylene glycol (Susanna L. Heikkinen et al., 2014; Mikkonen et al., 2009; P. Zhang & Whistler, 2004). The mentioned studies have also revealed that the oxygen permeability of AX films is not significantly affected by the presence or the type of plasticizer. Several other means have been suggested to improve the mechanical strength and permeability properties of AX films, including blending with lipids (Peroval, Debeaufort, Despre, & Voilley, 2002), reinforcement with other natural polymers such as cellulose (Saxena, Elder, Pan, & Ragauskas, 2009; Stevanic et al., 2011) or inorganic compounds (Sarossy et al., 2012), and crosslinking (Azeredo et al., 2015; Pereira et al., 2017).

Films from cereal AX confer functional properties due to their feruloylation that enables developing materials bearing antioxidant activity. This offers an advantage to avoid additional functionalization treatments of films such as the external addition of natural compounds to develop bioactive materials (Silva-Weiss, Ihl, Sobral, Gomez-Guillen, & Bifani, 2013). In addition to their antioxidant activity, the feruloylation of AX has recently been shown to administer antimicrobial and UV barrier properties to their films (Moreirinha et al., 2020).

2.4.2.2 Hydrogels from arabinoxylans

Hydrogels are three-dimensional polymeric materials, which have water absorption capacity that may reach up to thousands of times their dry weight. The integrity of hydrogels is governed by molecular interactions, secondary forces (i.e. ionic, hydrogen bonding and hydrophobic forces) and covalent crosslinks (Hoffman, 2012). Covalent crosslinking using oxidative enzymes, e.g. laccase or peroxidase, has been the main method to develop hydrogels from F-AX. Hydrogen bonding has been reported to play an additional role in the stability of enzymatically

crosslinked AX hydrogels (Carvajal-Millan, Guilbert, Morel, & Micard, 2005; Vansteenkiste, Babot, Rouau, & Micard, 2004; Xiaowei Zhang et al., 2019).

The morphology of AX hydrogels has been characterized by a porous and heterogeneous structure, usually with a honeycomb-like shape (Iravani, Fitchett, & Georget, 2011; Marquez-Escalante et al., 2018; Wang et al., 2019).

Rheological measurements are used to monitor the gelation ability of AX and the mechanical spectra of their gels. Viscosity measurements of AX hydrogels have shown that the apparent viscosity of AX hydrogels, as well as AX solutions, is concentration and shear rate dependent (M. S. Izydorczyk & Biliaderis, 2007; Wang et al., 2019; Xiaowei Zhang et al., 2019). Viscoelastic properties of AX hydrogels are usually studied by small amplitude oscillatory shear rheology. Studies have shown that the enzymatically crosslinked AX hydrogels exhibit strong gel characteristics where the storage modulus (G') is independent of frequency and greater than the loss modulus (G'') (Carvajal-Millan, Guigliarelli, et al., 2005; Kale, Hamaker, & Campanella, 2013; Marquez-Escalante et al., 2018; Vansteenkiste et al., 2004; Xiaowei Zhang et al., 2019). On the other hand, the rheological properties of AX hydrogels show a significant dependency on the FA content of AX, A/X ratio and concentration.

FA substitutions of AX are the junction points for the enzymatic crosslinking to occur, therefore the gelation ability and the rheological properties of AX hydrogels are largely related to the FA content. Many studies have reported that higher FA content led to the formation of stronger hydrogels (F. E. Ayala-Soto, Serna-Saldivar, Perez-Carrillo, & Garcia-Lara, 2014; F. E. Ayala-Soto, Serna-Saldivar, & Welte-Chanes, 2016; Carvajal-Millan, Guilbert, et al., 2005; Xiaowei Zhang et al., 2019). Kale et al. (2013) have shown that a 3-times higher FA content resulted in a 10-20-fold increase in the G' of a corn bran AX hydrogel (Kale et al., 2013).

A/X ratio may be another factor affecting the rheological properties of AX hydrogels. Marquez-Escalante et al. (2018) have shown that when the A/X ratio of wheat AX decreased from 0.68 to 0.51, the G' of its hydrogels increased by 60 Pa, which was due to the facilitated interaction between AX chains leading to the formation of di-FAs and tri-FAs (Marquez-Escalante et al., 2018).

The AX concentration also influences the properties of their hydrogels. Beyond a simple increase in the viscosity, an increase in the AX concentration has been reported to significantly

increase the G' and G'' of the hydrogels, independently from the FA content (Carvajal-Millan, Guilbert, et al., 2005; Martinez-Lopez et al., 2016).

Furthermore, the use of enzymes of different types (i.e. laccase or peroxidase) and different origin (e.g. laccase from *Myceliophthora thermophila* or *Pleurotus ostreatus*) has been shown to influence the gel characteristics (Martinez-Lopez et al., 2019; Munk et al., 2020).

In the past two decades, great research efforts have been focused on the development of hydrogels from F-AX to use in food and biomedical applications. Xylans are accepted as promising substrates for hydrogel applications owing to their intrinsic properties such as hydrophilicity, biodegradability and biocompatibility. Furthermore, reactive hydroxyl groups of xylans render them available for enzymatic (Parikka et al., 2010) and chemical (Gabrielii & Gatenholm, 1998; Kuzmenko, Hagg, Toriz, & Gatenholm, 2014) modifications. The hydrogels derived from corn and wheat AX have been successfully applied in various studies including encapsulation of biomolecules and pharmaceuticals, drug delivery and stabilization of blood glucose response (Iravani et al., 2011; Vansteenkiste et al., 2004; Vogel, Gallaher, & Bunzel, 2012). On the other hand, the use of xylan hydrogels as biological scaffolds for cell applications is still limited as these hydrogels are usually mechanically weak (Calvert, 2009). Consequently, the use of xylan hydrogels in such studies remains limited to their chemically modified forms (Kong et al., 2017). Hence, exploring alternative ways to produce strong hydrogel networks from native AX could open new possibilities for the design of biological scaffolds.

3 EXPERIMENTAL

3.1 MATERIALS AND CHEMICALS

3.1.1 Wheat bran

Fine granulometry wheat bran (WB) with 0.1 mm particle size was kindly provided by Lantmännen (Stockholm, Sweden) and stored in dark until use (used in the AX extraction, Paper I, II and III).

3.1.2 Corn bran

Corn bran was kindly provided by Cargill Deutschland GmbH (Krefeld, Germany) and stored in the dark until use (Paper IV).

3.1.3 Wheat endosperm arabinoxylan (WAX)

The arabinoxylan from wheat endosperm was purchased from Megazyme (Wicklow, Ireland) and used as a reference material in Paper II (Megazyme, Lot 160419b).

3.1.3 Chemicals and kits

Tap water was used for all the extractions. Total starch assay kit was purchased from Megazyme (Wicklow, Ireland). Dye reagent for the Bradford protein assay was purchased from Bio-Rad Laboratories (Sweden). The 5-5' and 8-8' dehydrodimers of ferulic acid were gifted by Prof. Florent Allais and Amandine Léa Flourat (AgroParisTech, Pomacle, France). The cellular ROS assay kit was purchased from Abcam B.V. (Amsterdam, Netherlands). Dialysis membranes were purchased from Spectrumlabs (Breda, Netherlands). All other chemicals, reagents and enzymes were purchased from Sigma-Aldrich (Stockholm, Sweden).

3.2 ARABINOXYLAN EXTRACTION (Paper I, II, III, IV)

Subcritical Water Extraction (SWE) of AX from wheat bran and corn bran was performed after a destarching step as pretreatment. Two different scales of SWE were used for the isolation of F-AX from destarched bran: laboratory scale and pilot scale. Alkaline extraction was employed for the extraction of AX without FA substitution and used for comparison with the F-AX.

3.2.1 Destarching of wheat and corn bran (Paper I-IV)

Starch present in cereal bran originates from the endosperm that adheres to the bran layers during the milling process (Apprich et al., 2014), and influences the yield of extraction and purity of AX. Therefore, both wheat and corn bran were pretreated before the AX extraction to remove starch from the starting biomass. Untreated wheat bran (WB) and low protein wheat bran (LP) were pretreated by porcine α -amylase to remove starch after gelatinization. The bran was gelatinized in 50 mM sodium phosphate buffer at pH 7.0 (1:10, w/v) for 8 min at 90 °C. α -amylase (16 U/mg starch) was then added to the mixture after equilibrating at 37 °C. The slurry was incubated at 37 °C for an initial 5 h and then the second dose of α -amylase was added followed by overnight incubation. Destarched bran was centrifuged (11,325 g, 30 min, 4 °C) and washed twice with cold ethanol (95 %) to recover the destarched wheat bran (DWB and DLP).

Corn bran was destarched by suspending in hot water at 80 °C for 4 h followed by filtration through a 25 μ m sieve and manual pressing of the solid residue.

3.2.2 Laboratory scale subcritical water extraction (Paper I)

The laboratory-scale extraction of F-AX from DWB was carried out using an accelerated solvent extractor (ASE) at 160 °C and 180 °C that applies 10-11 MPa pressure (Ruthes et al., 2017). In short, DWB was placed in extraction cells and four sequential cycles of extractions were applied to the same cell (5, 15, 30 and 60 min). The extracted fractions and resulting insoluble residues were freeze-dried and stored at room temperature until analysis. The yields of the extraction were determined gravimetrically.

3.2.3 Pilot scale subcritical water extraction (Paper II-IV)

The pilot scale extraction of F-AX from wheat bran was performed using a rotary autoclave submerged in polyethylene glycol (PEG). In short, wheat bran was suspended in tap water in autoclave vessels (1:10 w/v) that were then placed in the rotary apparatus. The extraction was performed at 160 °C for 30 min after a temperature ramp for 10 min. The resulting slurry was filtered, the filtrate was precipitated with 95 % ethanol (1:4, v/v) at 4 °C overnight and centrifuged (11,325 g, 15 min, 4 °C) to purify the extracted F-AX. The recovered fraction was resuspended in water and freeze-dried.

The pilot scale extraction of F-AX from corn bran was carried out in the pilot plant by Celabor (Chaineux, Belgium). The destarched corn bran cake was mixed with tap water (~1:15) and the

extraction was performed at 160 °C for four sequences (10, 30, 60 and 90 min). All the time fractions were combined and then freeze-dried to give the corn bran AX (CAX) used in Paper IV. The yields of the extractions were determined gravimetrically.

3.2.4 Alkaline extraction (Paper II)

For the alkaline extraction of AX, destarched wheat bran was suspended in 0.5 M NaOH (1:8, w/v) and incubated at 80 °C for 16 h under constant stirring. The resulting slurry was centrifuged (11,325 g, 30 min, 4 °C) and dialyzed for 72 h through a 20 kDa MWCO dialysis membrane. The recovered extract (NAX) was then freeze-dried and stored at room temperature until further use.

3.3 ACETYLATION OF ARABINOXYLANS (Paper II)

The acetylation of AX from the pilot scale subcritical water extraction (F-AX), alkaline extraction (NAX) and wheat endosperm (WAX) was performed by the per-*O*-acetylation method (Xueqin Zhang et al., 2016). In short, AXs were mixed with DMSO and *N*-methylimidazole (NMI) (22:2:1) at 100 °C for 5 h followed by cooling down to room temperature and further mixing for 19 h. As the acetylating agent, acetic anhydride (Aa) (0.99:1 Aa/AX) was added to the mixture and the reaction was allowed for 24 h at room temperature. The acetylated AXs were then purified by precipitation for 24 h using cold ethanol (80 %) at 4 °C. The purified fractions were recovered by centrifugation and then freeze-dried. Second acetylation was done on the freeze-dried fractions following the same protocol to improve the efficiency of the acetylation. The acetylation of FAX, NAX and WAX resulted in AcFAX, AcNAX and AcWAX, respectively.

3.4 FILM FORMATION (Paper II)

All films from the native and acetylated AX were produced by the solvent casting method.

3.4.1 Native arabinoxylan films

Films from the native AX were first prepared without plasticization. In short, FAX, NAX and WAX were suspended in distilled water (10 g/L) and mixed for 3 h at 50 °C. The film suspensions were then ultrasonicated for 5 min to remove air bubbles and then casted on Teflon plates followed by drying at 30 °C. However, the FAX film showed poor film-forming ability therefore plasticization by sorbitol was used for all the native AX. 30 % (w/w of AX) sorbitol was

mixed with the film suspensions that were then casted and dried as described above. The sorbitol plasticization yielded FAXSor, NAXSor and WAXSor films. Here, two more films were prepared with the external incorporation of FA into WAX. Pure FA was mixed with WAX (8 mg/g) corresponding to the content of covalently bound FA in FAX. The solutions were casted with and without sorbitol plasticization and dried as described above resulting in WAX+FA and WAXSor+FA films, respectively.

3.4.2 Acetylated arabinoxylan films

The films from AcFAX, AcNAX and AcWAX were also prepared with and without plasticization. However, these samples did not form continuous films without plasticization therefore only plasticized films of AcFAX, AcNAX and AcWAX were included in this work. Briefly, the acetylated AXs were suspended in acetylacetone as a nonpolar solvent (10 g/L) and then mixed with 30 % (v/w) triacetin as a nonpolar plasticizer. The solution casting was performed as described above.

3.5 PREPARATION OF HYDROGELS (Paper III, IV)

The preparation of hydrogels from AX extracted from wheat bran and corn bran was carried out by enzymatic crosslinking using laccase and horseradish peroxidase (HRP). Laccase crosslinking was performed for both wheat bran AX (FAX) and corn bran AX (CAX), while HRP crosslinking was only applied for CAX.

The laccase crosslinking of FAX included two different procedures. In the first procedure, FAX was solubilized in ultrapure water at 5 % (w/v) and then mixed with laccase from *Trametes versicolor* (0.1 U/mg AX). The reaction was allowed for 24 h at 30 °C with constant stirring, resulting in FAX-CL hydrogel. Here, O₂ in the air acted as the free radical generating agent. In the second procedure, the same crosslinking steps were followed by freeze-drying of FAX-CL. The freeze-dried fractions were then resuspended in citrate phosphate buffer at pH 2.0, 5.0 and 7.0. This process was called the regeneration of the hydrogels and resulted in FAX-CL-pH2, FAX-CL-pH5, and FAX-CL-pH7, respectively.

The laccase crosslinking of CAX was performed as described above using the same AX concentration (5 %) without including the regeneration, resulting in CAX-L hydrogel. The HRP crosslinking was performed by mixing the CAX solution with HRP solution at 0.03 U/mg AX. 30 % H₂O₂ (33 µL/mL CAX solution) was then added to the mixture as the free radical

generating agent. The HRP crosslinked hydrogel was formed instantly and named CAX-H hydrogel.

3.6 INSTRUMENTATION AND CHARACTERIZATION

3.6.1 Determination of starch content

The efficiency of the destarching was determined by measuring the starch content before and after the enzymatic pretreatment. The starch content was measured using the total starch assay kit by Megazyme (Wicklow, Ireland) (Paper I and II).

3.6.2. Determination of protein content

Proteins are another big constituent of cereal bran, which may affect the composition of the extracted fractions (Paper I), thus it is important to determine the protein content of the starting biomass as well as the resulting extracts. The protein content of the starting wheat bran was provided by the supplier as 14 %. The protein content of the low protein wheat bran and the destarched brans (DWB and DLP, Paper I) as well as the residues of the laboratory scale extraction (Paper I) was determined by the Dumas combustion method (AACC, 2003). The soluble protein content of the extracted fractions (Paper I and II) was measured by the Bradford assay (Bradford, 1976).

3.6.3 Radical scavenging activity

The radical scavenging activity of the extracted AX (Paper I and II) and the films produced from AX (Paper II) was determined according to the method of Brand-Williams, Cuvelier, and Berset (1995) with minor modifications. In short, 100 μM methanolic solution of 1,1-diphenyl-2-picrylhydrazyl (DPPH) radical was mixed with different concentrations of the aqueous solutions (3 – 6 mg/mL) of the extracts or films. The reactions were allowed for 30 min at room temperature in the dark and the resulting absorbances were recorded using a microplate reader (Clariostar Plus, BMG LABTECH, Ortenberg, Germany). The radical scavenging activity was expressed as half-maximal effective concentration (EC_{50}). A more detailed description of the DPPH assay is available in Paper I and II.

3.6.4 High-performance Anion Exchange Chromatography with Pulsed Amperometric Detection (HPAEC-PAD)

The monosaccharide composition of the starting brans, the reference wheat endosperm AX, and the AX fractions obtained after SWE, alkaline extraction and acetylation was analyzed by HPAEC-PAD. As these fractions were in the polymeric structure, hydrolysis was needed to be performed to degrade these to monomeric sugars. Different acidic hydrolysis methods can be used for the degradation of polysaccharides, which involve the use of sulfuric acid, trifluoroacetic acid (TFA) and two-step methanolysis. By sulfuric hydrolysis complex polysaccharides, including crystalline cellulose, can be hydrolyzed (Saeman, Moore, Mitchell, & Millett, 1954). Therefore, it was used to determine the monosaccharide composition of the starting brans (Paper I) in this work. However, sulfuric hydrolysis causes the degradation of uronic acids therefore TFA hydrolysis (Paper I) and two-step methanolysis (Paper II and IV) were used for the extracted and acetylated AX (Albersheim, Nevins, English, & Karr, 1967; Appeldoorn, Kabel, Van Eylen, Gruppen, & Schols, 2010).

The HPAEC-PAD system (Dionex ICS 3000, Sunnyvale, CA, USA) was equipped with a CarboPac PA1 (4 × 250 mm) column maintained at 30 °C with a flow rate of 1 mL min⁻¹. Monosaccharides were quantified using the calibration performed with neutral sugars and uronic acid standards (0.005-0.1 g/L).

3.6.5 High-Performance Liquid Chromatography (HPLC)

In this work, HPLC was used to determine the phenolic acid content and the degree of acetylation (DA) of AX.

The phenolic acid content was determined after saponification of the samples with NaOH (2 M) and extraction with ethyl acetate (Paper I-IV). The analysis was performed using an HPLC system (Waters 2695 separation module, Waters 2996 photodiode array detector) coupled to a UV/Vis detector and equipped with an SB-C18 separation column (Zorbax SB-C18 5 µm particle size, 4.6 × 250 mm, Agilent, Santa Clara, CA, USA) with a gradient of 2 % acetic acid and absolute methanol as the mobile phase (Szydłowska-Czerniak, Trokowski, & Szlyk, 2011). The phenolic acid content was calculated based on the standard calibration with caffeic, *p*-coumaric, ferulic, sinapic and cinnamic acid, and 5-5' and 8-8' di-FAs.

The DA was determined after saponification with NaOH (0.8 M) (Bi, Berglund, Vilaplana, McKee, & Henriksson, 2016) using an Ultimate-3000 HPLC system (Dionex, Sunnyvale, CA, USA) coupled to a UV/Vis detector (210 nm) and equipped with a Phenomenex Rezex ROA-Organic acid column (300 × 7.8 mm, Phenomenex, Torrance, CA, USA) with sulfuric acid (2.5 mM) as the mobile phase (Paper II). The DA was calculated based on the concentration of AX in the samples and the measured acetic acid concentration.

3.6.6 Size Exclusion Chromatography (SEC)

The size distribution of AX was determined by SEC (SECcurity 1260, Polymer Standard Services, Mainz, Germany) equipped with a GRAM pre-column, 100 Å and 10,000 Å analytical columns (Polymer Standard Services, Mainz, Germany) with DMSO + 0.5 % LiBr as the mobile phase. Detection was performed by refractive index (RI) detector to obtain the apparent molar mass distribution of AX (Paper I and II) using pullulan with a molecular weight of 342 to 708,000 Da as a standard. For the crosslinked samples (Paper III and IV), multi-angle laser light scattering (MALLS) detection was used to obtain the absolute molecular weight of the polysaccharides. In the case of MALLS detection, pullulan standards were used to relate the elution volume (V_{el}) to the hydrodynamic radius (R_h) using the Mark-Houwink equation (Vilaplana & Gilbert, 2010). The Mark-Houwink parameters for pullulan in DMSO-LiBr are $K = 2.427 \times 10^{-4} \text{ dL g}^{-1}$ and $a = 0.6804$.

3.6.7 High-Performance Liquid Chromatography-Electrospray Ionization-Mass Spectrometry (HPLC-ESI-MS)

The dehydrodimers of ferulic acid (di-FAs) were analyzed using an HPLC-ESI-MS system after the saponification of AX by NaOH (2 M) (Paper III and IV). The HPLC was equipped with an Eclipse Plus C18 column (Agilent Technologies, Santa Clara, CA, USA) and the mobile phase consisted of 0.1 % formic acid in water and 0.1 % formic acid in acetonitrile. The MS (Synapt G2, Waters, Milford, MA, USA) was used in positive mode with ion collision induced dissociation (CID) by nitrogen. The di-FAs were determined based on the fragmentation of the 369.1 m/z ion subjected to a collision of 20 eV.

3.6.8 Fourier Transform Infrared Spectrometry (FTIR)

An FTIR instrument (FTIR 100, Perkin Elmer, Norwalk, CT, USA) with an attenuated total reflection (ATR) unit (Golden Gate, Graseby Speac Ltd, Kent, England) was used to verify the

presence of FA and acetyl groups in the extracted and acetylated AX (Paper II). Spectra was recorded between 600 and 4000 cm^{-1} with 16 scans, and normalized using the Spectrum software (Perkin Elmer, Norwalk, CT, USA).

3.6.9 Field-Emission Scanning Electron Microscopy (FE-SEM)

The microstructure of the cross-sections of AX films was analyzed using FE-SEM (Hitachi TM-1000, Tokyo, Japan) operating at 1 – 5 kV (Paper II) after coating with Pt/Pd by a sputter coater (Cressington, Watford, UK).

3.6.10 Tensile testing

Tensile properties of the films were analyzed on a universal testing machine (Instron 5944, Norwood, MA, USA) after conditioning for a week at 23 °C and 50 % relative humidity. The films were cut into specimens with 5 mm width and ~20 mm length and tested at a stretching rate of 10 mm/min. Stress-strain curves were obtained for 5 specimens for each film and Young's modulus values were calculated using the linear region of the curves (Paper II).

3.6.11 Thermogravimetric Analysis (TGA)

The thermal stability of the AX films was analyzed using a TGA instrument (TGA/DSC1, Mettler Toledo, Columbus, OH, USA) operated from 25 °C to 750 °C under the nitrogen flow of 50 mL/min and with a heating rate of 10 °C/min (Paper II). The mass loss (%) and the initial decomposition temperature (T_{onset}) were determined from the thermogravimetric (TG) and the first derivative thermogravimetric (DTG) curves, respectively.

3.6.12 Differential Scanning Calorimetry (DSC)

The thermal behavior of the AX films was characterized by a DSC instrument (DSC1, Mettler Toledo, Greifensee, Switzerland) operated under the nitrogen flow of 50 mL/min and with a heating rate of 10 °C/min (Paper II). A temperature program was employed with 1st heating (25 – 125 °C), cooling (125 – (-25 °C)) and 2nd heating (-25 – 450 °C). The glass transition temperature (T_g) was determined from the 2nd heating cycle.

3.6.13 Oxygen Permeability (OP)

Polysaccharide-based films are well known to provide remarkably low permeability towards oxygen due to their hydrogen bonding network. To confirm this, the oxygen transmission rate

(OTR) of AX films was measured using an Ox-Tran instrument (MOCON 2/20, MN, USA) and the OP was calculated based on the average thickness of the films (Paper II).

3.6.14 Water Vapor Permeability (WVP)

The water vapor transmission rate (WVTR) of AX films was determined using the cup method (ASTM, 2016) at room temperature (Paper II). The WVP was calculated by considering the average thickness of the films and the vapor pressure difference between the inside and outside of the measuring cup. The calculated WVP values were corrected according to Gennadios, Weller, and Gooding (1994).

3.6.15 Rheological properties and gelation kinetics

The rheological properties (viscosity and viscoelasticity) of solutions and hydrogels produced from wheat bran F-AX were analyzed using a strain-controlled rheometer (ARES G2, TA Instruments, New Castle, DE, USA) equipped with a \varnothing 20.0 mm parallel plate (Paper III). Shear viscosity was measured with a gap of 0.5 mm at a shear rate of 1 – 100 s⁻¹. Dynamic storage modulus (G') and loss modulus (G'') were measured by subjecting the samples to a frequency sweep test over an angular frequency range of 0.6 to 125 s⁻¹ with a 0.5 % oscillation strain.

The rheological properties and gelation kinetics of the hydrogels produced from corn bran AX were studied using a strain-controlled rheometer (Discovery HR3, TA Instruments, New Castle, DE, USA) (Paper IV). The viscoelasticity measurements were carried out by a frequency sweep between 0.1 and 100 rad s⁻¹ on a 25.0 mm parallel plate at 25 °C. The oscillation strain was 1 % and the gap was 1 mm. The time course of the gelation of corn bran AX by two different enzymes (laccase and HRP) was monitored on the same rheometer by a time sweep at 25 °C with a constant frequency of 6.3 rad s⁻¹. The AX solution was loaded on the parallel plate and then the respective enzyme was added to the solution. The measurement was immediately started, and the reaction was followed for 2-5 h.

3.6.16 Cryogenic Scanning Electron Microscopy (Cryo-SEM)

Cryo-SEM is a powerful tool to characterize the microstructure of high water-containing materials such as hydrogels. An FE-SEM (Merlin, Carl Zeiss GmbH, Germany) fitted with a PP3000T cryo-SEM preparation system (Quorum Technologies, UK) was employed to analyze the surface morphology of the hydrogels produced from wheat bran F-AX (Paper III) and corn bran AX (Paper IV). Sample preparation is of critical importance for the cryo-SEM as different

techniques can result in artifacts such as ice-crystal damage. In this study, hydrogel samples were prepared using high pressure freezing (HPF) on an HPM100 system (Leica, Microsystems, Wetzlar, Germany) as this method is preferable to avoid cryofixation artifacts (Aston, Sewell, Klein, Lawrie, & Grøndahl, 2016). The analysis of the cryo-SEM images was performed using the open-source CellProfiler™ software. The porosity (%) was calculated as the ratio of the area of pores to the total image area.

3.6.17 Wide Angle (WAXS) and Small Angle X-ray Scattering (SAXS)

The degree of crystallinity of hemicelluloses is dependent on their degree of substitution and WAXS provides broad information for the crystal structure of materials. On the other hand, important information regarding macromolecular interactions in AX networks, which result in the hydrogel formation by enzymatic crosslinking, can be obtained using SAXS.

In this study, WAXS and SAXS measurements were performed using a laboratory-based X-ray source (Rigaku 003+ high brilliance microfocus Cu-radiation source, Rigaku Corp., Tokyo, Japan) at Chalmers University Materials Analysis Laboratory.

WAXS experiments were recorded on a Pilatus 100 K detector (Dectris, USA) with a sample-detector distance of ~134 mm (q range: $0.07 - 2.7 \text{ \AA}^{-1}$). WAXS profiles were used to determine the crystal peak positions and the degree of crystallinity (X_c) of wheat bran native and crosslinked F-AX (Paper III). Corn bran AX was also analyzed by WAXS however did not exhibit crystallinity (Paper IV).

SAXS measurements were performed using a 300 K detector (Dectris, USA) with a q range from 0.003 \AA^{-1} to 0.25 \AA^{-1} . The modeling of the SAXS data was carried out using the SasView 4.2.2 software package.

3.6.18 Scavenging of reactive oxygen species by hydrogels

Cellular stress, resulting from endo- or exogeneous reactive oxygen species (ROS) production, may result in the death of cells (cytotoxicity). AX-based hydrogels may provide a scavenging against ROS due to their intrinsic functional groups. In this study, firstly the response of the HT29-MTX human colon cell line to the corn bran AX hydrogels was assessed as a model for epithelial transporter cells. Secondly, the antioxidative potential of the AX hydrogels was evaluated using a cellular ROS assay kit. Tert-butyl hydroperoxide (TBHP) solution was diffused into the hydrogels and then the cells were seeded on the hydrogels in 96-well plates. After the

incubation at 37 °C for 20 min, the ROS production was monitored by measuring the fluorescence intensity every 30 min for 3 h (Paper IV). A more detailed description of the cytotoxicity and oxidative stress measurements is available in Paper IV.

4 RESULTS AND DISCUSSION

4.1 Sequential extraction of wheat bran proteins and arabinoxylans (Paper I)

For the utilization of F-AX and protein components of wheat bran, the implementation of efficient extraction and purification processes is fundamental. In this work, the effect of prior protein isolation on the SWE of wheat bran F-AX was investigated in a cascade process. WB was treated by Arte, Huang, Nordlund, and Katina (2019) to isolate the proteins in a two-step process combining fermentation and cold alkaline extraction (Arte et al., 2019). The residual wheat bran after the protein isolation was used as the low-protein counterpart (LP) in this thesis (Paper I).

The untreated (WB) and its low protein counterpart (LP) were subjected to sequential SWE (cumulative 5, 15, 30 and 60 min) at 160 °C and 180 °C for the extraction of F-AX. To study the effect of proteins on the subsequent F-AX extraction, a process without the initial protein isolation step was applied. For this study, SWE was applied using a laboratory-scale instrument. Prior to SWE, the two initial brans (WB and LP) were pretreated to remove starch and eliminate its possible hindrance to the extraction of F-AX.

The initial protein isolation step had considerable effects on the composition of wheat bran (**Table 1**). Firstly, the protein content was reduced from 14.0 % to 8.5 % by protein isolation. The reason for isolating only half of the initial proteins was likely the inaccessibility of the insoluble proteins in the aleurone layer by fermentation and cold alkaline extraction. The protein isolates were mostly composed of globulins, chitinases and β -amylase, which eliminated the presence of endogenous enzymes of the lactic acid bacteria used in the fermentation step. Secondly, the protein isolation did not substantially affect the AX content of LP and caused only a slight decrease in the FA content. This was unexpected as alkaline conditions are known to result in the cleavage of phenolic compounds. This result was due to the cold temperature of the alkaline extraction, which prevented the excessive loss of FA moieties.

By destarching, the starch content was reduced to below 2.0 % and 3 % in DWB and DLP, respectively. The destarching enriched the AX content of both brans and did not influence the A/X ratio or protein content. The reduction in the FA content of LP after destarching resulted

from the removal of free FA residues during the washing steps, which were cleaved during the alkaline treatment in the protein isolation.

Table 1. Chemical composition of untreated and pretreated wheat bran

Composition	Untreated (WB)	Low protein (LP)	Destarched (DWB)	Destarched low protein (DLP)
Moisture (%) [*]	8.2 ± 0.0	7.8 ± 0.0	2.6 ± 0.2	2.3 ± 0.0
Carbohydrate content (mg g ⁻¹ DW)	531.0 ± 28.0	683.0 ± 31.0	633.0 ± 21.0	678.0 ± 21.0
Glc (%)	45.0 ± 0.3	58.0 ± 0.6	28.0 ± 0.8	33.0 ± 2.1
Ara (%)	14.1 ± 0.2	12.1 ± 0.3	17.4 ± 1.0	18.4 ± 0.3
Xyl (%)	38.4 ± 0.4	28.3 ± 0.5	52.0 ± 0.6	45.0 ± 1.9
Gal (%)	2.0 ± 0.0	1.4 ± 0.0	1.8 ± 0.1	2.2 ± 0.1
AX (%)	52.6 ± 0.4	40.5 ± 0.5	69.0 ± 0.7	63.0 ± 2.2
A/X	0.4	0.4	0.3	0.4
Starch (%)	13.0 ± 0.3	32.0 ± 0.5	1.7 ± 0.1	2.4 ± 0.5
Protein Content (%)	14.0	8.5	12.8	8.1
Ferulic acid content (mg g ⁻¹ DW)	2.9 ± 0.0	2.3 ± 0.3	3.7 ± 0.5	1.9 ± 0.1

* Moisture content was determined gravimetrically after freeze-drying for 48 h.

DW: Dry weight

4.1.1 Effect of extraction conditions on the yields and molecular characteristics of F-AX

The total yields obtained from SWE of DWB and DLP at 160 °C and 180 °C were compared at respective extraction times. The protein isolation step did not substantially influence the extraction yields, and similar yields were obtained in the hydrothermal extracts of WB and LP (DWB-H and DLP-H) at respective temperatures. On the other hand, higher extraction temperature (180 °C) resulted in higher yield in both extracts as in agreement with previous observations (Ruthes et al., 2017).

As for the monosaccharide composition of the extracted fractions, a prominent content of arabinose and xylose was observed in the extracts of both DWB and DLP (**Figure 6a**). By implementing sequential extraction times, the mass transfer was enhanced with a fresh supply of water and hence, higher AX yields were obtained as the extraction extended. Starch was not detected in the extracts therefore, the measured glucose content was attributed to MLBG. The occurrence of glucose was especially higher in the 5-min extracts, which indicated the easier extractability of MLBG (Reisinger et al., 2013; Rudjito et al., 2019). The glucose measured in the residues (RWB and RLP) was attributed to insoluble cellulose that is resistant to hot water. With

regards to the protein isolation, higher AX content was obtained in the extracts of DLP, which was interesting as the AX content of the starting DLP was somewhat lower than that of DWB. This implied that the initial protein isolation loosened the cell wall network and hence, improved the extractability of AX.

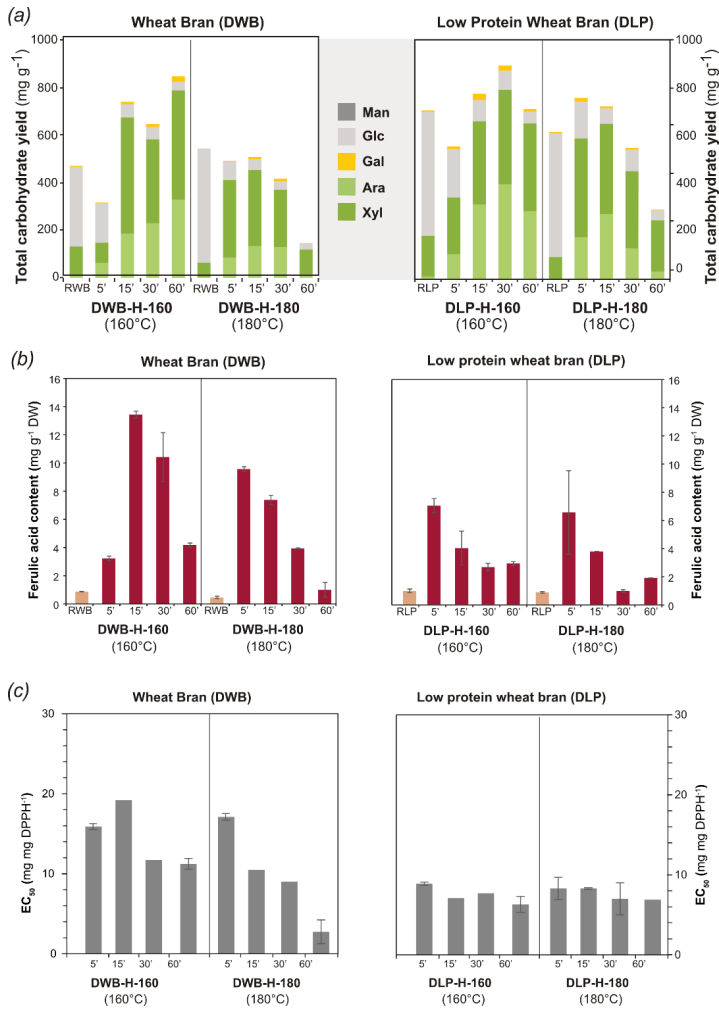


Figure 6. (a) Comparison of the monosaccharide composition of residues and extracts of DWB and DLP. (b) Comparison of the ferulic acid content of residues and extracts of DWB and DLP. (c) Comparison of antioxidant activity of extracts of DWB and DLP.

Regarding the effect of the extraction temperature, the total AX yields at 180 °C were slightly lower than those at 160 °C, despite the total solid yields were higher at the higher temperature. This was ascribed to the co-extraction of other crosslinked components of the cell wall (i.e. proteins and lignin). The extraction of AX occurred more rapidly at 180 °C and thus, lower AX was obtained as SWE prolonged to 60 min. The A/X ratio of the extracts of both DWB and DLP at 160 °C generally increased with time, corresponding to the progression of SWE from aleurone, containing AX with less *Araf*, to outer pericarp, containing AX with richer *Araf* units. Contrarily, a marked decrease was observed in the A/X ratio of the extracts at 180 °C, indicating both the tissue-specific characteristics of AX and the susceptibility of *Araf* residues to degradation at the higher temperature. Seemingly, the *Araf* substitutions were cleaved more easily at 180 °C as compared to 160 °C, yielding lower A/X ratios (Raisanen, Pitkanen, Halttunen, & Hurta, 2003).

The influence of the protein isolation and SWE conditions on the FA content of all the extracts is presented in **Figure 6b**. Firstly, the protein isolation resulted in lower FA in the extracts of DLP as compared to those of DWB. This was purely due to the lower FA content of the starting DLP, which was a consequence of the alkaline treatment step. Secondly, the SWE temperature did not influence the FA content of the extracts and similar FA content was measured in respective extracts (DWB-H-160 to DWB-H-180 and DLP-H-160 to DLP-H-180). This was ascribed to the thermal stability of the phenolic compounds as in agreement with previous studies (Santos et al., 2012). Finally, the FA content of the extracts did not correlate with their AX content, which was due to the presence of free and bound FA moieties as the extracts were not dialyzed. The feruloylated extracts of both DWB and DLP showed significant antioxidant activity (**Figure 6c**) however, this activity did not show a correlation with their FA content. Interestingly, the DLP extracts exhibited higher antioxidant activity despite their lower FA content as compared to the DWB extracts. This suggested that the radical scavenging activity cannot be only due to the feruloylation but possibly a result of the presence of other bioactive compounds present in the extracts (such as phytosterols) (Mateo Anson, Hemery, Bast, & Haenen, 2012).

The SEC analysis showed that the extracts of both DWB and DLP at 160 °C had bimodal distributions corresponding to the presence of low and high molar mass populations. In the 5-min fractions of these extracts, the presence of MLBG confirmed by the high molar mass peak observed at approximately 10^5 Da. The molar mass distributions evolved to monomodal as the

extraction progressed, verifying the presence of polymeric AX populations. On the other hand, longer extraction times resulted in a decrease in the molar mass of the AX populations. Regarding the effect of the protein isolation, the looser structure of the starting DLP resulted in a faster decrease in the molar mass of its extracts. As for the extracts at 180 °C, a substantial decrease was observed in the extracts of both DWB and DLP. This was related to the progressive hydrolysis of the polymeric AX at higher temperatures as observed by previous studies (Merali et al., 2015).

4.2 Arabinoxylan films (Paper II)

4.2.1 Upscaled SWE and alkaline extraction of arabinoxylans

Free standing films were prepared from wheat bran AX extracted by two different techniques and their film formation, material properties and antioxidant activity were compared to a reference film prepared from a commercially available wheat endosperm AX (WAX). The chemical composition and molecular structural parameters of these starting AX are shown in **Table 2**.

SWE was scaled up (33 times) for the extraction of feruloylated wheat bran AX (FAX), which has been proven to produce larger quantities of AX with sufficient yields (Rudjito et al., 2019). The monosaccharide analysis of FAX confirmed the dominating presence of AX (80 % of the total carbohydrates) however with a lower A/X ratio (0.2) than the AX from small scale SWE. Similar to the small scale SWE, this low DS of FAX was attributed to the susceptibility of Araf to high temperature. The phenolic acid content of FAX was measured as 10.3 mg/g DW, with 79.0 % FA, 19.9 % sinapic acid and 1.1 % 5-5' di-FA. Such high phenolic content of FAX, in turn, resulted in a high radical scavenging activity (EC_{50} : 17.7 mg/mg DPPH), implying the strong antioxidant properties of this extract. The polymeric characteristics of FAX were confirmed by the SEC analysis (M_w centered at 8×10^4 g/mol).

Alkaline extraction targeted the extraction of non-feruloylated AX (NAX). Alkaline extraction is a commonly used technique to isolate xylans from biomass and proceeds by cleaving the covalent and non-covalent bonds between cell wall components. Therefore, it is capable of extracting AX with high DS and with high yields. Thus, the yield of the alkaline extraction in this work was higher than that of SWE (31.1 % vs 7.5 %) and the AX content of NAX was 89.8 % (of the total carbohydrates) with an A/X ratio of 0.7. Phenolic acids were not detected in NAX and

hence, its radical scavenging activity was significantly lower (EC_{50} : 53.2 mg/mg DPPH). The M_w of NAX was higher (1.2×10^5 g/mol) with an additional presence of low molar mass populations.

The reference AX (WAX) was nearly completely pure (99.2 % AX) with an A/X ratio of 0.6 and did not contain any phenolic acids.

The effect of the A/X ratio, M_w and feruloylation of FAX, NAX and WAX on the material and radical scavenging properties of the films casted from their aqueous solutions were comprehensively investigated.

Table 2. Chemical composition and molecular parameters of the native AX extracted by SWE (FAX), alkaline extraction (NAX) and reference endosperm AX (WAX)

	FAX	NAX	WAX
Carbohydrate content (mg/g DW)	944.0 ± 51.0	822.0 ± 35.0	992.0 ± 96.0
Ara (%)	15.0 ± 0.1	36.6 ± 0.3	38.0 ± 0.1
Xyl (%)	65.7 ± 0.5	53.0 ± 0.6	61.0 ± 0.2
Glc (%)	18.0 ± 0.3	7.8 ± 1.0	0.3 ± 0.1
Gal (%)	1.3 ± 0.1	2.5 ± 0.1	0.6 ± 0.2
AX (%)	81.0 ± 0.4	90.0 ± 1.0	99.0 ± 0.2
Ara/Xyl	0.2	0.7	0.6
Starch content (%)	2.0 ± 0.1	3.3 ± 0.3	n.d. ^e
\bar{M}_n (10³ g/mol)	13.4	5.1	54.2
\bar{M}_w (10³ g/mol)	126.3	262.9	312.4
Dispersity index	9.4	51.3	5.8
Phenolic acid content (mg g⁻¹ DW)	10.3 ± 0.3	n.d.	n.d.
Ferulic acid (%)	79.0 ± 0.4	n.d.	n.d.
Sinapic acid (%)	20.0 ± 0.4	n.d.	n.d.
5-5AcFE (%)	1.0 ± 0.2	n.d.	n.d.

n.d. Not detected

4.2.2 Acetylation as a tool to improve the material properties of AX films

The polysaccharides extracted by different techniques; FAX, NAX and WAX, were chemically acetylated to different DA in order to reduce their hydrophilicity. The AX purity of the extracts influenced the acetylation process and DA of 1.2, 1.4 and 1.7 were measured for AcFAX, AcNAX and AcWAX, respectively. The acetylation was further confirmed by FTIR as presented in **Figure 7**. The spectral bands seen at 1735, 1360 and 1215 cm^{-1} in the spectra of the acetylated AX corresponded to carbonyl, C-CH₃ and carboxyl stretching, respectively, which indicated the presence of acetyl groups (Bi et al., 2016). Furthermore, the peak at 3300 cm^{-1} , showing the

hydroxyl stretching, decreased after acetylation due to the replacement of hydroxyl groups by acetyl groups.

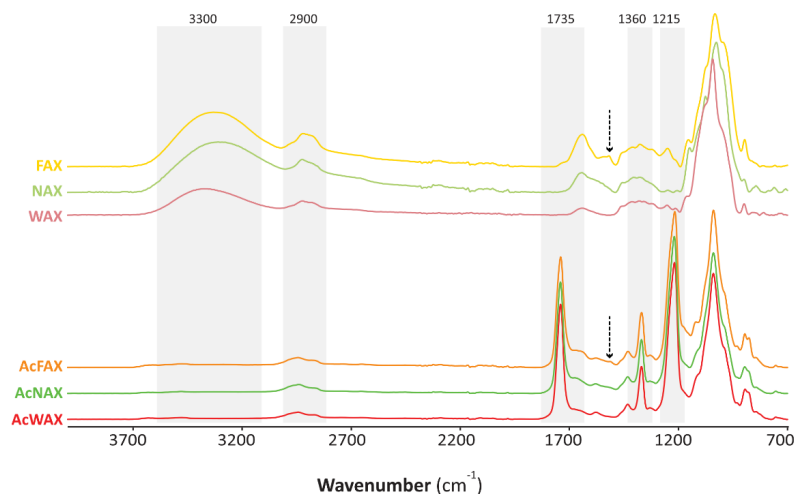


Figure 7. FTIR spectra of native and acetylated AX.

The total carbohydrate content decreased after acetylation as acetyl groups substituted for sugars (33-36 %). On the other hand, the AX content of the acetylated AX was slightly higher due to the loss of galactose and glucose units during purification steps after acetylation. The FA content of AcFAX decreased by half, which was attributed to hydrolysis. Similarly, the molar mass slightly decreased after acetylation, confirming the hydrolysis of polysaccharides due to the use of harsh chemicals in the acetylation reaction.

4.2.3 Material properties and bioactivity of native and acetylated AX films

The films from both native and acetylated AX were firstly casted without additional plasticizers. However, FAX did not form a continuous film, which was due to its lower molar mass and A/X ratio. The A/X ratio played a crucial role in the film-forming properties of AX as in agreement with previous studies (S. L. Heikkinen et al., 2013). Besides, the acetylated AX showed poor film-forming ability without plasticization, indicating the lack of adequate internal plasticization effect of the introduced acetyl groups, unlike in previous observations (Egues et al., 2014). Therefore, sorbitol and triacetin were employed as plasticizers for film casting from the native and acetylated AX, respectively. The plasticized films were homogeneous and smooth

(**Figure 8**) and suitable for evaluating their thermal, mechanical, permeability properties, and antioxidant activity. Additionally, external FA was incorporated into the WAXSor film to evaluate the impact of external FA addition on the radical scavenging activity as compared to bound FA in the FAXSor film.

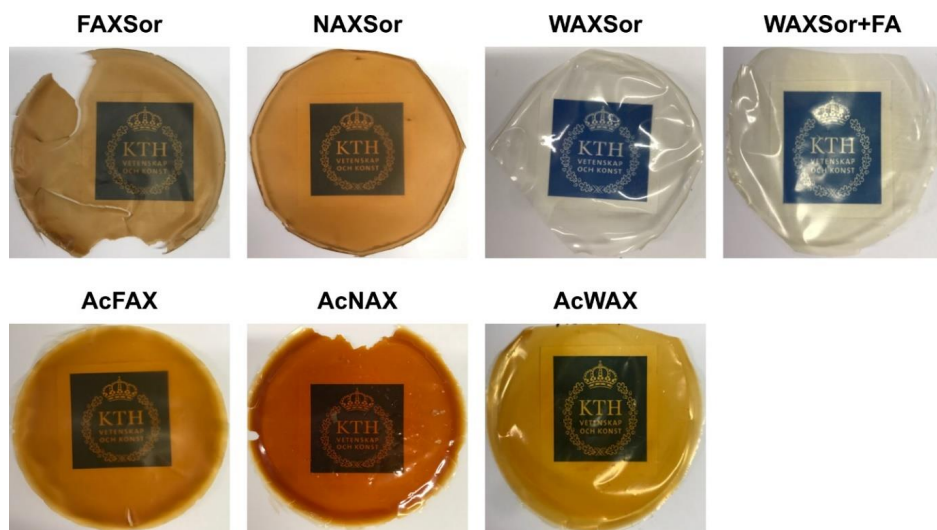


Figure 8. Plasticized and casted films of native (FAXSor, NAXSor, WAXSor, WAXSor+FA) and acetylated (AcFAX, AcNAX, AcWAX) AX.

The thermal properties of the plasticized films were analyzed by DSC as presented in **Figure 9a**. T_g of the films was determined and discussed as the indication of their thermal behavior. The T_g of FAXSor and WAXSor was similar however, NAXSor had a higher T_g , which was attributed to the low molar mass populations that hindered the chain mobility. Interestingly, the external FA in WAXSor+FA acted as a plasticizer and reduced the T_g by 10 °C. Regarding the acetylated films, a decrease in the T_g was observed after acetylation, suggesting the induction of internal plasticization by the introduced acetyl groups. Furthermore, the external plasticization by triacetin contributed to the decrease in the T_g by promoting polymer mobility.

As an important feature for the processing and applications of materials, the thermal stability of the films was evaluated as shown in **Figure 9b**. Two thermal decomposition regions were determined for the sorbitol plasticized films of the native AX, the first (25–150 °C) being due to the moisture loss and the second (180–600 °C) corresponding to the main thermal degradation

of the AX chains. The onset temperature of the decomposition (T_{onset}) in the second mass loss region was of interest to compare the thermal stability of the different films. Accordingly, FAXSor showed a lower T_{onset} than those of NAXSor and WAXSor, which was ascribed to the lower molar mass and purity of the FAX extract. As for the acetylated AX films, three thermal decomposition regions were defined: 100-160 °C, 160-250 °C and 300-600 °C. The first two regions were composed of two overlapping peaks and corresponded to the evaporation of the solvent (acetylacetone) and the decomposition of the plasticizer (triacetin), respectively. The third region showed the main decomposition of the acetylated AX chains, where all three films (AcFAX, AcNAX and AcWAX) exhibited similar T_{onset} values. After acetylation, T_{onset} significantly improved (by 80-100 °C), which indicated that the acetylation process limited the intramolecular dehydration of AX due to replacement of the hydroxyl groups and hence, delayed the thermal decomposition (Aburto et al., 1999; Fundador, Enomoto-Rogers, Takemura, & Iwata, 2012). This observation is in line with previous studies on acetylated xylans from different sources (Egues et al., 2014; Morais de Carvalho et al., 2019). In summary, the chemical acetylation of AX can be an efficient way of increasing their thermal stability.

The mechanical properties are another important aspect for the application of films therefore, the tensile strength, elongation at break and Young's modulus of the plasticized films were evaluated. The stress-strain curves of the films are presented in **Figure 9c**. Comparing the films from the native AX, FAXSor had the lowest tensile strength, elongation at break and Young's modulus values, which was attributed to its lower molar mass and A/X ratio. A/X ratio appeared to have a significant impact on the mechanical properties of the films, where the low A/X ratio of FAX promoted the intermolecular interaction between polysaccharide chains and thus, caused agglomeration. This, in turn, created stress concentration points that resulted in poorer mechanical properties, which is in agreement with previous studies (S. L. Heikkinen et al., 2013; Hojje et al., 2008). On the contrary, the combined effect of higher A/X ratio and higher molar mass of NAX and WAX yielded higher tensile strength and Young's modulus of their films. As for WAXSor+FA, a decrease was observed in the tensile properties by the addition of the external FA, which was explained by the low compatibility between FA and WAX (as also observed from the FE-SEM micrographs).

With regards to the acetylated AX films, all three films had similar tensile strength, elongation at break and Young's modulus values to each other. This indicated that the differences between the acetylated AX in terms of molar mass and the A/X ratio do not significantly influence the

tensile properties, and DA is the main factor determining the mechanical performance. Contrary to the expectations and previous observations (Egues et al., 2014; Stepan et al., 2012), acetylation did not improve the mechanical properties as compared to the native AX. This could be partly explained by the decreased molar mass of AX after acetylation.

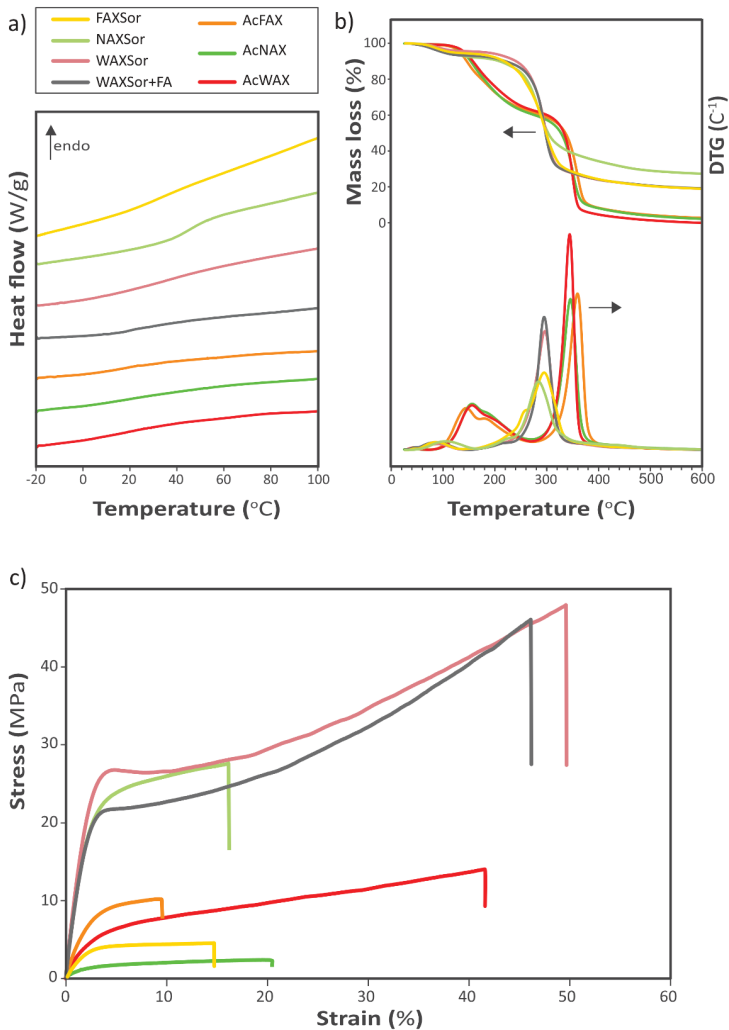


Figure 9. (a) DSC curves of AX films, (b) TGA curves of AX films, and (c) Stress-strain curves of AX films.

Hemicellulose films can be excellent barrier materials to oxygen due to the extensive hydrogen bonding between the chains. The oxygen permeability (OP) of the films was therefore evaluated and presented in **Table 3**. The plasticized films of the native AX had similar OP to each other between 0.7-1.0 cm³ μm/m² d kPa, regardless of the intrinsic differences between the native AX (i.e. molar mass, A/X ratio, external FA). The OP measurement of the native AX films confirmed that these films would be excellent barriers, as a good oxygen barrier film is characterized with OP between 1-10 cm³ μm/m² d kPa (Krochta & DeMulder-Johnston, 1997). As for the acetylated AX films, the OP values of AcFAX, AcNAX and AcWAX were significantly higher, which was merely due to the lack of hydroxyl groups disrupting the hydrogen bonding network.

Table 3. Barrier properties and radical scavenging activity AX films

	OP (cm ³ μm/m ² d kPa)	WVP (g mm/kPa m ² d)	EC ₅₀ (mg film/mg DPPH)
FAXSor	1.0 ± 0.2 ^a	0.9 ± 0.2 ^a	13.3 ± 0.5 ^a
NAXSor	0.8 ± 0.1 ^a	0.7 ± 0.3 ^a	43.8 ± 4.1 ^b
WAXSor	0.9 ± 0.2 ^a	1.4 ± 0.1 ^a	n.a.
WAXSor+FA	0.7 [*]	1.6 ± 0.2 ^a	n.a.
FAX film	n.a.	n.a.	15.8 ± 0.1 ^a
NAX film	n.d.	3.0 ± 0.6 ^{c,e}	45.0 ± 5.0 ^b
WAX film	n.d.	5.7 ± 0.5 ^{d,f}	n.a.
WAX+FA film	n.d.	4.5 ± 0.8 ^{e,f}	n.a.
AcFAX	79.0 [*]	4.2 ± 1.0 ^b	n.d.
AcNAX	155.0 [*]	2.0 ± 0.4 ^{a,b}	n.d.
AcWAX	101.5 ± 24.0 ^b	2.8 ± 0.2 ^b	n.d.

n.a. Not applicable; n.d. Not determined; * Only one successful measurement; Superscript letters: Results with different letters have statistical differences (t-test, p < 0.05)

Water vapor permeability (WVP) of the films was assessed as an indication of their barrier properties against moisture in potential packaging applications. The WVP values of all the films are presented in **Table 3**. The plasticized films of the native AX had WVP between 0.7-1.6 g mm/kPa m² d, demonstrating a moderate moisture barrier (Krochta & DeMulder-Johnston, 1997). The WVP of the non-plasticized films of NAX, WAX, and WAX+FA was also measured to evaluate the effect of plasticization. Accordingly, the sorbitol-plasticized films showed

significantly lower water vapor affinity, which was due to the formation of hydrogen bonds between AX and sorbitol. Regarding the WVP of the acetylated AX films, these films had significantly lower WVP than that of the non-plasticized films. This was expected as the hydroxyl groups were replaced by acetyl groups, which reduced the affinity towards moisture. On the other hand, the WVP values of the acetylated AX films were lower than those of the sorbitol-plasticized films of the native AX. This strongly suggested that plasticization by sorbitol is a more powerful tool for developing AX films with good barrier properties, which also represents a simple strategy.

The radical scavenging activity of the films was evaluated against the DPPH radical (**Table 3**). The effect of the external addition of FA on the radical scavenging activity of the WAXSor film was compared to FAXSor that contained ester-bound FA. The acetylated AX films did not dissolve in the solvents of the DPPH assay (methanol/water) therefore their radical scavenging activity was not determined. The radical scavenging activity was expressed as EC_{50} (mg film/mg DPPH) which corresponds to the concentration of film required to decrease the initial concentration of the DPPH radical by 50 %, meaning a higher radical scavenging activity when the EC_{50} is lower. FAXSor showed a lower EC_{50} than NAXSor, and WAXSor did not show any activity. This indicated that the purest nature of WAX prevented any antioxidant effect of phytochemicals. The incorporation of external FA (WAXSor+FA) brought about DPPH scavenging activity however, this film did not achieve a 50 % reduction. This verified that free FA cannot confer as much radical scavenging activity as the ester-bound FA in the FAXSor film. Therefore, it can be concluded that the dominant contribution to the radical scavenging activity of cereals originates from covalently linked phenolic compounds as in agreement with previous work (Liyana-Pathirana & Shahidi, 2006; Pang et al., 2018; Yang, Dang, & Fan, 2018). It is worth noting that sorbitol plasticization did not influence radical scavenging activities. These results are important to show the strong antioxidant potential of the bio-based films derived from subcritical water extracted AX, which can build a promising feedstock for packaging films. These future packaging films would be especially useful in applications targeting the protection of food-stuff that are prone to oxidation.

4.3 Arabinoxylan hydrogels (Paper III and IV)

Laccase is often used for the crosslinking of F-AX and this renders hydrogels with various properties depending on the molecular characteristics (DS, FA content, Mw) of the source AX.

In this work, a series of hydrogels were prepared from feruloylated wheat bran AX by laccase crosslinking and a subsequent regeneration process involving freeze-drying of the crosslinked F-AX and resuspension in different pH buffers. Peroxidase is another enzyme employed for the crosslinking of AX, which may generate hydrogels with different structural properties compared to laccase-crosslinked hydrogels. Therefore, the laccase and peroxidase crosslinking were performed to produce hydrogels from highly feruloylated corn bran AX and the properties of the resulting hydrogels were compared. The hydrogels developed from both wheat bran F-AX and corn bran AX were characterized in terms of chemical and structural changes upon crosslinking using biochemical, rheological and biophysical techniques to elucidate the multiscale assembly mechanism of AX hydrogels.

4.3.1 Properties of crosslinked AX from wheat bran

Different forms of dehydrodimers of FA (di-FAs), namely 5-5', 8-5', 8-8' and 8-O-4' di-FAs, may be present in F-AX and these are expected to change in form and quantity with crosslinking as monomeric FA is converted into di-FAs. To identify the di-FAs before (FAX) and after laccase crosslinking (FAX-CL), HPLC-ESI-MS² was performed as presented in **Figures 10a and 10b**. 6 different di-FAs were identified in both FAX and FAX-CL, corresponding to 8-8'-cyclic, 8-8'-noncyclic (NC), two different forms of the 5-5' di-FA (Ac-Am 5-5' and Di-Am 5-5'), 8-O-4' and 8-5' di-FAs. The peak intensity of the 8-8'-NC, 5-5'-Di-Am, and 8-5' di-FAs increased after crosslinking whereas the 5-5'-Ac-Am decreased. The former of these changes implied that the monomeric FA was converted into these di-FAs and the latter suggested that the 5-5'-Ac-Am di-FA was likely converted to the 5-5'-Di-Am di-FA.

The changes in the phenolic acid content following the crosslinking were further determined by HPLC and presented in **Figure 10c**. The predominant phenolic acid in FAX before crosslinking was found as FA and minor contents of *p*-coumaric acid, 8-8' di-FA and 5-5' di-FA were also observed. Some small peaks eluting after the 8-8' and 5-5' di-FAs were detected, which were defined as putative di-FAs and quantified using the response factors of the 8-8' and 5-5' di-FAs. After crosslinking, a depletion in the monomeric FA content of FAX by 45 % was observed, which corresponded to the total increase in the amount of the di-FAs (8-8' di-FA, 5-5' di-FA and putative di-FAs). This demonstrated that the oxidation of FA in the F-AX from wheat bran was achieved using laccase. The profile of di-FAs detected in the crosslinked F-AX in this study were different from those previously observed (Khalighi, Berger, & Ersoy, 2019; Martinez-Lopez et

al., 2019; Xiaowei Zhang et al., 2019). This was expected as the oxidative coupling of FA proceeds with the formation of phenoxy radicals, the position of which varies due to resonance stabilization. The phenoxy radicals may be located in different sites of the FA molecule and thus create different forms of dehydrodimers.

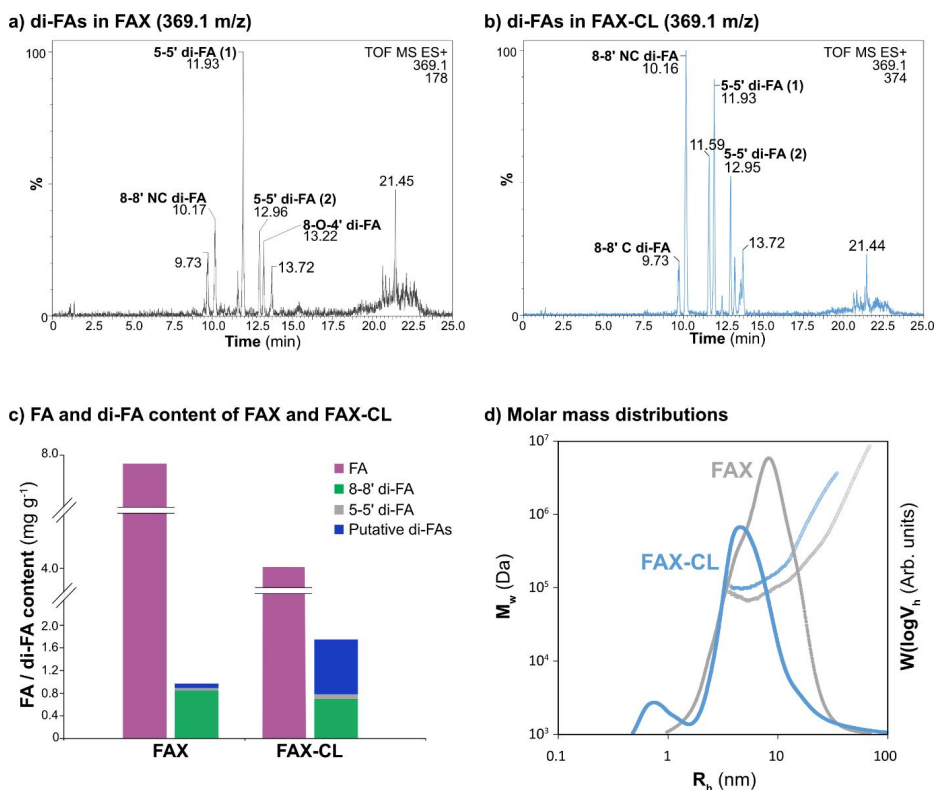


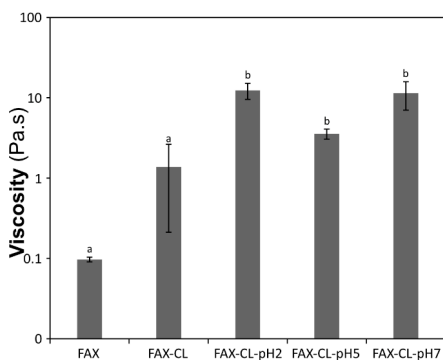
Figure 10. (a) Phenolic acid profile of FAX before enzymatic crosslinking, (b) Phenolic acid profile of FAX-CL after enzymatic crosslinking, (c) Changes in the phenolic acid content of FAX following enzymatic crosslinking, and (d) Changes in the SEC profiles of FAX following enzymatic crosslinking.

The molar mass distributions of AX before (FAX) and after crosslinking (FAX-CL) were analyzed by SEC as an indication of their macromolecular structure. The number-average molecular weight (M_n) and weight-average molecular weight (M_w) of FAX and FAX-CL was

determined by light scattering detection. The SEC weight distribution ($w(\log V_h)$) and the size dependence of the weight-average molecular weight ($M_w(V_h)$) were defined as a function of hydrodynamic radius (R_h) as shown in **Figure 10d**. FAX showed a monomodal molar mass distribution with an M_n of 97.1 kDa. After crosslinking, a shift in the $w(\log V_h)$ to lower sizes was observed together with a higher absolute molar mass ($M_w(V_h)$) at a certain R_h . It was evidenced with these two effects that the covalent crosslinking of FAX chains increased the absolute molecular weight and resulted in macromolecular structures with more compact hydrodynamic conformations.

The gelation after the laccase crosslinking of FAX, and the changes in the viscosity and viscoelasticity occurred after the regeneration process were monitored by rheological measurements. Shear viscosity measurements were performed to determine the viscosity behavior at a shear rate of 10 s^{-1} . The viscosity of the FAX solution before and after crosslinking and the results are presented in **Figure 11a**. FAX showed the lowest viscosity among the samples with a shear thinning behavior. After crosslinking, the viscosity increased by approximately one order of magnitude, confirming the formation of a covalently-bound AX hydrogel. After regeneration at different pHs (2.0-7.0), the samples displayed significantly higher viscosity.

a) Viscosity at 10 s^{-1}



b) Viscoelasticity

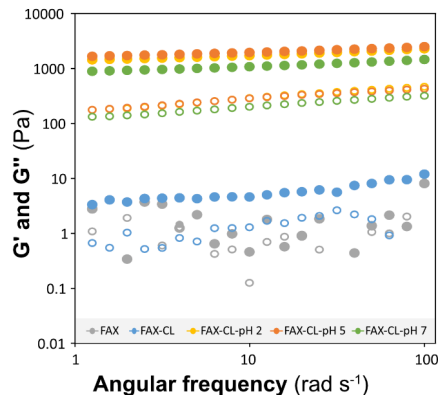


Figure 11. Rheological properties native and regenerated hydrogels from wheat bran F-AX. (a) Viscosity at the shear rate of 10 s^{-1} and (b) Viscoelasticity of FAX, FAX-CL, FAX-CL-pH2, FAX-CL-pH5 and FAX-CL-pH7 (all samples at 5 %). Full symbols show storage modulus (G') and open symbols show loss modulus (G'').

To further understand the rheological behavior of the hydrogels, G' and G'' were measured as shown in **Figure 11b**. The FAX solution showed a typical solution behavior with fluctuating G' and G'' values. When crosslinked (FAX-CL), gel characteristics were observed, where G' was higher than G'' and the G' was independent of frequency. The regeneration process substantially increased the G' and G'' values, which indicated the formation of mechanically stronger hydrogels. The pH of the regeneration, on the other hand, did not influence the viscoelasticity. The boosting effect of the regeneration on the rheological properties of the FAX hydrogels was attributed to the chain re-arrangement of AX in the freeze-drying step during the regeneration process, which likely arose from backbone interactions between the unsubstituted regions of AX. Freeze-drying was hypothesized to increase the hydrogen bonding between AX, resulting in closer polysaccharide chains with higher viscosity/viscoelasticity.

The morphology of the FAX hydrogels was characterized by cryo-SEM as shown in **Figure 12**. The differences between the hydrogels were discussed in terms of pore sizes and porosity. Among the hydrogels, FAX-CL had the highest porosity, confirming a typical characteristic of polysaccharide gels. After regeneration, all the hydrogels showed less porosity compared to FAX-CL, which indicated the formation of a more compact microstructure by the regeneration process. Among the regenerated hydrogels, FAX-CL-pH2 had the lowest porosity and the porosity increased with increased regeneration pH. As for the pore sizes of the hydrogels, FAX-CL-pH2 had the smallest pores and the pore sizes increased as the regeneration pH was increased, similar to the trend in the porosity values. The lower porosity of the regenerated hydrogels was attributed to the restricted chain mobility of the polysaccharides as a result of the freeze-drying step. This was also correlated with higher G' and G'' values of the regenerated hydrogels, which likely resulted from their stiffer network. The differences in the porosity of the hydrogels suggested that physical interactions between the AX chains increased at low pH and thus, created tighter domains.

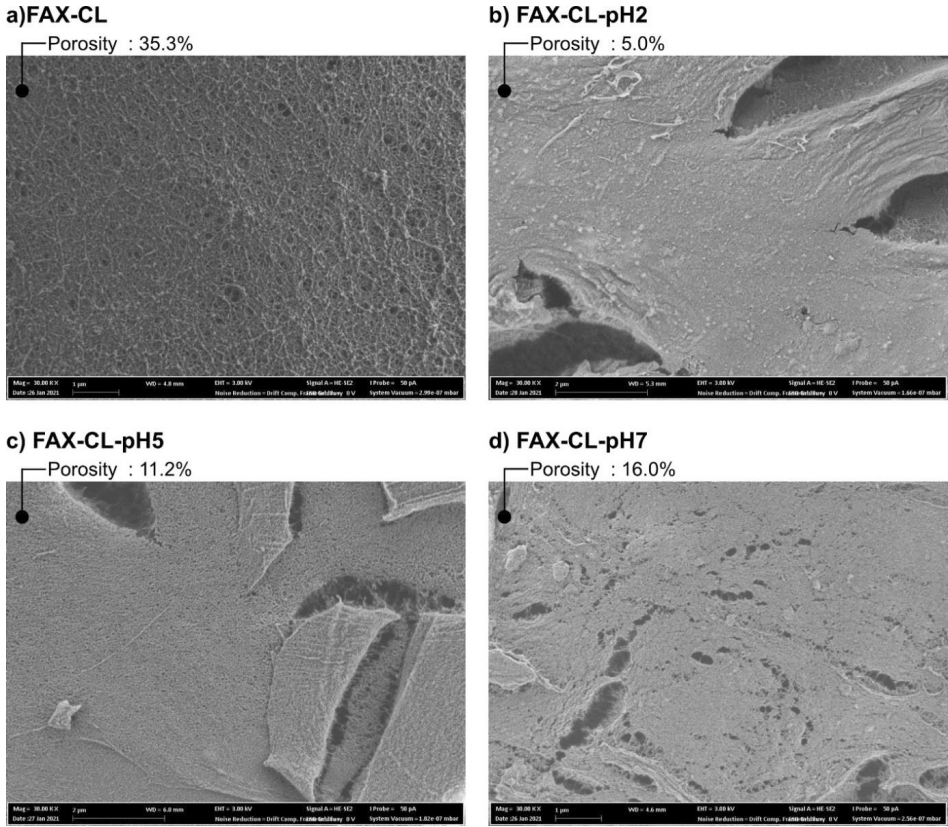


Figure 12. Cryo-SEM images of native and regenerated hydrogels from wheat bran F-AX. (a) FAX-CL, (b) FAX-CL-pH2, (c) FAX-CL-pH5, and (d) FAX-CL-pH7.

The crystalline behavior of the FAX solution, the crosslinked FAX-CL and the regenerated FAX-CL-pH2 was determined by WAXS and presented in **Figure 13a**. Five common crystalline peaks and a wide amorphous peak at $2\theta=21^\circ$ were observed in the three samples. The d-spacing values of the samples were calculated using Bragg's law ($\lambda = 2d \times \sin \theta$). The crystalline and amorphous peaks were fitted to determine the degree of crystallinity (X_c). The d-spacing values for the common crystalline peaks were determined as $d_1= 8.34 \text{ \AA}$, $d_2= 7.30 \text{ \AA}$, $d_3= 4.8 \text{ \AA}$ and $d_4= 4.0 \text{ \AA}$ and $d_5= 3.6 \text{ \AA}$ (**Figure 13b**), which was in agreement with previous observations (Nieduszynski & Marchessault, 1972). The FAX solution was found to be semi-crystalline with an X_c of 15.86 %, which was a consequence of the low DS of the source AX. Hemicelluloses are

widely accepted as amorphous materials (Werner, Pommer, & Broström, 2014); however, xylans may be semi-crystalline ($X_c = 12\text{-}20\%$) when they have low DS (Hoije et al., 2008; Stevanic et al., 2011; Y. Zhang et al., 2011). Considering the low DS of the feruloylated AX from wheat bran in this work ($A/X = 0.2$), the crystalline behavior of the FAX solution was in agreement with previous studies (S. L. Heikkinen et al., 2013; Nieduszynski & Marchessault, 1972). The X_c doubled following the laccase crosslinking, indicating a higher level of organization in FAX-CL. On the other hand, the regeneration did not significantly affect the crystalline behavior and a similar X_c of FAX-CL-pH2 was measured to that of FAX-CL. The changes that occurred in the crystalline behavior of the F-AX after crosslinking inferred a couple of aspects. Firstly, the enzymatic crosslinking created a more compact structure in the hydrogels compared to the FAX solution by increasing the proximity of AX chains. Secondly, the increased X_c after crosslinking suggests the presence of secondary interactions in the hydrogel networks, likely hydrogen bonding. WAXS measurements revealed that the gelation mechanism of moderately branched F-AX is partly related to their large-scale order (i.e. crystallinity). Interestingly, the crystallinity cannot explain alone the structural changes that occurred by regeneration as the same crystalline behavior was observed in FAX-CL-pH2.

To understand the overall gelation mechanism of F-AX from wheat bran and particularly the structural changes that occurred after the regeneration process, SAXS of FAX-CL and FAX-CL-pH2 was performed. The correlation length model, described by Equation 1, was used to fit the SAXS data. This model has a first term describing the power-law function from clusters in the low q region and a second term describing the Lorentzian function of scattering from polymer chains in the high q region.

$$I(q) = \frac{A}{q^n} + \frac{C}{1+(q\xi)^m} + B \quad (1)$$

where n is the power-law exponent, A is the power-law coefficient, m is the Lorentz exponent, C is the Lorentz coefficient, ξ is the correlation length for the polymer chains and B is the background. The correlation length, ξ , is related to the size of the growing aggregates in the hydrogels (Bode et al., 2013). The fitted scattering curves and the fitting parameters are presented in **Figures 13c and 13d**, respectively. Both hydrogels (FAX-CL and FAX-CL-pH2) were found to be mass fractals as their power-law exponents were in the range of $1 < n < 3$. The n value of FAX-CL-pH2 was higher than that of FAX-CL, indicating a higher density of the crosslinked AX clusters in FAX-CL-pH2. In the high q range, the Lorentz exponents (m) of FAX-

CL and FAX-CL-pH2 were similar, which indicated similar compactness of these hydrogels. On the other hand, the correlation length, ξ of the two hydrogels was different, FAX-CL-pH2 having a higher value. This indicated that the regeneration process leads to the formation of larger aggregates. This difference between the hydrogels suggested that auxiliary physical interactions between AX chains may be contributing to the network formation in the case of regeneration. As observed by the rheological measurements, hydrogen bonding is promoted during the freeze-drying step in regeneration and thus, leading to larger aggregates. The density of the crosslinked aggregates is partly increased by the physical interactions during regeneration, which results in remarkably higher viscoelasticity of the regenerated hydrogels.

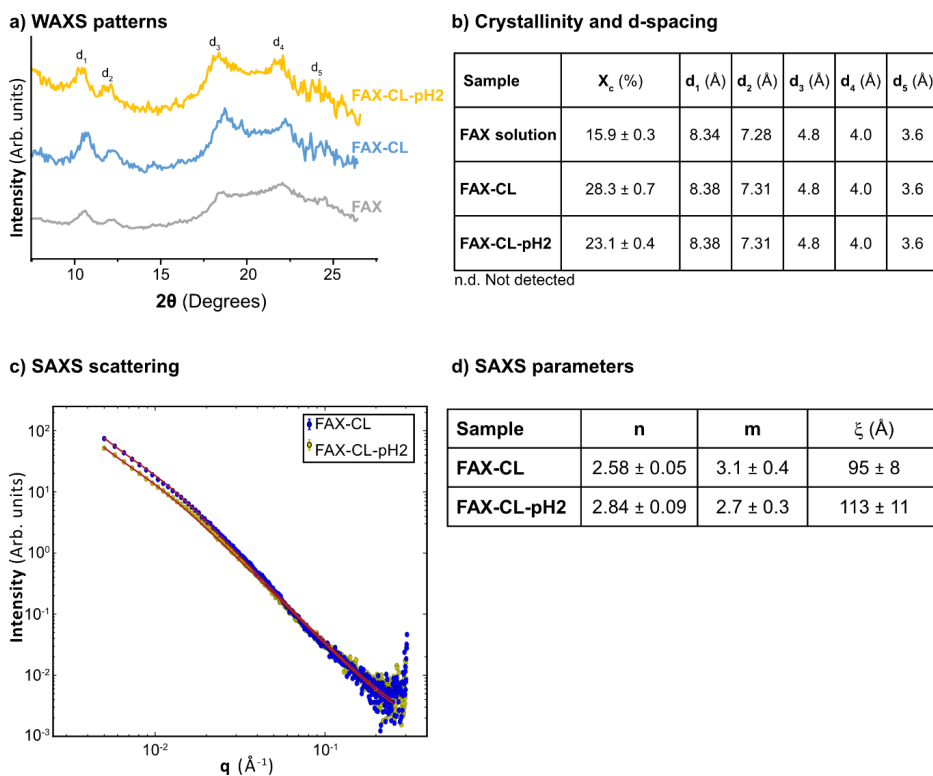


Figure 13. Scattering data of FAX solution, FAX-CL and FAX-CL-pH2. (a) WAXS curves, (b) Degree of crystallinity (X_c) and d-spacing, (c) SAXS curves with fittings, and (d) Fitting parameters of the correlation length model of SAXS data.

4.3.2 Comparison of laccase and peroxidase crosslinking of corn bran AX

AX with high DS and high FA content readily forms hydrogels with high viscosity and mechanical strength, differently from AX with low FA content and DS such as wheat bran AX. As a complex polysaccharide with high feruloylation, the crosslinking of corn bran AX may result in structurally different hydrogels. Therefore, enzymatic crosslinking of corn bran AX was performed using laccase and peroxidase and the properties of the resulting hydrogels were investigated. Moreover, to study the potential of AX hydrogels in biomedical applications, the oxidative response of human colon cell line to exposed to AX hydrogels with oxidative stress was explored as proof of concept.

The differences between laccase and peroxidase crosslinking were analyzed in terms of the conversion of monomeric FA into its dimeric forms. Firstly, the time evolution of the crosslinking reaction by both enzymes was determined by monitoring the decrease in the FA content together with the increase in the di-FA content by HPLC. The reaction by laccase (CAX-L) lasted approximately 24 h to reach the constant FA and di-FA content (**Figure 14a**). For the reaction by HRP (CAX-H), the plateau was reached almost instantly after 5 min (**Figure 14b**). This large difference indicated that the peroxidase enzyme catalyzed the crosslinking reaction faster as the coupling of FA occurs through direct interaction with H₂O₂. The coupling reaction by laccase, on the other hand, takes place rather indirectly where the electron transfer occurs in the copper cluster of laccase and thus, requires more time to reach the maximum conversion of FA.

Secondly, the phenolic acid content of CAX-L and CAX-H was measured at 48 hours of the reaction to evaluate the efficiency of the crosslinking and compared to that of uncrosslinked CAX. The phenolic acid content of CAX, CAX-L and CAX-H is presented in **Figure 14c**. CAX was strikingly rich in monomeric FA as in agreement with previous observations (Fabiola E. Ayala-Soto et al., 2014; Rudjito, Jiménez-Quero, Hamzaoui, Kohnen, & Vilaplana, 2020), which particularly emphasized the efficiency of SWE in maintaining the functional groups of hemicelluloses. Other phenolic acids as *p*-coumaric acid, sinapic acid, 5-5' di-FA and 8-8' di-FA were also observed in CAX. As occurred in the crosslinking of wheat bran AX, small peaks eluting after the 8-8' and 5-5' di-FAs were also detected in CAX. These were considered to be other forms of di-FAs, namely the 8-O-4' and 8-5' di-FAs and quantified as putative di-FAs using the response factors of the 8-8' and 5-5' di-FAs.

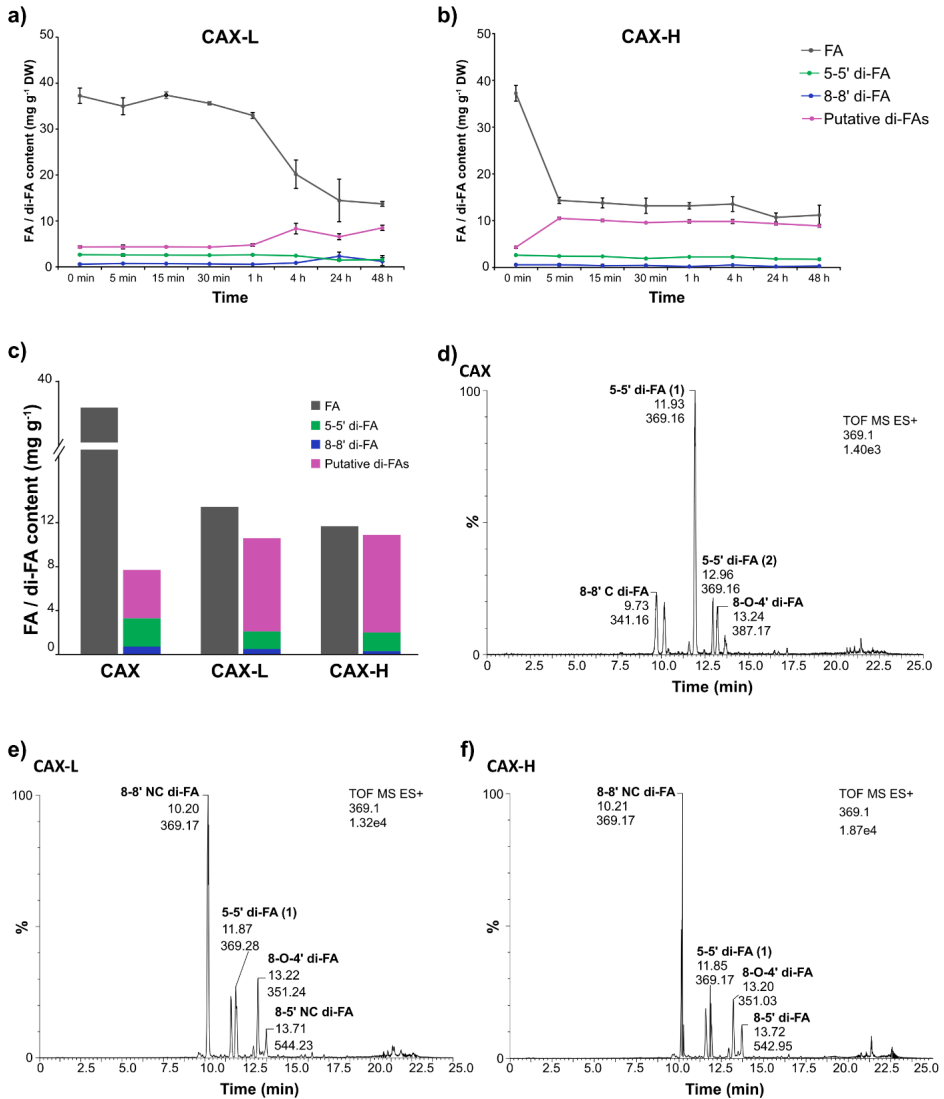


Figure 14. Decrease in FA content and increase in di-FA content by time of (a) CAX-L and (b) CAX-H, (c) Changes in the phenolic acid content of CAX after enzymatic crosslinking by laccase (CAX-L) and horseradish peroxidase (CAX-H), and (d-f) Ion extracted HPLC-ESI-MS chromatograms of CAX, CAX-L and CAX-H, respectively.

CAX contained a considerably high amount of putative di-FAs as in agreement with previous studies (Munk et al., 2020). After crosslinking by both laccase and HRP, monomeric FA content significantly decreased, and the putative di-FAs increased, verifying the successful covalent crosslinking. Comparing CAX-L and CAX-H, 62 % and 67 % of the initial FA were converted by the two enzymes, respectively. This difference could be explained by the formation of higher amounts of tri-FAs by HRP, as similar di-FA contents were measured in CAX-L and CAX-H. The results of the HPLC analysis revealed that laccase and peroxidase catalyze the oxidative coupling reaction of FA by oxidizing different positions of the molecule and hence, lead to the formation of different amounts of di-FAs and tri-FAs.

Thirdly, the different forms of di-FAs in CAX, CAX-L and CAX-H were further identified by HPLC-ESI-MS² as shown in **Figure 14d-f**. The presence of the 5-5' and 8-8' di-FAs in CAX was confirmed with two forms of each di-FA (cyclic and non-cyclic forms of the 8-8' di-FA and Ac-Am and Di-Am forms of the 5-5' di-FA). The 8-O-4' and 8-5' di-FAs were also identified in CAX, which corresponded to the assigned putative di-FAs in the HPLC chromatograms. After crosslinking, identical changes were observed in CAX-L and CAX-H in terms of the presence and intensity of the di-FA peaks. The peak eluting at 9.7 min in CAX was not detected in CAX-L and CAX-H and the intensity of the peaks at 11.9 and 12.9 min decreased. This showed that the 5-5' and 8-8'-C di-FAs were converted to other forms of di-FAs. The peaks corresponding to the 8-8' and 8-O-4' di-FAs intensified after crosslinking, as in correlation with the increase in the putative di-FAs observed in the HPLC results. The results of the HPLC-ESI-MS² analysis demonstrated that both laccase and HRP produce the same forms of di-FAs by oxidatively coupling the FA molecules.

4.3.3 Physicochemical properties and antioxidative potential of hydrogels from corn bran AX

The time evolution of G' and G'' of CAX-L and CAX-H was monitored using small amplitude oscillatory shear as presented in **Figure 15a**. Prior to the enzymatic crosslinking, the G' and G'' of the initial CAX solution were 0.2 Pa and 0.03 Pa, respectively. When the laccase crosslinking was initiated (CAX-L), a lag phase of G' was observed for approximately 65 min followed by a slight increase until 90 min, after which a sharp increase was seen and finally, a plateau region was reached at approximately 200 min. As for CAX-H, an instant increase in its G' was seen following the addition of HRP and H₂O₂, which was in correlation with the time evolution of the

FA and di-FA content of CAX-H (**Figure 14b**). Monitoring the development of G' and G'' of both hydrogels over time demonstrated that the mechanical strength of these hydrogels is directly related to the increased density of the covalent links formed by the two enzymes.

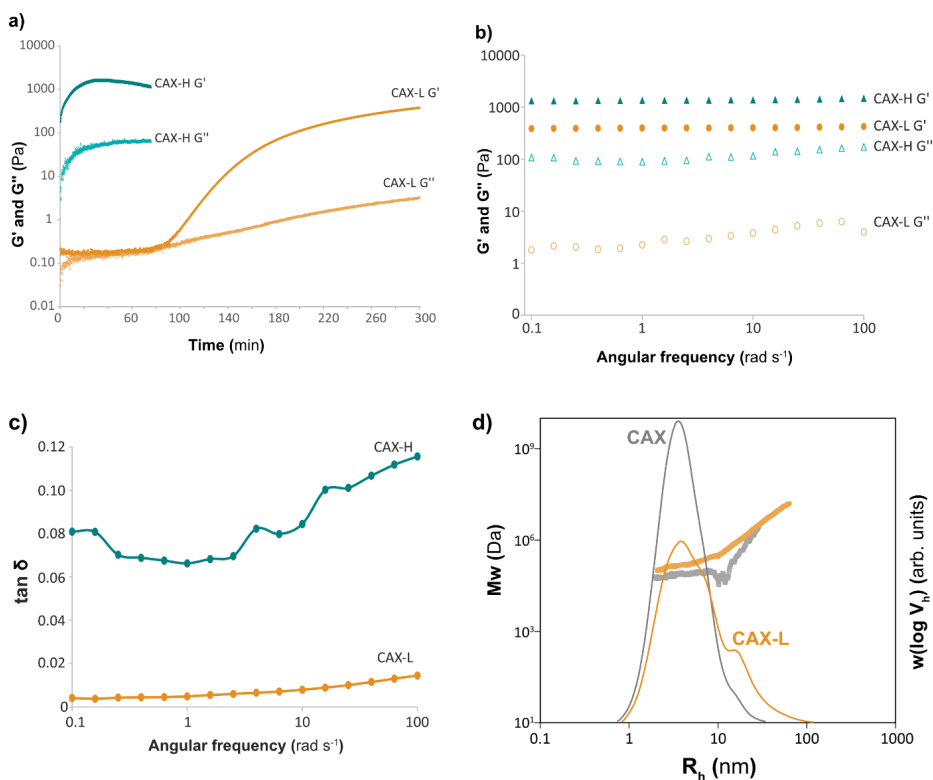


Figure 15. (a) Time evolution of gelation by laccase (CAX-L) and HRP (CAX-H), (b) Viscoelasticity of fully formed CAX hydrogels, (c) Loss tangent of CAX hydrogels, and (d) SEC of CAX solution and hydrogels.

Viscoelasticity of the hydrogels at the end of the gelation reactions was also investigated and presented in **Figure 15b**. Both CAX-L and CAX-H showed $G' > G''$ and the G' values were independent of the measured frequency, confirming their gel state. CAX-L had a lower G' than that of CAX-H however, G'' of CAX-H was significantly higher than that of CAX-L. To understand this difference between the two hydrogels, their loss tangents ($\tan \delta$) were compared as an indication of the network strength (**Figure 15c**). The $\tan \delta$ values of both hydrogels were

close to zero, which demonstrated that elastic properties prevailed (i.e. gel-like network). On the other hand, the $\tan \delta$ of CAX-L was 10-fold lower than that of CAX-H, indicating a more elastic network of CAX-L. Despite the similar number of covalent crosslinks in CAX-L and CAX-H (**Figure 14c**), this different rheological behavior of the hydrogels was attributed to (1) the different placement of the new crosslinks between AX polymers, and (2) the different reaction kinetics of laccase and HRP. According to hypothesis (1), the two enzymes place the new crosslinks on different positions, where laccase crosslinks fewer AX polymers and HRP crosslinks more individual polymers. Hence, this leads to a more heterogeneous network organization in CAX-H, which results in a lower elasticity. According to hypothesis (2), the slower reaction kinetics of laccase enable the formation of non-covalent interactions between AX aggregates in addition to the covalent crosslinks. This places the polymer chains closer to each other and contributes to the formation of a more elastic network in CAX-L.

The macromolecular structure of the CAX solution and the CAX-L and CAX-H hydrogels was characterized by SEC with MALLS detection. **Figure 15d** shows the SEC weight distribution ($w(\log V_h)$) and the size dependence of the weight-average molecular weight ($M_w(V_h)$) as a function of hydrodynamic radius (R_h). The CAX solution displayed a monomodal molar mass distribution, implying that it was composed of high molar mass AX populations as in agreement with previous observations (Rudjito et al., 2020). After crosslinking by laccase (CAX-L), a shift in the $w(\log V_h)$ to lower sizes and a higher absolute molar mass ($M_w(V_h)$) at a certain R_h was observed. These two concurrent effects indicated that the laccase crosslinking of CAX increased the absolute molar mass and lead to more compact hydrodynamic conformations. As for CAX-H, no reliable data could be obtained from the SEC analysis because it was likely filtered out during sample preparation prior to injection. This suggested that CAX-H was composed of larger covalent crosslinked polymers that could not be filtered through and detected. This was partly ascribed to the different specificity of the enzymes, as laccase appears to act on smaller polyphenols (as in early stages of lignification) and HRP can act as well on larger polymeric polyphenols (i.e. larger lignin and lignin-carbohydrate complexes) (Oinonen, Zhang, Lawoko, & Henriksson, 2015; Wallace & Fry, 1999).

The differences between the CAX hydrogels at the nanoscale level were investigated by SAXS. The correlation length model (Equation 1) was used to fit the SAXS data of CAX-L and CAX-H. The scattering curves with fitting and the fitting parameters are presented in **Figures 16a and 16b**, respectively.

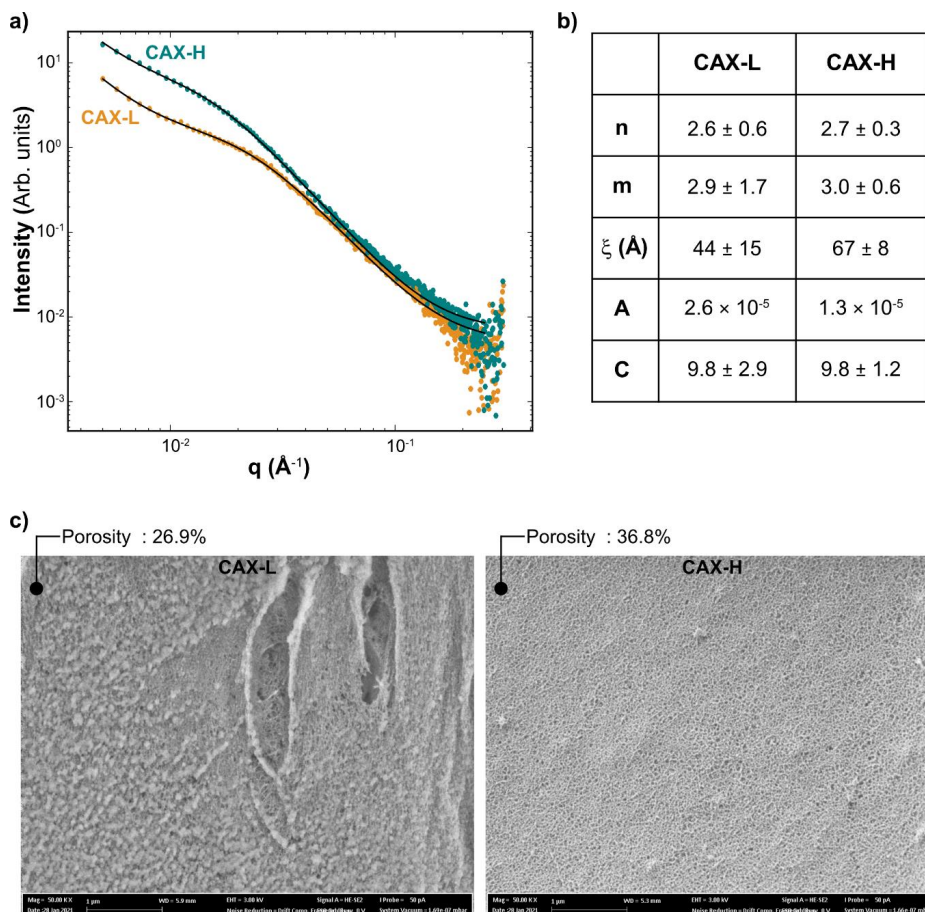


Figure 16. (a) SAXS curve of CAX-L and CAX-H, (b) Fitting parameters of the correlation length model of SAXS data, and (c) Cryo-SEM images of CAX-L and CAX-H with corresponding porosity values.

In the high q range, the Lorentz exponents (m) and the Lorentz coefficients of the two hydrogels were similar however, CAX-H had a higher correlation length, ξ . The similar m values demonstrated the similar compactness of the individual polymer chains in both hydrogels. Furthermore, both hydrogels were composed of polymer globules as indicated by their high m

values (B. Hammouda, 2016). The higher ξ of CAX-H showed that this hydrogel had larger aggregates as compared to CAX-L. This demonstrated that HRP crosslinking created larger polymeric aggregates in CAX-H, verifying the observations from the SEC-MALLS analysis. In the low q range, both hydrogels were mass fractals as their power-law exponents were in the range of $1 < n < 3$. The same n values revealed that the gel large scale structures (density of clusters) of these hydrogels were similar. On the other hand, the different power-law coefficients (A) implied differences in terms of the clustering strength (A/q^n) at the lowest measured q (0.003 \AA^{-1}) (Boualem Hammouda, Ho, & Kline, 2004). The clustering strength of CAX-L was higher (94.3) than that of CAX-H (84.3), which was likely related to the higher network strength of CAX-L as observed by viscoelasticity measurements (**Figure 15b**). As indicated by the similar compactness of the polymer chains and density of clusters, both hydrogels are of similar cluster sizes. However, their different clustering strength and correlation length suggest that the HRP crosslinking leads to the association of more polymers in the cluster networks compared to laccase and hence, results in the clumping of macromolecular chains. From the combined results of the SEC and SAXS analyses, it was hypothesized that the slow action of laccase on F-AX creates smaller and potentially homogeneous aggregates resulting in stronger and more organized clusters. HRP, on the other hand, crosslinks F-AX quickly and thus, creates larger polymeric aggregates that are possibly organized in more heterogeneous network clusters.

The morphology of CAX-L and CAX-H was studied by cryo-SEM after high pressure freezing. The microstructure of the hydrogels together with their porosity are presented in **Figure 16c**. CAX-L and CAX-H were of porous microstructure with porosity values of 26.88 % and 36.76 %, respectively. These findings indicated that CAX-L had a less dense microstructure whereas CAX-H was of a denser macromolecular organization. Seemingly, the larger polymer networks formed by HRP rendered a more porous microstructure.

Polysaccharide-based hydrogels find wide uses in biomedical applications such as wound healing and tissue engineering (Hu & Xu, 2020; Zhu et al., 2019). In this direction, AX-based hydrogels hold great potential as they are potentially non-toxic and biocompatible. Moreover, the FA substitutions of cereal AX can provide the AX hydrogels with remarkable antioxidant activity, further increasing their application potential. Therefore, the protective effects of the CAX hydrogels against ROS were evaluated by seeding the human epithelial cell line, HT-29-MTX on top of the hydrogels. The ROS production of the cells on CAX-L and CAX-H was monitored over time after inducing oxidative stress using tert-butyl hydroperoxide (TBHP) and

compared to that of alginate gel as presented in **Figure 17a-c**. The cell viability was also measured, and it was ensured that the cells survived the 3-h oxidative stress as shown in **Figure 17d**.

The cells on the alginate gel gradually produced ROS as the oxidative stress was prolonged and the concentration of TBHP was increased (**Figure 17a**). This indicated that the alginate gel was not capable of introducing a protective effect against oxidative stress and the cells suffered from injury on this gel.

The cells seeded on CAX-L and CAX-H produced significantly lower ROS compared to alginate for all the TBHP concentrations applied (**Figure 17b and 17c**). This verified that both CAX hydrogels scavenged the ROS produced by the cells, which was attributed to the antioxidant activity of the FA units attached to the source AX against intra- and extracellular ROS (Zdunska, Dana, Kolodziejczak, & Rotsztejn, 2018). A gradual increase was observed in the ROS production of the cells on CAX-L with the increased TBHP concentration and it remained constant for the concentrations of 0, 0.15 and 0.6 mM. When the TBHP concentration was 30 mM, cells produced significantly higher ROS and the viability of the cells at this concentration was lower, but still higher than in alginate (**Figure 17d**). These two effects together suggested that the cells did not survive, and CAX-L was not capable of scavenging this concentration of TBHP. As for CAX-H, the ROS production was constant at the TBHP concentrations of 0, 0.15 and 0.6 mM, similar to CAX-L. When the TBHP concentration was increased to 30 mM, the ROS production remained similar to the lower concentrations. This indicated that CAX-H is capable of providing a more powerful antioxidative function even at excessive oxidative stress as compared to CAX-L. The higher activity of CAX-H was ascribed to its higher porosity, which provides a larger surface area to scavenge the oxidants.

The results of the ROS measurements revealed that the CAX hydrogels are capable of providing protective effects against chemically-induced ROS. Among the two hydrogels, CAX-H is expected to administer better scavenging properties as it provided the HT-29-MTX cell line with higher antioxidative potential, but CAX-L is expected to provide a stronger scaffold for cell applications with its higher mechanical strength.

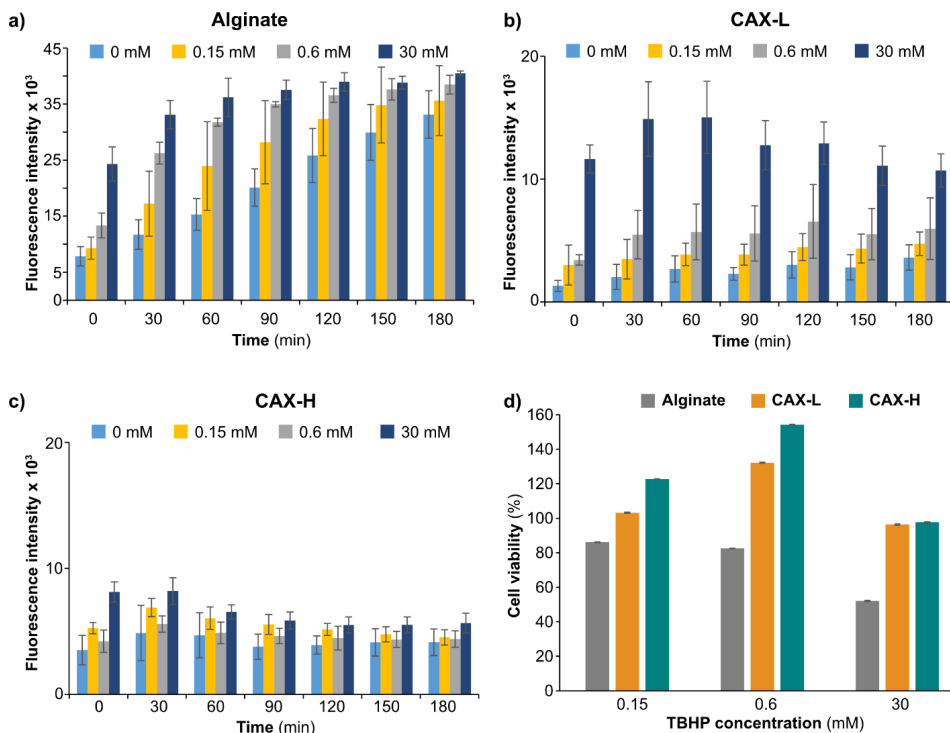


Figure 17. (a-c) Cellular ROS production after oxidative stress of alginate gel, CAX-L and CAX-H, respectively, and (d) Cell viability of HT-29-MTX cells after exposure to tert-butyl hydroperoxide (TBHP)-induced oxidative stress.

4.3.4 Comparison of the gelation mechanisms of wheat bran and corn bran AX

In this thesis, two different biomass, wheat bran and corn bran were exploited to isolate their hemicellulose fractions using subcritical water extraction. Extracted feruloylated AX from wheat bran and feruloylated AX from corn bran were then used to develop hydrogels by enzymatic crosslinking. The assembly mechanisms of these hydrogels were influenced by the molecular differences between these two hemicellulose fractions. In this section, the effect of the degree of substitution, branching pattern and feruloylation degree of these fractions on their gelation is comparatively discussed.

One of the main factors influencing the formation of hydrogels from feruloylated AX is the quantity of the FA units attached to the AX chains (Carvajal-Millan, Landillon, et al., 2005). On the other hand, other structural parameters, i.e. the degree of substitution of AX and the conformation of the chains, were observed to play a significant role in their gelation mechanism. While the highly feruloylated/highly substituted corn bran AX was able to readily form hydrogels in neutral conditions (Paper IV), wheat bran F-AX formed hydrogels with lower mechanical strength (Paper III) compared to corn bran AX. Therefore, an additional step for the wheat bran F-AX, i.e. regeneration, was necessary to induce the formation of hydrogels with mechanical spectra comparable to those of corn bran AX. Similar mechanical spectra were indeed reached when regeneration was employed on the crosslinked wheat bran F-AX (FAX-CL), regardless of the pH conditions. The results obtained from SEC, rheology, WAXS and SAXS measurements indicated that enzymatic crosslinking of F-AX leads to the re-organization of the polymeric chains and increases intermolecular (backbone) interactions. This, in turn, results in more compact polymeric conformations and higher-ordered chain packing. The heterogeneous localization of the crosslinks randomly forms ordered structures, which results in the formation of polysaccharide aggregates and larger clusters (composed of aggregates). When FAX-CL was regenerated at pH 2.0 after freeze-drying, physical interactions between F-AX chains were observed to increase and the distance between the chains decreased. In the regenerated hydrogel (FAX-CL-pH2) the aggregates further grow and form larger and expanded clusters. These clusters result in higher viscoelasticity of the regenerated hydrogel, which is similar to that of the laccase-crosslinked corn bran AX hydrogel (CAX-L).

Corn bran AX, on the other hand, possesses a very complex molecular structure with oligomeric side branches, restricting interactions between the xylan backbones compared to low-substituted wheat bran AX. Therefore, the gelation mechanism of corn bran AX is hypothesized to depend on interactions between side chains (intra- or intermolecular), together with covalent crosslinks formed between FA moieties. The high feruloylation of corn bran AX further makes the covalent crosslinks denser than those seen in lower feruloylated wheat bran AX. In the WAXS patterns of corn bran AX, no crystal peaks were observed, confirming that crystallinity does not play a role in the gelation of this xylan. Based on these hypotheses, a schematic comparison of the gelation mechanisms of low-substituted wheat bran F-AX and highly substituted corn bran F-AX is presented in **Figure 18**. Note that this comparison is based on laccase crosslinking of both AX as peroxidase crosslinking of wheat bran F-AX was not carried out in this study.

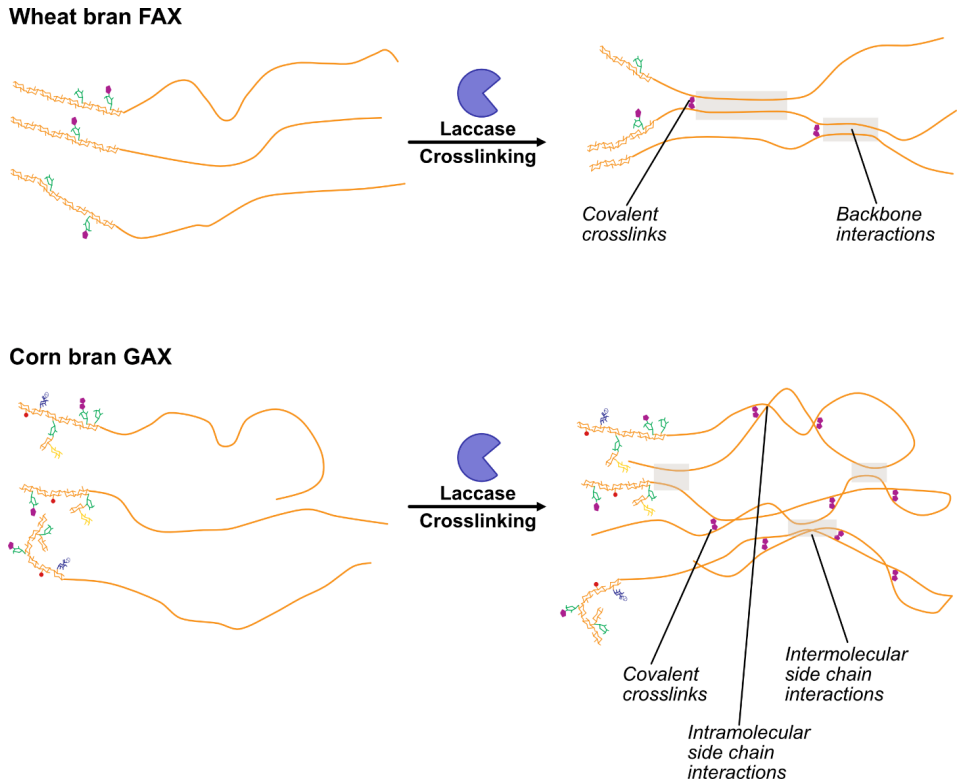


Figure 18. Schematic comparison of the gelation mechanism of low-substituted wheat bran feruloylated AX and highly substituted corn bran feruloylated AX. The gelation of wheat bran AX proceeds through covalent crosslinks and intermolecular interactions between unsubstituted regions of the xylan backbone, and/or larger-scale aggregative network interactions. The gelation of corn bran AX occurs through covalent crosslinks and intra- and intermolecular side chain interactions.

5 CONCLUSIONS

Hemicelluloses were fractionated from cereal bran and valorized into films and hydrogels using various strategies.

The impact of the prior protein isolation on SWE of feruloylated arabinoxylans was evaluated at two different temperatures. The protein isolation step loosened up the microstructure of wheat bran, enabling higher polysaccharide yields in the subsequent SWE and preserving available FA moieties. The time extracts contained different amounts of monosaccharides demonstrating the gradual progression of subcritical water through the cell wall. Higher extraction temperatures enhanced the yields with faster isolation of the polysaccharides but significantly reduced the molar mass. The protein isolation step or extraction temperatures did not substantially influence the FA content of the extracts and all extracts demonstrated considerable antioxidant activity.

Feruloylated arabinoxylans were further isolated from wheat bran by scaled-up SWE and alkaline extraction. SWE led to the isolation of AX with low DS (A/X: 0.2), significant FA content (10.3 mg/g) and polymeric molar mass (8×10^4 Da). The alkaline extraction resulted in AX with high yields and higher molar mass however without any feruloylation. Chemical modification of subcritical water- and alkaline-extracted wheat bran AX and a reference wheat endosperm AX was achieved by acetylation. The DA of AXs was affected by the purity of the extracts and a lower DA was obtained for the subcritical water extracted AX (DA: 1.2) compared to the alkaline extracted AX (DA: 1.4) and endosperm AX (DA: 1.7).

Barrier films were prepared from the native and acetylated AX, and the influence of their structural features on the film properties was evaluated. The higher molar mass and DS of the native AX resulted in better thermal stability and mechanical properties. Sorbitol plasticization of the films significantly improved their water vapor permeability. The oxygen permeability of the films from the native AX was excellent regardless of their structural differences. The acetylation of AXs improved the thermal stability of their films however, the mechanical and barrier properties were not influenced by this modification. Higher WVVP of the acetylated films compared to the sorbitol-plasticized films from the native AX demonstrated the potency of sorbitol plasticization for developing bio-based films with good barrier properties. Furthermore, the influence of external incorporation of free FA on the antioxidant properties of

the films was evaluated in comparison with AX with bound FA. Higher antioxidant activity was measured in the AX films with bound FA, which demonstrated the potential use of subcritical water extracted AX in active food packaging applications.

Feruloylated AX from wheat bran was transformed into hydrogels by laccase crosslinking, and a subsequent regeneration process. The efficiency of the crosslinking was verified by the conversion of monomeric FA into its dehydromers. The enzymatic crosslinking increased the molecular weight and resulted in a closer-packing of the AX chains. The regeneration process significantly increased the viscosity and viscoelasticity of the resulting hydrogels for all tested pH (2.0-7.0). It was demonstrated that the rheological properties of the feruloylated AX hydrogels could be tuned by chemical and physical effects. The microstructure of both the crosslinked and regenerated hydrogels was porous, the former exhibiting higher porosity. The gelation of the low-substituted wheat bran AX was shown to be governed not only by the covalent crosslinks but also by the crystallinity, and physical interactions between the unsubstituted regions in the xylan backbone and between larger-scale AX aggregates.

Hydrogels were also developed from corn bran feruloylated AX using laccase and peroxidase crosslinking. Peroxidase crosslinking occurred faster than laccase however, both enzymes formed the same forms of FA dehydromers. Laccase formed hydrogels with a more elastic network while peroxidase resulted in the occurrence of larger covalent crosslinked polymers. The network of the peroxidase-crosslinked hydrogel was composed of larger aggregates than that of the laccase-crosslinked one and its clustering strength was lower. The protective effect of the corn bran AX hydrogels against oxidative stress was evaluated in direct contact with human colon cells. Both AX hydrogels had adequate scavenging activity against the reactive oxygen species produced by the cells under chemically-induced oxidative stress. The scavenging activity of the peroxidase-crosslinked hydrogel was higher, promising a better biological matrix for cell applications.

In this study, the conversion of cereal bran hemicelluloses into multifunctional materials has been demonstrated. The role of the molecular properties of hemicelluloses in their material formation ability has been targeted. The adjustability of the properties of these polysaccharides opens up new possibilities for their future use. From an application aspect, the studied materials demonstrated potential to be applied in food and biomedical products where pH stability and antioxidant properties are essential.

6 UNITED NATIONS SUSTAINABLE DEVELOPMENT GOALS

The United Nations (UN) has adopted 17 sustainable development goals (SDGs) as a universal call to ensure a sustainable future. This thesis aiming at the improved use of hemicelluloses from cereal by-products is well-suited with the four of these goals. The development of bio-based materials from cereal bran is strongly associated with SDG 3 – No Hunger as the materials developed during this thesis have the potential to minimize food waste and extend the shelf life of foodstuff. SDG 9 – Industry, Innovation and Infrastructure describes the need for innovative work for energy efficiency and promotes the implementation of high-tech products. This thesis is related to this goal as it has generated innovative future materials. The work presented here is particularly associated with SDG 12 – Responsible Production and Consumption as the materials developed in this thesis contribute to the aim of ‘doing more with less’. Global material consumption is increasing and therefore, the importance of resource efficiency is highlighted with this goal. In this direction, using cereal by-products as renewable and underutilized resources would help to use earth’s resources more efficiently by valorizing them into innovative products. Moreover, SDG 14 – Life Below Water highlights the need for more environmentally friendly materials and eliminating plastic waste from our oceans and promotes attempts towards the conservation of ecosystems and biodiversity. Considering that oil-based materials are currently the largest pollutants to oceans, this thesis would provide more ocean-friendly materials that could help to reduce the use of oil sources. The outputs of this work have the potential to be used as biodegradable products that will not accumulate in oceans.

7 FUTURE PERSPECTIVES

This thesis focused on efficient fabrication and comprehensive characterization of arabinoxylan-based films and hydrogels. Several other aspects can still be addressed in order to reach the full potential of cereal arabinoxylans. Some suggestions for further studies that could follow up on this thesis are listed as follows.

- Developing more effective chemical modification strategies for arabinoxylans to enhance their hydrophobicity and hence improve the barrier properties of their films.
- Implementing thermo-mechanical processing (e.g. by extrusion or compression molding) of arabinoxylan-based films on large scale to investigate their commercial potential.
- Validating the potential of arabinoxylan-based films and hydrogels in actual food (packaging, texturizing gelling agents) and biomedical (drug release, wound healing, tissue engineering) applications.
- Studying the interactions between all components of the cereal cell wall (cellulose, arabinoxylan, mixed linkage β -glucans, and lignin) to understand its assembly and also to fabricate materials with advanced properties.

8 ACKNOWLEDGEMENTS

I would like to express my sincere gratitude to my supervisor Assoc. Prof. Francisco Vilaplana for providing me with the opportunity to work with you. Your guidance, dedication and all-time positive approach enabled me to confidently work on this project. Many thanks to Dr. Rosana Moriana for your endless source of knowledge and for being a mentor for me. Many thanks to my co-supervisor Dr. Amparo Jiménez Quero for your help, technical knowledge, practicality and energy.

I had the pleasure of working with many great collaborators and co-authors. Thanks to Dr. Carolin Menzel for your invaluable help and friendship. Thanks to Dr. Elisa Arte, Assoc. Prof. Kati Katina, Dr. Danila Carvalho, Prof. Mikael Lindström, Assoc. Prof. Olena Sevastyanova, and Assist. Prof. Thomas Crouzier. Special thanks to Dr. Patricia Lopez-Sanchez for spending so much time with me, and for me during experiments and writing. Your guidance and knowledge are invaluable. Million thanks to Dr. Tomás Plivelic for patiently teaching me and helping to unravel the mystery of X-rays.

The Swedish Research Council FORMAS and Lantmännen Research Foundation are thanked for funding my PhD project. I would like to acknowledge Dr. Annelie Moldin for helpful discussions. Sweden's innovation agency VINNOVA and Tresearch are acknowledged for providing sources for SAXS and cryo-SEM. Dr. Barbara Berke, Dr. Cheng Choo and Dr. Sara Henriksson are sincerely thanked for their generous help.

Thanks to Prof. Per Berglund for reviewing my thesis.

My deepest thanks to all members of the Division of Glycoscience, and colleagues at the Department of Industrial Biotechnology on Plan 2 for making our environment so warm and friendly. I would also like to thank colleagues at the Department of Fiber and Polymer Technology for spending time with me and sharing their precious equipment. Many thanks to previous and current members of the Vilaplana Group.

My closest colleagues Kun and Reskandi, thank you for your candid friendship! Kun, special thanks for your endless patience with me during the cell experiments. Reskandi, special thanks for hearing my complaints. You are both great, and I believe you will reach all your goals in life.

Finally, I would like to thank my beloved family, Sibel, Orhan and Sare Yilmaz for your constant love and support. My deepest gratitude goes to my husband Kadir, the dearest person in my life. Thank you for supporting me on this adventure and all paths of life!

9 REFERENCES

- AACC. (2003). Approved Methods of the American Association of Cereal Chemists Approved Methods of Analysis (11th ed.). St. Paul: AACC International.
<http://methods.aaccnet.org/summaries/44-15-02.aspx>.
- Aburto, J., Alric, I., Thiebaut, S., Borredon, E., Bikiaris, D., Prinos, J., & Panayiotou, C. (1999). Synthesis, characterization, and biodegradability of fatty-acid esters of amylose and starch. *Journal of Applied Polymer Science*, 74(6), 1440-1451. doi:10.1002/(sici)1097-4628(19991107)74:6<1440::Aid-app17>3.0.Co;2-v
- Adom, K. K., & Liu, R. H. (2002). Antioxidant activity of grains. *J Agric Food Chem*, 50(21), 6182-6187. doi:10.1021/jf0205099
- Aguedo, M., Fougnyes, C., Dermience, M., & Richel, A. (2014). Extraction by three processes of arabinoxylans from wheat bran and characterization of the fractions obtained. *Carbohydr Polym*, 105(Supplement C), 317-324. doi:10.1016/j.carbpol.2014.01.096
- Albersheim, P., Nevins, D. J., English, P. D., & Karr, A. (1967). A method for the analysis of sugars in plant cell-wall polysaccharides by gas-liquid chromatography. *Carbohydrate Research*, 5(3), 340-345. doi:10.1016/s0008-6215(00)80510-8
- Anderson, C., & Simsek, S. (2019). How Do Arabinoxylan Films Interact with Water and Soil? *Foods*, 8(6). doi:10.3390/foods8060213
- Antoine, C., Peyron, S., Mabilille, F., Lapiere, C., Bouchet, B., Abecassis, J., & Rouau, X. (2003). Individual contribution of grain outer layers and their cell wall structure to the mechanical properties of wheat bran. *J Agric Food Chem*, 51(7), 2026-2033. doi:10.1021/jf0261598
- Appeldoorn, M. M., Kabel, M. A., Van Eylen, D., Gruppen, H., & Schols, H. A. (2010). Characterization of oligomeric xylan structures from corn fiber resistant to pretreatment and simultaneous saccharification and fermentation. *J Agric Food Chem*, 58(21), 11294-11301. doi:10.1021/jf102849x
- Apprich, S., Tirpanalan, Ö., Hell, J., Reisinger, M., Böhmendorfer, S., Siebenhandl-Ehn, S., . . . Kneifel, W. (2014). Wheat bran-based biorefinery 2: Valorization of products. *LWT - Food Science and Technology*, 56(2), 222-231. doi:10.1016/j.lwt.2013.12.003
- Arte, E., Huang, X., Nordlund, E., & Katina, K. (2019). Biochemical characterization and technofunctional properties of bioprocessed wheat bran protein isolates. *Food Chem*, 289, 103-111. doi:10.1016/j.foodchem.2019.03.020
- ASTM. (2016). Standard Test Methods for Water Vapor Transmission of Materials, Designation E96/E96M - 16. In.
- Aston, R., Sewell, K., Klein, T., Lawrie, G., & Grøndahl, L. (2016). Evaluation of the impact of freezing preparation techniques on the characterisation of alginate hydrogels by cryo-SEM. *European Polymer Journal*, 82, 1-15. doi:10.1016/j.eurpolymj.2016.06.025
- Ayala-Soto, F. E., Serna-Saldívar, S. O., García-Lara, S., & Pérez-Carrillo, E. (2014). Hydroxycinnamic acids, sugar composition and antioxidant capacity of arabinoxylans extracted from different maize fiber sources. *Food Hydrocolloids*, 35, 471-475. doi:10.1016/j.foodhyd.2013.07.004
- Ayala-Soto, F. E., Serna-Saldívar, S. O., Pérez-Carrillo, E., & García-Lara, S. (2014). Relationship between hydroxycinnamic profile with gelation capacity and rheological properties of arabinoxylans extracted from different maize fiber sources. *Food Hydrocolloids*, 39, 280-285. doi:10.1016/j.foodhyd.2014.01.017

- Ayala-Soto, F. E., Serna-Saldivar, S. O., & Weltri-Chanes, J. (2016). Effect of processing time, temperature and alkali concentration on yield extraction, structure and gelling properties of corn fiber arabinoxylans. *Food Hydrocolloids*, *60*, 21-28. doi:10.1016/j.foodhyd.2016.03.014
- Azeredo, H. M. C., Kontou-Vrettou, C., Moates, G. K., Wellner, N., Cross, K., Pereira, P. H. F., & Waldron, K. W. (2015). Wheat straw hemicellulose films as affected by citric acid. *Food Hydrocolloids*, *50*, 1-6. doi:10.1016/j.foodhyd.2015.04.005
- Barron, C., Surget, A., & Rouau, X. (2007). Relative amounts of tissues in mature wheat (*Triticum aestivum* L.) grain and their carbohydrate and phenolic acid composition. *Journal of Cereal Science*, *45*(1), 88-96. doi:10.1016/j.jcs.2006.07.004
- Bi, R., Berglund, J., Vilaplana, F., McKee, L. S., & Henriksson, G. (2016). The degree of acetylation affects the microbial degradability of mannans. *Polymer Degradation and Stability*, *133*, 36-46. doi:10.1016/j.polymdegradstab.2016.07.009
- Bode, F., da Silva, M. A., Smith, P., Lorenz, C. D., McCullen, S., Stevens, M. M., & Dreiss, C. A. (2013). Hybrid processes in enzymatically gelled gelatin: impact on , macroscopic properties and cellular response. *Soft Matter*, *9*(29), 6986-6999. doi:10.1039/c3sm00125c
- Borjesson, M., Larsson, A., Westman, G., & Strom, A. (2018). Periodate oxidation of xylan-based hemicelluloses and its effect on their thermal properties. *Carbohydr Polym*, *202*, 280-287. doi:10.1016/j.carbpol.2018.08.110
- Borjesson, M., Westman, G., Larsson, A., & Strom, A. (2019). Thermoplastic and Flexible Films from Arabinoxylan. *ACS Applied Polymer Materials*, *1*(6), 1443-1450. doi:10.1021/acsapm.9b00205
- Bradford, M. M. (1976). A rapid and sensitive method for the quantitation of microgram quantities of protein utilizing the principle of protein-dye binding. *Anal Biochem*, *72*(1), 248-254. doi:10.1006/abio.1976.9999
- Brand-Williams, W., Cuvelier, M. E., & Berset, C. (1995). Use of a free radical method to evaluate antioxidant activity. *LWT - Food Science and Technology*, *28*(1), 25-30. doi:10.1016/s0023-6438(95)80008-5
- Buanafina, M. M. d. O. (2009). Feruloylation in grasses: current and future perspectives. *Mol Plant*, *2*(5), 861-872. doi:10.1093/mp/ssp067
- Buchanan, C. M., Buchanan, N. L., Debenham, J. S., Gatenholm, P., Jacobsson, M., Shelton, M. C., . . . Wood, M. D. (2003). Preparation and characterization of arabinoxylan esters and arabinoxylan ester/cellulose ester polymer blends. *Carbohydrate Polymers*, *52*(4), 345-357. doi:10.1016/s0144-8617(02)00290-4
- Calvert, P. (2009). Hydrogels for Soft Machines. *Advanced Materials*, *21*(7), 743-756. doi:10.1002/adma.200800534
- Carvajal-Millan, E., Guigliarelli, B., Belle, V., Rouau, X., & Micard, V. (2005). Storage stability of laccase induced arabinoxylan gels. *Carbohydrate Polymers*, *59*(2), 181-188. doi:10.1016/j.carbpol.2004.09.008
- Carvajal-Millan, E., Guilbert, S., Morel, M. H., & Micard, V. (2005). Impact of the structure of arabinoxylan gels on their rheological and protein transport properties. *Carbohydrate Polymers*, *60*(4), 431-438. doi:10.1016/j.carbpol.2005.02.014
- Carvajal-Millan, E., Landillon, V., Morel, M. H., Rouau, X., Doublier, J. L., & Micard, V. (2005). Arabinoxylan gels: impact of the feruloylation degree on their structure and properties. *Biomacromolecules*, *6*(1), 309-317. doi:10.1021/bm049629a
- Chateigner-Boutin, A. L., Ordaz-Ortiz, J. J., Alvarado, C., Bouchet, B., Durand, S., Verherbruggen, Y., . . . Saulnier, L. (2016). Developing Pericarp of Maize: A Model to Study Arabinoxylan Synthesis and Feruloylation. *Front Plant Sci*, *7*(1476), 1476. doi:10.3389/fpls.2016.01476

- Cocero, M. J., Cabeza, Á., Abad, N., Adamovic, T., Vaquerizo, L., Martínez, C. M., & Pazo-Cepeda, M. V. (2018). Understanding biomass fractionation in subcritical & supercritical water. *The Journal of Supercritical Fluids*, *133*, 550-565. doi:10.1016/j.supflu.2017.08.012
- Cui, S. W., Wu, Y., & Ding, H. (2013). The range of dietary fibre ingredients and a comparison of their technical functionality. In J. A. Delcour & K. Poutanen (Eds.), *Fibre-Rich and Wholegrain Foods* (pp. 96-119): Woodhead Publishing.
- Deralia, P. K., du Poset, A. M., Lund, A., Larsson, A., Strom, A., & Westman, G. (2021). Hydrophobization of arabinoxylan with n-butyl glycidyl ether yields stretchable thermoplastic materials. *Int J Biol Macromol*, *188*, 491-500. doi:10.1016/j.ijbiomac.2021.08.041
- Deralia, P. K., du Poset, A. M., Lund, A., Larsson, A., Ström, A., & Westman, G. (2021). Oxidation Level and Glycidyl Ether Structure Determine Thermal Processability and Thermomechanical Properties of Arabinoxylan-Derived Thermoplastics. *ACS Applied Bio Materials*, *4*(4), 3133-3144. doi:10.1021/acsbam.0c01550
- Doner, L. W., Chau, H. K., Fishman, M. L., & Hicks, K. B. (1998). An Improved Process for Isolation of Corn Fiber Gum. *Cereal Chemistry Journal*, *75*(4), 408-411. doi:10.1094/cchem.1998.75.4.408
- Ebringerová, A. (2005). Structural Diversity and Application Potential of Hemicelluloses. *Macromolecular Symposia*, *232*(1), 1-12. doi:10.1002/masy.200551401
- Ebringerová, A., & Heinze, T. (2000). Xylan and xylan derivatives – biopolymers with valuable properties, 1. Naturally occurring xylans structures, isolation procedures and properties. *Macromolecular Rapid Communications*, *21*(9), 542-556. doi:10.1002/1521-3927(20000601)21:9<542::aid-marc542>3.3.co;2-z
- Ebringerová, A., Hromádková, Z., & Berth, G. (1994). Structural and molecular properties of a water-soluble arabinoxylan-protein complex isolated from rye bran. *Carbohydrate Research*, *264*(1), 97-109. doi:10.1016/0008-6215(94)00183-9
- Egues, I., Stepan, A. M., Eceiza, A., Toriz, G., Gatenholm, P., & Labidi, J. (2014). Corncob arabinoxylan for new materials. *Carbohydrate Polymers*, *102*, 12-20. doi:10.1016/j.carbpol.2013.11.011
- Fang, J. M., Sun, R., Fowler, P., Tomkinson, J., & Hill, C. A. S. (1999). Esterification of wheat straw hemicelluloses in the N,N-dimethylformamide/lithium chloride homogeneous system. *Journal of Applied Polymer Science*, *74*(9), 2301-2311. doi:10.1002/(sici)1097-4628(19991128)74:9<2301::aid-app20>3.0.co;2-7
- FAOSTAT. (2019). FAO Statistics Division, 2019: <http://www.Fao.Org/faostat/en/#data/qcl>.
- Figuerola-Espinoza, M. C., Poulsen, C., Borch Soe, J., Zargahi, M. R., & Rouau, X. (2004). Enzymatic solubilization of arabinoxylans from native, extruded, and high-shear-treated rye bran by different endo-xylanases and other hydrolyzing enzymes. *J Agric Food Chem*, *52*(13), 4240-4249. doi:10.1021/jf034809h
- Fincher, G. B., & Stone, B. A. (2004). CEREALS | Chemistry of Nonstarch Polysaccharides. In *Encyclopedia of Grain Science* (pp. 206-223). Oxford: Elsevier.
- Fundador, N. G. V., Enomoto-Rogers, Y., Takemura, A., & Iwata, T. (2012). Syntheses and characterization of xylan esters. *Polymer*, *53*(18), 3885-3893. doi:10.1016/j.polymer.2012.06.038
- Gabrieli, I., & Gatenholm, P. (1998). Preparation and properties of hydrogels based on hemicellulose. *Journal of Applied Polymer Science*, *69*(8), 1661-1667. doi:10.1002/(sici)1097-4628(19980822)69:8<1661::Aid-app19>3.0.Co;2-x
- Gartaula, G., Dhital, S., Pleming, D., & Gidley, M. J. (2017). Isolation of wheat endosperm cell walls: Effects of non-endosperm flour components on structural analyses. *Journal of Cereal Science*, *74*, 165-173. doi:10.1016/j.jcs.2017.02.004

- Gáspár, M., Juhász, T., Szengyel, Z., & Réczey, K. (2005). Fractionation and utilisation of corn fibre carbohydrates. *Process Biochemistry*, 40(3-4), 1183-1188. doi:10.1016/j.procbio.2004.04.004
- Gennadios, A., Weller, C. L., & Gooding, C. H. (1994). Measurement errors in water vapor permeability of highly permeable, hydrophilic edible films. *Journal of Food Engineering*, 21(4), 395-409. doi:10.1016/0260-8774(94)90062-0
- Gong, L. X., Wang, H. N., Wang, T. X., Liu, Y. L., Wang, J., & Sun, B. G. (2019). Feruloylated oligosaccharides modulate the gut microbiota in vitro via the combined actions of oligosaccharides and ferulic acid. *Journal of Functional Foods*, 60, 103453. doi:ARTN 103453 10.1016/j.jff.2019.103453
- Gröndahl, M., & Gatenholm, P. (2007). Oxygen Barrier Films Based on Xylans Isolated from Biomass. In *Materials, Chemicals, and Energy from Forest Biomass* (Vol. 954, pp. 137-152): American Chemical Society.
- Gwirtz, J. A., & Garcia-Casal, M. N. (2014). Processing maize flour and corn meal food products. *Ann N Y Acad Sci*, 1312(1), 66-75. doi:10.1111/nyas.12299
- Hammouda, B. (2016). Probing Nanoscale Structures—The SANS Toolbox https://www.ncnr.nist.gov/staff/hammouda/the_SANS_toolbox.pdf. National Institute of Standards Technology Center for Neutron Research; Gaithersburg, MD.
- Hammouda, B., Ho, D. L., & Kline, S. (2004). Insight into Clustering in Poly(ethylene oxide) Solutions. *Macromolecules*, 37(18), 6932-6937. doi:10.1021/ma049623d
- Heikkinen, S., Jacquemin, L., Rouilly, A., Sablayrolles, C., Tenkanen, M., & Pontalier, P.-Y. (2016). Comparison of two wheat bran extracts in the sheet extrusion process. *Industrial Crops and Products*, 91, 1-5. doi:10.1016/j.indcrop.2016.06.020
- Heikkinen, S. L., Mikkonen, K. S., Koivisto, P., Heikkilä, M. I., Pirkkalainen, K., Liljeström, V., . . . Tenkanen, M. (2014). Long-Term Physical Stability of Plasticized Hemicellulose Films. *BioResources; Vol 9, No 1 (2014)*.
- Heikkinen, S. L., Mikkonen, K. S., Pirkkalainen, K., Serimaa, R., Joly, C., & Tenkanen, M. (2013). Specific enzymatic tailoring of wheat arabinoxylan reveals the role of substitution on xylan film properties. *Carbohydrate Polymers*, 92(1), 733-740. doi:10.1016/j.carbpol.2012.09.085
- Hemery, Y., Rouau, X., Lullien-Pellerin, V., Barron, C., & Abecassis, J. (2007). Dry processes to develop wheat fractions and products with enhanced nutritional quality. *Journal of Cereal Science*, 46(3), 327-347. doi:10.1016/j.jcs.2007.09.008
- Hoffman, A. S. (2012). Hydrogels for biomedical applications. *Advanced drug delivery reviews*, 64, 18-23. doi:10.1016/j.addr.2012.09.010
- Höije, A., Gröndahl, M., Tømmeraaas, K., & Gatenholm, P. (2005). Isolation and characterization of physicochemical and material properties of arabinoxylans from barley husks. *Carbohydrate Polymers*, 61(3), 266-275. doi:10.1016/j.carbpol.2005.02.009
- Hoije, A., Sternemalm, E., Heikkinen, S., Tenkanen, M., & Gatenholm, P. (2008). Material properties of films from enzymatically tailored arabinoxylans. *Biomacromolecules*, 9(7), 2042-2047. doi:10.1021/bm800290m
- Hollmann, J., Elbegzaya, N., Pawelzik, E., & Lindhauer, M. G. (2009). Isolation and characterization of glucuronoarabinoxylans from wheat bran obtained by classical and ultrasound-assisted extraction methods. *Quality Assurance and Safety of Crops & Foods*, 1(4), 231-239. doi:10.1111/j.1757-837X.2009.00039.x
- Hromadkova, Z., Paulsen, B. S., Polovka, M., Kostalova, Z., & Ebringerova, A. (2013). Structural features of two heteroxylan polysaccharide fractions from wheat bran with anti-complementary and antioxidant activities. *Carbohydr Polym*, 93(1), 22-30. doi:10.1016/j.carbpol.2012.05.021

- Hu, H., & Xu, F. J. (2020). Rational design and latest advances of polysaccharide-based hydrogels for wound healing. *Biomater Sci*, 8(8), 2084-2101. doi:10.1039/d0bm00055h
- Huisman, M. M. H., Schols, H. A., & Voragen, A. G. J. (2000). Glucuronoarabinoxylans from maize kernel cell walls are more complex than those from sorghum kernel cell walls. *Carbohydrate Polymers*, 43(3), 269-279. doi:10.1016/s0144-8617(00)00154-5
- Iiyama, K., Lam, T., & Stone, B. A. (1994). Covalent Cross-Links in the Cell Wall. *Plant Physiol*, 104(2), 315-320.
- Iiyama, K., Lam, T. B. T., & Stone, B. A. (1990). Phenolic acid bridges between polysaccharides and lignin in wheat internodes. *Phytochemistry*, 29(3), 733-737. doi:10.1016/0031-9422(90)80009-6
- Iravani, S., Fitchett, C. S., & Georget, D. M. R. (2011). Physical characterization of arabinoxylan powder and its hydrogel containing a methyl xanthine. *Carbohydrate Polymers*, 85(1), 201-207. doi:10.1016/j.carbpol.2011.02.017
- Izydorczyk, M. S., & Biliaderis, C. (2007). Arabinoxylans: Technologically and Nutritionally Functional Plant Polysaccharides. In *Functional Food Carbohydrates*: CRC Press.
- Izydorczyk, M. S., & Biliaderis, C. G. (1995). Cereal arabinoxylans: advances in structure and physicochemical properties. *Carbohydrate Polymers*, 28(1), 33-48. doi:10.1016/0144-8617(95)00077-1
- Izydorczyk, M. S., & MacGregor, A. W. (2000). Evidence of intermolecular interactions of β -glucans and arabinoxylans. *Carbohydrate Polymers*, 41(4), 417-420. doi:10.1016/s0144-8617(99)00151-4
- Jerkovic, A., Kriegl, A. M., Bradner, J. R., Atwell, B. J., Roberts, T. H., & Willows, R. D. (2010). Strategic distribution of protective proteins within bran layers of wheat protects the nutrient-rich endosperm. *Plant Physiol*, 152(3), 1459-1470. doi:10.1104/pp.109.149864
- Jordbruksverket. (2009). Facts about Swedish Agriculture. *Jordbruksverket*, https://www2.jordbruksverket.se/webdav/files/SJV/trycksaker/Pdf_ovriqt/ovr2qb.pdf.
- Kale, M. S., Hamaker, B. R., & Campanella, O. H. (2013). Alkaline extraction conditions determine gelling properties of corn bran arabinoxylans. *Food Hydrocolloids*, 31(1), 121-126. doi:10.1016/j.foodhyd.2012.09.011
- Kelzer, J. M., Kononoff, P. J., Tedeschi, L. O., Jenkins, T. C., Karges, K., & Gibson, M. L. (2010). Evaluation of protein fractionation and ruminal and intestinal digestibility of corn milling co-products. *J Dairy Sci*, 93(6), 2803-2815. doi:10.3168/jds.2009-2460
- Khalighi, S., Berger, R. G., & Ersoy, F. (2019). Cross-Linking of Wheat Bran Arabinoxylan by Fungal Laccases Yields Firm Gels. *Processes*, 8(1). doi:doi.org/10.3390/pr8010036
- Kong, W. Q., Gao, C. D., Hu, S. F., Ren, J. L., Zhao, L. H., & Sun, R. C. (2017). Xylan-Modified-Based Hydrogels with Temperature/pH Dual Sensitivity and Controllable Drug Delivery Behavior. *Materials (Basel)*, 10(3), 304. doi:10.3390/ma10030304
- Krochta, J. M., & DeMulder-Johnston, C. (1997). Edible and biodegradable polymer films: Challenges and opportunities. *Food Technology*, 51(2), 61-74.
- Kuzmenko, V., Hagg, D., Toriz, G., & Gatenholm, P. (2014). In situ forming spruce xylan-based hydrogel for cell immobilization. *Carbohydr Polym*, 102, 862-868. doi:10.1016/j.carbpol.2013.10.077
- Liyana-Pathirana, C. M., & Shahidi, F. (2006). Importance of insoluble-bound phenolics to antioxidant properties of wheat. *Journal of Agricultural and Food Chemistry*, 54(4), 1256-1264. doi:10.1021/jf052556h
- Maes, C., & Delcour, J. (2002). *Structural Characterisation of Water-extractable and Water-unextractable Arabinoxylans in Wheat Bran* (Vol. 35).

- Maes, C., & Delcour, J. A. (2002). Structural characterisation of water-extractable and water-unextractable arabinoxylans in wheat bran. *J Cer Sci*, 35. doi:10.1006/jcrs.2001.0439
- Marquez-Escalante, J. A., Carvajal-Millan, E., Yadav, M. P., Kale, M., Rascon-Chu, A., Gardea, A. A., . . . Faulds, C. B. (2018). Rheology and microstructure of gels based on wheat arabinoxylans enzymatically modified in arabinose to xylose ratio. *J Sci Food Agric*, 98(3), 914-922. doi:10.1002/jsfa.8537
- Martinez-Lopez, A. L., Carvajal-Millan, E., Marquez-Escalante, J., Campa-Mada, A. C., Rascon-Chu, A., Lopez-Franco, Y. L., & Lizardi-Mendoza, J. (2019). Enzymatic cross-linking of ferulated arabinoxylan: effect of laccase or peroxidase catalysis on the gel characteristics. *Food science and biotechnology*, 28(2), 311-318. doi:10.1007/s10068-018-0488-9
- Martinez-Lopez, A. L., Carvajal-Millan, E., Micard, V., Rascon-Chu, A., Brown-Bojorquez, F., Sotelo-Cruz, N., . . . Lizardi-Mendoza, J. (2016). In vitro degradation of covalently cross-linked arabinoxylan hydrogels by bifidobacteria. *Carbohydr Polym*, 144, 76-82. doi:10.1016/j.carbpol.2016.02.031
- Mateo Anson, N., Hemery, Y. M., Bast, A., & Haenen, G. R. (2012). Optimizing the bioactive potential of wheat bran by processing. *Food Funct*, 3(4), 362-375. doi:10.1039/c2fo10241b
- McKeen, L. W. (2017). Polyolefins, Polyvinyls, and Acrylics. In L. W. McKeen (Ed.), *Permeability Properties of Plastics and Elastomers* (pp. 157-207): William Andrew Publishing.
- Megazyme. (Lot 160419b). WHEAT ARABINOXYLAN (Low Viscosity) Data Sheet.
- Mendez-Encinas, M. A., Carvajal-Millan, E., Rascon-Chu, A., Astiazaran-Garcia, H. F., & Valencia-Rivera, D. E. (2018). Ferulated Arabinoxylans and Their Gels: Functional Properties and Potential Application as Antioxidant and Anticancer Agent. *Oxid Med Cell Longev*, 2018, 2314759. doi:10.1155/2018/2314759
- Merali, Z., Collins, S. R., Elliston, A., Wilson, D. R., Kasper, A., & Waldron, K. W. (2015). Characterization of cell wall components of wheat bran following hydrothermal pretreatment and fractionation. *Biotechnol Biofuels*, 8, 23. doi:10.1186/s13068-015-0207-1
- Mikkelsen, D., Flanagan, B. M., Wilson, S. M., Bacic, A., & Gidley, M. J. (2015). Interactions of arabinoxylan and (1,3)(1,4)-beta-glucan with cellulose networks. *Biomacromolecules*, 16(4), 1232-1239. doi:10.1021/acs.biomac.5b00009
- Mikkonen, K. S., Heikkinen, S., Soovre, A., Peura, M., Serimaa, R., Talja, R. A., . . . Tenkanen, M. (2009). Films from Oat Spelt Arabinoxylan Plasticized with Glycerol and Sorbitol. *Journal of Applied Polymer Science*, 114(1), 457-466. doi:10.1002/app.30513
- Mikkonen, K. S., & Tenkanen, M. (2012). Sustainable food-packaging materials based on future biorefinery products: Xylans and mannans. *Trends in Food Science & Technology*, 28(2), 90-102. doi:10.1016/j.tifs.2012.06.012
- Morais de Carvalho, D., Berglund, J., Marchand, C., Lindström Mikael, E., Vilaplana, F., & Sevastyanova, O. (2019). Improving the thermal stability of different types of xylan by acetylation. *Carbohydrate Polymers*, 220, 132-140. doi:10.1016/j.carbpol.2019.05.063
- Moreirinha, C., Vilela, C., Silva, N. H. C. S., Pinto, R. R. J., Almeida, A., Rocha, M. A. M., . . . Freire, C. S. R. (2020). Antioxidant and antimicrobial films based on brewers spent grain arabinoxylans, nanocellulose and feruloylated compounds for active packaging. *Food Hydrocolloids*, 105836. doi:10.1016/j.foodhyd.2020.105836
- Munk, L., Muschiol, J., Li, K., Liu, M., Perzon, A., Meier, S., . . . Meyer, A. S. (2020). Selective Enzymatic Release and Gel Formation by Cross-Linking of Feruloylated Glucurono-Arabinoxylan from Corn Bran. *ACS Sustainable Chemistry & Engineering*, 8(22), 8164-8174. doi:10.1021/acssuschemeng.0c00663

- Ng, A., Greenshields, R. N., & Waldron, K. W. (1997). Oxidative cross-linking of corn bran hemicellulose: formation of ferulic acid dehydrodimers. *Carbohydrate Research*, 303(4), 459-462. doi:10.1016/s0008-6215(97)00193-6
- Nieduszynski, I. A., & Marchessault, R. H. (1972). Structure of β ,D(1 \rightarrow 4')-xylan hydrate. *Biopolymers*, 11(7), 1335-1344. doi:10.1002/bip.1972.360110703
- Nilsson, M. (1996). Water unextractable polysaccharides from three milling fractions of rye grain. *Carbohydrate Polymers*, 30(4), 229-237. doi:10.1016/s0144-8617(96)00071-9
- Nino-Medina, G., Carvajal-Millan, E., Rascon-Chu, A., Marquez-Escalante, J. A., Guerrero, V., & Salas-Munoz, E. (2010). Feruloylated arabinoxylans and arabinoxylan gels: structure, sources and applications. *Phytochemistry Reviews*, 9(1), 111-120. doi:10.1007/s11101-009-9147-3
- Nylander, F., Svensson, O., Josefson, M., Larsson, A., & Westman, G. (2019). New features of arabinoxylan ethers revealed by using multivariate analysis. *Carbohydr Polym*, 204, 255-261. doi:10.1016/j.carbpol.2018.09.062
- Oinonen, P., Zhang, L., Lawoko, M., & Henriksson, G. (2015). On the formation of lignin polysaccharide networks in Norway spruce. *Phytochemistry*, 111, 177-184. doi:10.1016/j.phytochem.2014.10.027
- Onipe, O. O., Jideani, A. I. O., & Beswa, D. (2015). Composition and functionality of wheat bran and its application in some cereal food products. *International Journal of Food Science & Technology*, 50(12), 2509-2518. doi:10.1111/ijfs.12935
- Pang, Y., Ahmed, S., Xu, Y., Beta, T., Zhu, Z., Shao, Y., & Bao, J. (2018). Bound phenolic compounds and antioxidant properties of whole grain and bran of white, red and black rice. *Food Chemistry*, 240, 212-221. doi:10.1016/j.foodchem.2017.07.095
- Parikka, K., Leppanen, A. S., Pitkanen, L., Reunanen, M., Willfor, S., & Tenkanen, M. (2010). Oxidation of polysaccharides by galactose oxidase. *J Agric Food Chem*, 58(1), 262-271. doi:10.1021/jf902930t
- Parker, M. L., Ng, A., & Waldron, K. W. (2005). The phenolic acid and polysaccharide composition of cell walls of bran layers of mature wheat (*Triticum aestivum* L. cv. Avalon) grains. *J Sci Food Agri*, 85. doi:10.1002/jsfa.2304
- Pereira, P. H., Waldron, K. W., Wilson, D. R., Cunha, A. P., Brito, E. S., Rodrigues, T. H., . . . Azeredo, H. M. (2017). Wheat straw hemicelluloses added with cellulose nanocrystals and citric acid. Effect on film physical properties. *Carbohydr Polym*, 164, 317-324. doi:10.1016/j.carbpol.2017.02.019
- Peroval, C., Debeaufort, F., Despre, D., & Voilley, A. (2002). Edible arabinoxylan-based films. 1. Effects of lipid type on water vapor permeability, film structure, and other physical characteristics. *J Agric Food Chem*, 50(14), 3977-3983.
- Piber, M., & Koehler, P. (2005). Identification of dehydro-ferulic acid-tyrosine in rye and wheat: evidence for a covalent cross-link between arabinoxylans and proteins. *J Agric Food Chem*, 53(13), 5276-5284. doi:10.1021/jf050395b
- Rabemanolontsoa, H., & Saka, S. (2016). Various pretreatments of lignocellulosics. *Bioresour Technol*, 199, 83-91. doi:10.1016/j.biortech.2015.08.029
- Ragaee, S. M., Wood, P. J., Wang, Q., Tosh, S. M., Brummer, Y., & Huang, X. (2008). Isolation, Fractionation, and Structural Characteristics of Alkali-Extractable β -Glucan from Rye Whole Meal. *Cereal Chemistry Journal*, 85(3), 289-294. doi:10.1094/cchem-85-3-0289
- Raisanen, U., Pitkanen, I., Halttunen, H., & Hurta, M. (2003). Formation of the main degradation compounds from arabinose, xylose, mannose and arabinitol during pyrolysis. *Journal of Thermal Analysis and Calorimetry*, 72(2), 481-488. doi:10.1023/A:1024557011975

- Reisinger, M., Tirpanalan, O., Pruckler, M., Huber, F., Kneifel, W., & Novalin, S. (2013). Wheat bran biorefinery--a detailed investigation on hydrothermal and enzymatic treatment. *Bioresource Technology*, *144*, 179-185. doi:10.1016/j.biortech.2013.06.088
- Rhodes, D. I., & Stone, B. A. (2002). Proteins in Walls of Wheat Aleurone Cells. *Journal of Cereal Science*, *36*(1), 83-101. doi:10.1006/jcres.2001.0450
- Rogowski, A., Briggs, J. A., Mortimer, J. C., Tryfona, T., Terrapon, N., Lowe, E. C., . . . Bolam, D. N. (2015). Glycan complexity dictates microbial resource allocation in the large intestine. *Nat Commun*, *6*, 7481. doi:10.1038/ncomms8481
- Rosa-Sibakov, N., Poutanen, K., & Micard, V. (2015). How does wheat grain, bran and aleurone structure impact their nutritional and technological properties? *Trends in Food Science & Technology*, *41*(2), 118-134. doi:10.1016/j.tifs.2014.10.003
- Rose, D. J., & Inglett, G. E. (2010). Production of feruloylated arabinoxylo-oligosaccharides from maize (*Zea mays*) bran by microwave-assisted autohydrolysis. *Food Chemistry*, *119*(4), 1613-1618. doi:10.1016/j.foodchem.2009.09.053
- Rose, D. J., Patterson, J. A., & Hamaker, B. R. (2010). Structural differences among alkali-soluble arabinoxylans from maize (*Zea mays*), rice (*Oryza sativa*), and wheat (*Triticum aestivum*) brans influence human fecal fermentation profiles. *J Agric Food Chem*, *58*(1), 493-499. doi:10.1021/jf9020416
- Rudjito, R. C., Jiménez-Quero, A., Hamzaoui, M., Kohnen, S., & Vilaplana, F. (2020). Tuning the molar mass and substitution pattern of complex xylans from corn fibre using subcritical water extraction. *Green Chemistry*. doi:10.1039/d0gc02897e
- Rudjito, R. C., Ruthes, A. C., Jiménez-Quero, A., & Vilaplana, F. (2019). Feruloylated arabinoxylans from wheat bran: Optimization of extraction process and validation at pilot scale. *ACS Sustainable Chemistry & Engineering*, *7*(15), 13167-13177. doi:10.1021/acssuschemeng.9b02329
- Rumpagaporn, P., Reuhs, B. L., Kaur, A., Patterson, J. A., Keshavarzian, A., & Hamaker, B. R. (2015). Structural features of soluble cereal arabinoxylan fibers associated with a slow rate of in vitro fermentation by human fecal microbiota. *Carbohydr Polym*, *130*, 191-197. doi:10.1016/j.carbpol.2015.04.041
- Ruthes, A. C., Martínez-Abad, A., Tan, H.-T., Bulone, V., & Vilaplana, F. (2017). Sequential fractionation of feruloylated hemicelluloses and oligosaccharides from wheat bran using subcritical water and xylanolytic enzymes. *Green Chemistry*, *19*(8), 1919-1931. doi:10.1039/c6gc03473j
- Saeman, J. F., Moore, W. E., Mitchell, R. L., & Millett, M. A. (1954). Techniques for the determination of pulp constituents by quantitative paper chromatography. *Tappi J*, *37*(8), 336-343.
- Santos, N. A., Cordeiro, A. M. T. M., Damasceno, S. S., Aguiar, R. T., Rosenhaim, R., Carvalho Filho, J. R., . . . Souza, A. G. (2012). Commercial antioxidants and thermal stability evaluations. *Fuel*, *97*, 638-643. doi:10.1016/j.fuel.2012.01.074
- Sarossy, Z., Blomfeldt, T. O., Hedenqvist, M. S., Koch, C. B., Ray, S. S., & Plackett, D. (2012). Composite films of arabinoxylan and fibrous sepiolite: morphological, mechanical, and barrier properties. *ACS Appl Mater Interfaces*, *4*(7), 3378-3386. doi:10.1021/am3002956
- Sárossy, Z., Tenkanen, M., Pitkänen, L., Bjerre, A.-B., & Plackett, D. (2013). Extraction and chemical characterization of rye arabinoxylan and the effect of β -glucan on the mechanical and barrier properties of cast arabinoxylan films. *Food Hydrocolloids*, *30*(1), 206-216. doi:10.1016/j.foodhyd.2012.05.022
- SasView. <http://www.sasview.org/> (accessed Jan 1, 2021).
- Saulnier, L., Marot, C., Chanliaud, E., & Thibault, J.-F. (1995). Cell wall polysaccharide interactions in maize bran. *Carbohydrate Polymers*, *26*(4), 279-287. doi:10.1016/0144-8617(95)00020-8

- Saulnier, L., Vigouroux, J., & Thibault, J. F. (1995). Isolation and partial characterization of feruloylated oligosaccharides from maize bran. *Carbohydr Res*, 272(2), 241-253. doi:10.1016/0008-6215(95)00053-v
- Saxena, A., Elder, T. J., Pan, S., & Ragauskas, A. J. (2009). Novel nanocellulosic xylan composite film. *Composites Part B-Engineering*, 40(8), 727-730. doi:10.1016/j.compositesb.2009.05.003
- Schendel, R. R., Meyer, M. R., & Bunzel, M. (2015). Quantitative Profiling of Feruloylated Arabinoxylan Side-Chains from Gramineous Cell Walls. *Front Plant Sci*, 6(1249), 1249. doi:10.3389/fpls.2015.01249
- Schooneveld-Bergmans, M. E. F., Hopman, A. M. C. P., Beldman, G., & Voragen, A. G. J. (1998). Extraction and partial characterization of feruloylated glucuronoarabinoxylans from wheat bran. *Carbohydrate Polymers*, 35(1-2), 39-47. doi:10.1016/s0144-8617(97)00229-4
- Silva-Weiss, A., Ihl, M., Sobral, P. J. A., Gomez-Guillen, M. C., & Bifani, V. (2013). Natural Additives in Bioactive Edible Films and Coatings: Functionality and Applications in Foods. *Food Engineering Reviews*, 5(4), 200-216. doi:10.1007/s12393-013-9072-5
- Srinivasan, M., Sudheer, A. R., & Menon, V. P. (2007). Ferulic Acid: Therapeutic Potential Through Its Antioxidant Property. *Journal of Clinical Biochemistry and Nutrition*, 40(2), 92-100. doi:10.3164/jcfn.40.92
- Stepan, A. M., Höjje, A., Schols, H. A., de Waard, P., & Gatenholm, P. (2012). Arabinose content of arabinoxylans contributes to flexibility of acetylated arabinoxylan films. *Journal of Applied Polymer Science*, 125(3), 2348-2355. doi:10.1002/app.36458
- Sternemalm, E., Højje, A., & Gatenholm, P. (2008). Effect of arabinose substitution on the material properties of arabinoxylan films. *Carbohydrate Research*, 343(4), 753-757. doi:10.1016/j.carres.2007.11.027
- Stevanic, J. S., Joly, C., Mikkonen, K. S., Pirkkalainen, K., Serimaa, R., Remond, C., . . . Salmen, L. (2011). Bacterial Nanocellulose-Reinforced Arabinoxylan Films. *Journal of Applied Polymer Science*, 122(2), 1030-1039. doi:10.1002/app.34217
- Stevenson, L., Phillips, F., O'Sullivan, K., & Walton, J. (2012). Wheat bran: its composition and benefits to health, a European perspective. *Int J Food Sci Nutr*, 63(8), 1001-1013. doi:10.3109/09637486.2012.687366
- Stoklosa, R. J., Latona, R. J., Bonnaillie, L. M., & Yadav, M. P. (2019). Evaluation of arabinoxylan isolated from sorghum bran, biomass, and bagasse for film formation. *Carbohydr Polym*, 213, 382-392. doi:10.1016/j.carbpol.2019.03.018
- Swennen, K., Courtin, C. M., Lindemans, G. C. J. E., & Delcour, J. A. (2006). Large-scale production and characterisation of wheat bran arabinoxyloligosaccharides. *Journal of the Science of Food and Agriculture*, 86(11), 1722-1731. doi:10.1002/jsfa.2470
- Szydłowska-Czerniak, A., Trokowski, K., & Sztyk, E. (2011). Optimization of extraction conditions of antioxidants from sunflower shells (*Helianthus annuus* L.) before and after enzymatic treatment. *Industrial Crops and Products*, 33(1), 123-131. doi:10.1016/j.indcrop.2010.09.016
- Thuvander, J., Arkell, A., & Jönsson, A. S. (2014). Centrifugation as pretreatment before ultrafiltration of hemicelluloses extracted from wheat bran. *Separation and Purification Technology*, 138, 1-6. doi:10.1016/j.seppur.2014.10.003
- Vansteenkiste, E., Babot, C., Rouau, X., & Micard, V. (2004). Oxidative gelation of feruloylated arabinoxylan as affected by protein. Influence on protein enzymatic hydrolysis. *Food Hydrocolloids*, 18(4), 557-564. doi:10.1016/j.foodhyd.2003.09.004

- Velkova, N., Doliška, A., Fras Zemljič, L., Vesel, A., Saake, B., & Strnad, S. (2015). Influence of carboxymethylation on the surface physical-chemical properties of glucuronoxylan and arabinoxylan films. *Polymer Engineering & Science*, *55*(12), 2706-2713. doi:10.1002/pen.24059
- Verma, B., Hucl, P., & Chibbar, R. N. (2009). Phenolic acid composition and antioxidant capacity of acid and alkali hydrolysed wheat bran fractions. *Food Chemistry*, *116*(4), 947-954. doi:10.1016/j.foodchem.2009.03.060
- Vilaplana, F., & Gilbert, R. G. (2010). Two-Dimensional Size/Branch Length Distributions of a Branched Polymer. *Macromolecules*, *43*(17), 7321-7329. doi:10.1021/ma101349t
- Vinkx, C. J. A., & Delcour, J. A. (1996). Rye (*Secale cereale* L.) Arabinoxylans: A Critical Review. *Journal of Cereal Science*, *24*(1), 1-14. doi:10.1006/jcsc.1996.0032
- Vogel, B., Gallaher, D. D., & Bunzel, M. (2012). Influence of cross-linked arabinoxylans on the postprandial blood glucose response in rats. *J Agric Food Chem*, *60*(15), 3847-3852. doi:10.1021/jf203930a
- Wallace, G., & Fry, S. C. (1999). Action of diverse peroxidases and laccases on six cell wall-related phenolic compounds. *Phytochemistry*, *52*(5), 769-773. doi:10.1016/s0031-9422(99)00342-8
- Wang, L., Zhang, L., Qiu, S., Liu, C., Zhang, P., Yin, L., & Chen, F. (2019). Rheological properties and structural characteristics of arabinoxylan hydrogels prepared from three wheat bran sources. *Journal of Cereal Science*, *88*, 79-86. doi:10.1016/j.jcs.2019.05.003
- Werner, K., Pommer, L., & Broström, M. (2014). Thermal decomposition of hemicelluloses. *Journal of Analytical and Applied Pyrolysis*, *110*(Supplement C), 130-137. doi:<https://doi.org/10.1016/j.jaap.2014.08.013>
- Xu, F., Liu, C. F., Geng, Z. C., Sun, J. X., Sun, R. C., Hei, B. H., . . . Je, J. (2006). Characterisation of degraded organosolv hemicelluloses from wheat straw. *Polymer Degradation and Stability*, *91*(8), 1880-1886. doi:10.1016/j.polymdegradstab.2005.11.002
- Yadav, M. P., Johnston, D. B., Hotchkiss, A. T., & Hicks, K. B. (2007). Corn fiber gum: A potential gum arabic replacer for beverage flavor emulsification. *Food Hydrocolloids*, *21*(7), 1022-1030. doi:10.1016/j.foodhyd.2006.07.009
- Yang, X. J., Dang, B., & Fan, M. T. (2018). Free and bound phenolic compound content and antioxidant activity of different cultivated blue highland barley varieties from the Qinghai-Tibet plateau. *Molecules*, *23*(4), 879. doi:10.3390/molecules23040879
- Zdunska, K., Dana, A., Kolodziejczak, A., & Rotsztejn, H. (2018). Antioxidant Properties of Ferulic Acid and Its Possible Application. *Skin Pharmacol Physiol*, *31*(6), 332-336. doi:10.1159/000491755
- Zeitoun, R., Pontalier, P. Y., Marechal, P., & Rigal, L. (2010). Twin-screw extrusion for hemicellulose recovery: influence on extract purity and purification performance. *Bioresour Technol*, *101*(23), 9348-9354. doi:10.1016/j.biortech.2010.07.022
- Zhang, P., & Whistler, R. L. (2004). Mechanical properties and water vapor permeability of thin film from corn hull arabinoxylan. *Journal of Applied Polymer Science*, *93*(6), 2896-2902. doi:10.1002/app.20910
- Zhang, X., Chen, T., Lim, J., Gu, F., Fang, F., Cheng, L., . . . Hamaker, B. R. (2019). Acid gelation of soluble laccase-crosslinked corn bran arabinoxylan and possible gel formation mechanism. *Food Hydrocolloids*, *92*, 1-9. doi:10.1016/j.foodhyd.2019.01.032
- Zhang, X., Zhang, A., Liu, C., & Ren, J. (2016). Per-O-acylation of xylan at room temperature in dimethylsulfoxide/N-methylimidazole. *Cellulose*, *23*(5), 2863-2876. doi:10.1007/s10570-016-0997-8

- Zhang, Y., Pitkanen, L., Douglade, J., Tenkanen, M., Remond, C., & Joly, C. (2011). Wheat bran arabinoxylans: Chemical structure and film properties of three isolated fractions. *Carbohydrate Polymers*, *86*(2), 852-859. doi:10.1016/j.carbpol.2011.05.036
- Zhou, S., Liu, X., Guo, Y., Wang, Q., Peng, D., & Cao, L. (2010). Comparison of the immunological activities of arabinoxylans from wheat bran with alkali and xylanase-aided extraction. *Carbohydrate Polymers*, *81*(4), 784-789. doi:10.1016/j.carbpol.2010.03.040
- Zhu, T., Mao, J., Cheng, Y., Liu, H., Lv, L., Ge, M., . . . Lai, Y. (2019). Recent Progress of Polysaccharide-Based Hydrogel Interfaces for Wound Healing and Tissue Engineering. *Advanced Materials Interfaces*, *6*(17), 1900761. doi:10.1002/admi.201900761
- Zitterman, A. (2003). DIETARY FIBER | Bran. In B. Caballero (Ed.), *Encyclopedia of Food Sciences and Nutrition* (pp. 1844-1850). Oxford: Academic Press.

